TECHNICAL REPORT STANDARD TITLE PAGE

1. Report No.	2. Government Accession No.	3. Recipient's Catalog No.
TX-91/0989-1F		

4. Title and Subtitle	5. Report Date
Comparison of Two Protected-Permitted Lead-Lag Left-Turn Phasing Arrangements	May 1991
	6. Performing Organization Code

7. Author (s)	8. Performing Organization Report No.
Daniel B. Fambro, Gilmer D. Gaston, and Christopher M. Hoff	Research Report 0989-1F

9. Performing Organization Name and Address	10. Work Unit No.
Texas Transportation Institute Texas A&M University System College Station, Texas 77843-3135	11. Contract or Grant No. Study No. 2-18-89-0989
	13. Type of Report and Period Covered Final - August 1989 May 1991
12. Sponsoring Agency Name and Address Texas State Dept. of Highways & Public Transportation Transportation Planning Division P.O. Box 5051 Austin, Texas 78763	14. Sponsoring Agency Code

15. Supplementary Notes

Study Title: Operational Data for Comparison of Two Left-Turn Phasing Alternatives.
This research was funded by the State of Texas.

16. Abstract

This report documents an analysis of the operations of a special type of lead-lag left-turn phasing sequence developed and used by traffic engineers in Dallas and Richardson, Texas. This phasing, known as the Dallas phasing, is prohibited by existing standards for left-turn phasing set forth in the *Manual for Uniform Traffic Control Devices* (MUTCD). The objective of this research was to use field and simulation data to evaluate the operational characteristics and benefits of this type of left-turn phasing arrangement. Operational data were collected at four intersections in the Dallas area that utilized the phasing. Measured and predicted stopped delays were used as the primary operational measures of comparison.

The results of this study indicate that the Dallas phasing can be accurately modelled with existing left-turn models. In addition, this study presents new values for several parameters used in protected-permitted left-turn models; i.e., values for critical gap, left-turn headway, and the average number of sneakers. The results of this study also indicate that the Dallas phasing results in less delay for both left-turning and through movements than the MUTCD phasing, and that at intersections along high volume coordinated arterial streets, the Dallas phasing offers significant operational benefits.

17. Key Words	18. Distribution Statement
lead-lag, left-turns, protected/permitted left-turns, left-turn delay, permitted left-turn characteristics	No restrictions. This document is available to the public through the National Technical Information Service, 5285 Port Royal Road Springfield, Virginia 22161

19. Security Classif. (of this report)	20. Security Classif. (of this page)	21. No. of Pages	22. Price
Unclassified	Unclassified	119	

Form DOT F 1700.7 (8-69)

COMPARISON OF TWO PROTECTED-PERMITTED LEAD-LAG LEFT-TURN PHASING ARRANGEMENTS

by

Daniel B. Fambro, P.E.
Assistant Research Engineer

Gilmer D. Gaston
Research Assistant

and

Christopher M. Hoff
Student Technician

Research Report 0989-1F
Research Study Number 2-18-89-0989
Study Title: Operational Data for Comparison of Two Left-Turn Phasing Alternatives

Sponsored by the

Texas State Department of Highways and Public Transportation

May 1991

TEXAS TRANSPORTATION INSTITUTE
The Texas A&M University System
College Station, Texas 77843-3135

METRIC (SI*) CONVERSION FACTORS

APPROXIMATE CONVERSIONS TO SI UNITS

Symbol	When You Know	Multiply By	To Find	Symbol
LENGTH				
in	inches	2.54	centimetres	cm
ft	feet	0.3048	metres	m
yd	yards	0.914	metres	m
mi	miles	1.61	kilometres	km
AREA				
in²	square inches	645.2	centimetres squared	cm ²
ft²	square feet	0.0929	metres squared	m²
yd²	square yards	0.836	metres squared	m²
mi²	square miles	2.59	kilometres squared	km²
ac	acres	0.395	hectares	ha
MASS (weight)				
oz	ounces	28.35	grams	g
lb	pounds	0.454	kilograms	kg
T	short tons (2000 lb)	0.907	megagrams	Mg
VOLUME				
fl oz	fluid ounces	29.57	millilitres	mL
gal	gallons	3.785	litres	L
ft³	cubic feet	0.0328	metres cubed	m³
yd³	cubic yards	0.0765	metres cubed	m³

NOTE: Volumes greater than 1000 L shall be shown in m³.

TEMPERATURE (exact)

°F	Fahrenheit temperature	5/9 (after subtracting 32)	Celsius temperature	°C

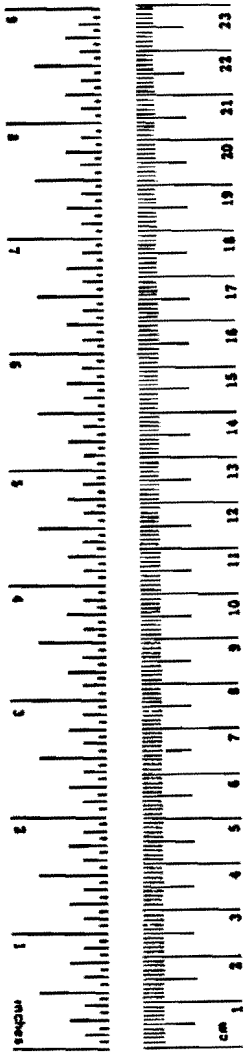

APPROXIMATE CONVERSIONS TO SI UNITS

Symbol	When You Know	Multiply By	To Find	Symbol
LENGTH				
mm	millimetres	0.039	inches	in
m	metres	3.28	feet	ft
m	metres	1.09	yards	yd
km	kilometres	0.621	miles	mi
AREA				
mm²	millimetres squared	0.0016	square inches	in²
m²	metres squared	10.764	square feet	ft²
km²	kilometres squared	0.39	square miles	mi²
ha	hectores (10 000 m²)	2.53	acres	ac
MASS (weight)				
g	grams	0.0353	ounces	oz
kg	kilograms	2.205	pounds	lb
Mg	megagrams (1 000 kg)	1.103	short tons	T
VOLUME				
mL	millilitres	0.034	fluid ounces	fl oz
L	litres	0.264	gallons	gal
m³	metres cubed	35.315	cubic feet	ft³
m³	metres cubed	1.308	cubic yards	yd³

TEMPERATURE (exact)

°C	Celsius temperature	9/5 (then add 32)	Fahrenheit temperature	°F

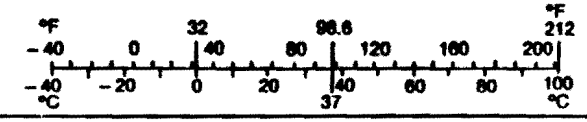

These factors conform to the requirement of FHWA Order 5190.1A.

* SI is the symbol for the International System of Measurements

ABSTRACT

This report documents an analysis of the operations of a special type of lead-lag left-turn phasing sequence developed and used by traffic engineers in Dallas and Richardson, Texas. This phasing, known as the Dallas phasing, is prohibited by existing standards for left-turn phasing set forth in the *Manual for Uniform Traffic Control Devices* (MUTCD). The objective of this research was to use field and simulation data to evaluate the operational characteristics and benefits of this type of left-turn phasing arrangement. Operational data were collected at four intersections in the Dallas area that utilized the phasing. Measured and predicted stopped delays were used as the primary operational measures of comparison.

The results of this study indicate that the Dallas phasing can be accurately modelled with existing left-turn models. In addition, this study presents new values for several parameters used in protected-permitted left-turn models; i.e., values for critical gap, left-turn headway, and the average number of sneakers. The results of this study also indicate that the Dallas phasing results in less delay for both left-turning and through movements than the MUTCD phasing, and that at intersections along high-volume coordinated arterial streets, the Dallas phasing offers significant operational benefits.

EXECUTIVE SUMMARY

Accommodating left-turning vehicles at signalized intersections have long been a source of concern for transportation engineers. As the number of left-turning vehicles increases, average delay and accident potential for both through and left-turning vehicles also increase. Separate left-turn lanes and protected left-turn phases are commonly used to minimize the impacts of left-turning vehicles. When an exclusive left-turn phase is used, however, the time to provide that phase must be taken from the through phases. Other decisions the engineer must make is the type of left-turn phasing that best satisfies the left-turn demand, and if the intersection is located on an arterial street, the left-turn phase sequence that maximizes progression.

One type of left-turn phasing that has been used to successfully increase the operational efficiency of some signalized intersections is protected-permitted phasing. This type of phasing can provide benefits under low to moderate traffic volumes because it allows left-turning vehicles to not only utilize a protected phase but also a permitted phase, if suitable gaps exist, for turning left. Phase sequence flexibility is an important factor when providing progression along an arterial street, and in many situations progression is maximized by the selection of lead-lag phasing at some of the intersections along the arterial. Permitted left turns opposing a protected lagging left turn, however, have been found to cause some left-turning drivers to assume that opposing traffic is simultaneously seeing a yellow indication at the end of the through phase. This situation can occur whenever a protected-permitted lead-lag left-turn is used. Thus, primarily as a result of safety concerns, protected-permitted phasing typically is not used with lead-lag left-turns.

In an effort to both increase the operational efficiency of individual intersections and also to maximize progression along the arterial street, traffic engineers in Dallas developed a new type of protected-permitted lead-lag left-turn signal phasing (i.e., Dallas phasing). The Dallas phasing uses overlaps to display circular greens (permitted left turn) to left-turning traffic during the opposing protected left-turn phase, thus increasing the length of the permitted phase. This phasing has been used at over 80 intersections for the past several years without any apparent safety problems. Unfortunately, current guidelines set forth in *The Manual on Uniform Traffic Control Devices* (MUTCD), prohibit the use of the Dallas arrangement. The purpose of this research was to provide an operational comparison of the Dallas phasing with MUTCD phasing arrangements. The following paragraphs summarize the results of this study.

FIELD STUDIES

Study Design. Field data were collected at four sites in Dallas and Richardson, Texas -- Mockingbird Lane at Inwood Road and Garland Road at Buckner Boulevard in Dallas, and Coit Road at Arapaho Road and Plano Road at Beltline Road in Richardson. At each of these intersections, data were collected for two hours in the morning peak, two

hours in the morning off-peak, two hours in afternoon off-peak, and two hours in the afternoon off-peak. Thus, there was a possibility of 64 hours of useable data (eight hours per direction for each of the four intersections). Each of the intersections was operated under the Dallas protected-permitted lead-lag left-turn phasing arrangement. During the two peak periods, the intersections were operated as a part of a coordinated system and during the two off-peak periods, they were operated independently of adjacent intersections. In all time periods, the study intersections were operated in the pretimed mode.

The data collection system consisted of three components -- manual data collection, electronic data collection, and video data collection. The manual data collection system was used to measure average stopped delay for both the through and left-turning movements in each direction. The electronic data collection system was used to collect traffic volume counts and percentages of heavy vehicles by movement and by lane at the intersection. The video data collection system was used to verify the signal timing information provided by the cities, determine saturation flow headway for each intersection, determine critical gaps and turning headway for left-turning vehicles at each of the intersections, and determine conflict rates between left-turning and opposing through vehicles.

Results. After discarding data blocks with missing or incorrect data (one of the intersections could not be operated in the desired phasing arrangement), 100 15-minute blocks (25 hours) of useable data remained. This data set contained signal timing information, traffic volume information, traffic flow information, and average stopped delay by 15-minute block. For each 15-minute block representing a leading protected-permitted left-turn movement, there was a corresponding 15-minute block representing the opposing lagging protected-permitted left turn movement. On a by-site basis, the final data set contained 8 hours of data from Mockingbird Lane, 6 hours of data from Garland Road, 8.5 hours of data from Coit Road, and 2.5 hours of data from Plano Road.

Cycle lengths ranged from 90 to 180 seconds, protected left-turn phases from 10 to 20 seconds, and permitted left-turn phases from 40 to 80 seconds. Left turning movement flow rates ranged from 100 to 300 vehicles per hour and opposing through movement flow rates ranged from 500 to 2000 vehicles per hour (250 to 700 vehicles per hour per lane). Critical gaps and turning headway for left-turning vehicles during the permitted portion of the phase ranged from 5.0 to 5.7 seconds and from 2.2 to 2.6 seconds, respectively. Both ranges are consistent with previous studies of permitted left turn operation reported in the literature. Saturation flow rates for opposing through movements ranged from 1600 to 1900 passenger cars per hour per lane. This finding also is consistent with previous studies.

The percentage of the left turns made on the permitted portion of the left-turn phase ranged from 0 to 80 percent; however, 75 percent of the observations were between 10 and 60 percent of the left turns being made on the permitted phase. The average delay for all left-turning vehicles ranged from 10 to 80 seconds per vehicle. Thus, the data set represents a wide range of operating conditions. The delay measured in the field for each 15-minute

block was then compared to that predicted by a conceptual model based on the left-turn modeling contained in PASSER II. The results of this comparison were that when the effects of progression were taken into account, the model accurately predicted the delay that was measured in the field. Because these results were consistent for all conditions, it was concluded that the conceptual model and/or PASSER II was suitable for comparing the MUTCD and Dallas protected-permitted lead-lag left-turn phasing.

SIMULATION STUDIES

Study Design. In order to compare the differences between the Dallas and conventional protected-permitted lead-lag left-turn phasing, a wide range of operating conditions was desirable. Two cycle lengths (90 and 120 seconds), three green time to cycle length ratios (0.4, 0.5, and 0.6), two types of left-turn phasing (MUTCD protected-permitted lead-lag left-turns, and Dallas protected-permitted lead-lag left-turns), five left-turn volumes (100 to 300 vehicles per hour in steps of 50), and six opposing through volumes (300 to 800 vehicles per hour per lane in steps of 100) were studied. This design resulted in 360 different combinations of traffic conditions being evaluated by PASSER II.

Results. For all conditions evaluated, protected-permitted lead-lag left-turn phasing resulted in less delay than did protected only lead-lag left-turn phasing. Reductions resulting from the change in phasing ranged from 20 to 50 percent (from 10 to 20 seconds per left-turn vehicle). Interestingly, delay reductions were greater for the left-turn movement with the leading protected phase. For this situation, the protected phase is being used to clear the queue of left-turning vehicles, the first portion of the permitted phase is effectively red because of the dissipation of the opposing queue, and the remainder of the permitted phase is being used to clear the left-turning vehicles that arrived during green. Thus, the protected portion of the phase occurs when the left-turn demand is the heaviest.

For the opposite situation (i.e., lagging protected phase), the first portion of the permitted phase is effectively red because of the dissipation of the opposing queue, the remainder of the permitted phase is being used to clear the waiting queue of left-turning vehicles, and the protected phase is being used to clear the remainder of the queued vehicles and those left-turning vehicles that arrived during green. In this case, the permitted portion of the phase occurs when the left-turn demand is the heaviest.

When comparing the Dallas to MUTCD protected-permitted lead-lag left-turn phasing, the Dallas phasing generally resulted in less delay. There were no conditions for which the Dallas phasing was worse than MUTCD protected-permitted phasing. Reductions in delay resulting from the change to the Dallas phasing range from 10 to 50 percent in most cases. As with the previous comparison, delay reductions were greater for the left-turn movement with the leading protected phase. This difference is a result of the additional

time for the permitted movement with the lagging protected phase being added during the time the opposing queue is dissipating.

CONCLUSIONS

Based on the results of this study, the following conclusions about the Dallas protected-permitted lead-lag left-turn phasing can be drawn:

1. The Dallas protected-permitted lead-lag left-turn phasing resulted in similar behavior by left-turning vehicles when compared to behavior during other types of permitted left-turn phasing; i.e., critical gaps, turning headway, and saturation flow rates were consistent to those reported in the literature.

2. The Dallas protected-permitted lead-lag left-turn phasing results in less delay for both the left-turning and through movements than MUTCD protected-permitted lead-lag left-turn phasing. This reduction in delay is slightly greater for the case where the protected phase leads the permitted phase than it is for the case where the protected phase lags the permitted phase.

3. At high volume intersections where protected-permitted left-turn phasing is beneficial from a capacity standpoint, and lead-lag left-turn phasing is necessary from a progression standpoint, Dallas left-turn phasing offers an operationally efficient alternative.

ACKNOWLEDGEMENTS

The research reported herein was performed as part of a study entitled "Operational Comparison of Two Left-Turn Phasing Arrangements" by the Texas Transportation Institute and sponsored by the Texas State Department of Highways and Public Transportation. Dr. Daniel B. Fambro and Dr. Carroll J. Messer of the Texas Transportation Institute served as co-research supervisors, and Mr. Ricky Collins of the Texas State Department of Highways and Public Transportation served as technical coordinator.

The authors wish to thank Mr. Herman Haenel of the Texas State Department of Highways and Public Transportation for his assistance, insight and constructive suggestions throughout the duration of this study. The authors also wish to thank Mr. Gerry DeCamp of the City of Las Vegas Department of Transportation, formerly of the City of Dallas Department of Transportation, Ms. Beth Ramirez of the City of Dallas Department of Transportation, and Mr. Walter Ragsdale of the City of Richardson Department of Transportation for their help in identifying study locations and assisting in the data collection effort for this research. Finally, a special thanks is extended to Dr. Carroll Messer for his insight into the internal workings of the PASSER II model.

The authors wish to acknowledge the student technicians at the Texas Transportation Institute who helped collect, reduce, and analyze the data for this research. Specifically, Mr. Marc Williams, Ms. Patricia Jackson, and Ms. Stacy Hall worked several long days in the hot August sun; Ms. Ellen Grubbs, Mr. Jerry Henderson, Ms. Patricia Jackson, Mr. Marty Springer, and Mr. Steve Venglar worked many long hours reducing data from video tape; Mr. John Habermann, Mr. Chris Hoff, and Mr. Kevin Shunk simulated more than 1,000 different left-turn conditions with PASSER II-90; and Mr. Christopher Amarante, Ms. Laura Arabie, Ms. Sarah Lillo, Ms. Dana Mixson, and Mr. Way En Yong prepared many of the report's graphics and assisted in typing and editing this report.

DISCLAIMER

The contents of this report reflect the views of the authors who are responsible for the opinions, findings, and conclusions presented herein. The contents do not necessarily reflect the official views or policies of the Texas State Department of Highways and Public Transportation. This report does not constitute a standard, specification, or regulation.

TABLE OF CONTENTS

LIST OF TABLES

LIST OF FIGURES

I. INTRODUCTION

Background

Accommodating left-turning vehicles at signalized intersections has long been a source of concern for transportation engineers. As the number of left-turning vehicles increases, average delay and accident potential for both through and left-turning vehicles also increases. Separate left-turn lanes and protected left-turn phases are commonly used to minimize the impacts of left-turning vehicles. When an exclusive left-turn phase is used, however, the time to provide that phase must be taken from the through phases. Other decisions the engineer must make are the type of left-turn phasing that best satisfies the left-turn demand, and if the intersection is located on an arterial street, the left-turn phase sequence that maximizes progression.

One type of left-turn phasing that has been used to successfully increase the operational efficiency of some signalized intersections is protected-permitted left-turn phasing. This type of phasing can provide benefits under low to moderate traffic volumes because it allows left-turning vehicles to not only utilize a protected phase but also a permitted phase, if suitable gaps exist, for turning left. Phase sequence flexibility is an important factor when providing progression along an arterial street, and in many situations progression is maximized by the selection of lead-lag phasing at some of the intersections along the arterial. Permitted left turns opposing a protected lagging left turn, however, have been found to cause some left-turning drivers to assume that opposing traffic is simultaneously seeing a yellow indication at the end of their adjacent through phase. This situation can occur whenever a protected-permitted lead-lag left-turn phasing sequence is used. Thus, primarily as a result of safety concerns, protected-permitted phasing typically is not used with lead-lag left-turns.

Problem Statement

Flexibility in the use of left-turn phase sequences is especially important when providing progression for traffic along an arterial street. Arterial progression opportunities are often maximized by using lead-lag phase sequences at several key intersections. Under current *Manual of Uniform Traffic Control Devices*(1), MUTCD, phase sequencing guidelines, however, protected-permitted lead-lag left-turn phase sequences are discouraged because of safety concerns. In an effort to increase the operational efficiency of individual intersections and to maximize progression along the arterial street, traffic engineers in Dallas and Richardson developed an experimental type of left-turn signal phasing which provides for lead-lag protected-permitted left-turns. This type of phasing has been used at over 80 intersections for the past several years with no apparent safety problems.

A phasing diagram illustrating the differences between the MUTCD and Dallas phasing is presented in Figure 1. As illustrated in this figure, the main difference between the two types of phasing are that with the Dallas phasing, permitted left turns are allowed during both the concurrent through phase and the opposing protected left-turn phase.

The current guidelines set forth in MUTCD which prohibits the Dallas phasing are located on page 4B-12.(1) The statement is reproduced as follows:

> "(c) Protected and Permitted Mode - When the protected mode and the permitted mode can occur during the same cycle, a separate signal face is not required for the left turn, but, if provided, shall be considered an approach signal face, and shall meet the following requirements:
>
> 1. During the protected left turn movement, a GREEN ARROW shall be displayed simultaneously with a CIRCULAR RED or CIRCULAR GREEN on the same approach with the protected left turn and simultaneously with a CIRCULAR RED for traffic on the opposing approach."

Note that this statement explicitly states that during the protected left-turn phase, signal heads on the opposing approach must have a circular red indication.

Several prior studies have indicated that this signal phasing provides operational benefits of increased left-turn capacity and reduced vehicular delay. One study performed by the city of College Station's Traffic Engineering Section utilized the TRANSYT-7F program to compare the MUTCD and Dallas phasing alternatives for an arterial in College Station, Texas.(2) Collins compared the MUTCD and Dallas protected-permitted lead-lag phasing arrangements for isolated intersections using the TEXAS simulation model.(3) Both studies indicated that the Dallas phasing reduced left turn-delay for intersections where permitted left-turn capacity is available. Neither of these studies, however, had the resources to validate their results with field data.

Objectives

The objectives of this research were to provide an operational comparison between the MUTCD and Dallas phasing arrangements. This comparison involved three types of information -- analytical modelling, data from field studies, and data from the PASSER II-90 computer program. In order to accomplish the study objectives, the following tasks were conducted:

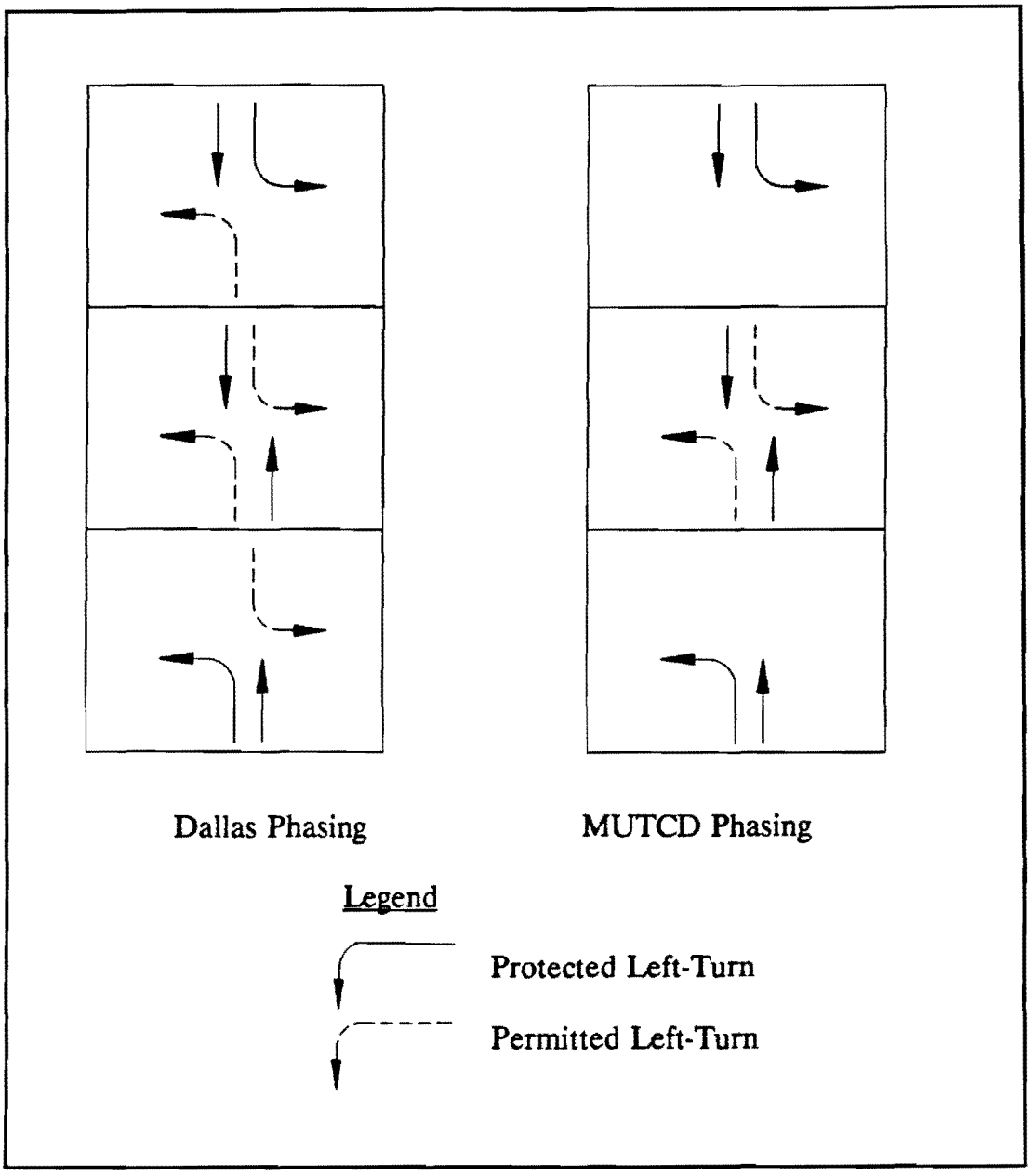

Figure 1: Dallas and MUTCD Phasing Comparison

1. Conduct state-of-the-art review;
2. Develop analytical models;
3. Conduct field studies;
4. Conduct simulation studies; and
5. Compare MUTCD and Dallas phasing.

Safety concerns with the Dallas phasing arrangement were addressed as part of the overall research effort by traffic engineers at the Texas State Department of Highways and Public Transportation (SDHPT). Those results are not included in this report.

Organization

This report consists of five major sections and five appendices. Section I contains a brief overview of the MUTCD and Dallas phasing schemes and the objectives of this research. Section II presents a discussion of the various types of protected-permitted left-turn phasing, guidelines for their use, and analytical models for evaluating their operational effectiveness. Section III describes an analytical model for predicting protected-permitted lead-lag left-turn delay and the procedures for collection, reduction, and analysis of the field study data. Section IV discusses the results from the field studies, subsequent validation of the analytical model, and the PASSER II-90 simulation study of protected-permitted lead-lag left-turn phasing which compared the MUTCD and Dallas phasing arrangements. Conclusions and recommendations resulting from this research are presented in Chapter V. The appendices contain the field data that were collected and documentation for many of the statistical tests that were conducted.

II. STATE-OF-THE-ART REVIEW

Traffic signals are used to allow the orderly movement of two or more conflicting traffic or pedestrian movements at roadway intersections. Under certain volume conditions, traffic signals can increase the traffic carrying capacity of intersections and reduce the frequency of certain types of accidents. In summary, traffic signals are used to:

1. Provide for the orderly movement of traffic;
2. Provide time for pedestrians and other vehicles to cross or enter the traffic stream;
3. Reduce the frequency of certain types of accidents; and
4. Increase the traffic carrying capacity of intersections.

Traffic signals use signal phases to control the flow of traffic. In its simplest form, a traffic signal phase can be represented by a combination of movements that are allowed to proceed concurrently as indicated by a green, yellow, red sequence. In the more complex case of left-turn phasing, the signal indications for protected-only and protected-permitted left-turn phasing, respectively, are:

1. Green arrow - yellow arrow - red ball; and
2. Green arrow - yellow arrow - green ball - yellow ball -red ball; or green ball - green arrow - yellow ball - red ball.

Each signal phase provides the right-of-way for one or more traffic movements. A traffic movement is the directional path of a vehicle approaching and leaving an intersection. The path includes left-turns, right turns, and through traffic. A left-turn movement includes both the left-turn arrival and departure paths. The remainder of this section discusses the different treatments for accommodating left-turn movements, guidelines for selecting the appropriate left-turn treatment, and a review of several analytical models for modelling permitted left-turn movements.

Left-Turn Treatments

The number of signal phases has a significant impact upon the efficiency of a traffic signal. Fewer phases increase the efficiency of traffic signal operation. Additional signal phases require more clearance intervals which reduce the amount of time available for the movement of traffic. Clearance intervals are required at the termination of each green phase. Clearance intervals provide for the orderly change of right-of-way between conflicting traffic movements. Additional clearance intervals reduce the percentage of time available to move traffic, thereby reducing intersection capacity.

This reduction in capacity is most severe when the additional phases provide protected-only left-turns. The reduced capacity can be regained by increasing the cycle length. Longer cycle lengths increase delay; therefore, it is desirable to keep the number of signal phases to a minimum and keep the cycle length as short as possible while providing adequate capacity for all of the intersection movements.

Left-Turn Phasing Types. Three types of left-turn phasing exist, and they are best described by whether or not the left-turn movement is protected by a separate phase or permitted to turn through gaps in the opposing traffic stream. The phasing types are usually referred to as follows:

1. Protected-only, also known as Exclusive;
2. Permitted-only; and
3. Protected-Permitted, or Exclusive-Permitted.

Protected-only left-turn phasing has the lowest accident potential but is also the most restrictive on traffic flow. With this type of phasing, left-turn movements are allowed only during the green arrow phase. Protected-only phasing is often used at locations that experience high traffic volumes, accident experience, or both. Permitted-only left-turn phasing is less restrictive to traffic flow, but it has the highest accident potential. Permitted-only phasing is normally used at intersections with low left-turn volumes.

Protected-permitted phasing, when applicable, can increase left-turn capacity without increasing the length of the protected phase or the cycle length. The additional left-turn capacity is created by allowing permitted left-turns during the opposing through phase. Permitted left-turn capacity is a function of the opposing traffic volume and the amount of time available to make a permitted left-turn movement. When the opposing traffic volume is low, the resulting increase in the permitted left-turn capacity can reduce the required length of the protected phase. This reduction can result in lower intersection delay and improve the quality of progression for the through movements along the arterial street.

Left-Turn Phasing Sequences. In order to maximize the time available to progress traffic along a coordinated street, it is often desirable to use different left-turn phasing sequences at some signalized intersections along the arterial. The phase sequence selected should place the protected left-turn phase at a time during the signal cycle that eliminates or minimizes interference with traffic progression along the major street. Three different phase sequences are associated with protected-only and protected-permitted left-turn phasing. The sequences are named according to the order of the left-turn phase with respect to the through phase, as follows:

1. Leading left-turn movements;
2. Lagging left-turn movements; and
3. Lead-lag left-turn movements.

Leading left-turns means that the two opposing left-turns receive the green arrow simultaneously before the two opposing through movements receive the green ball indication. In contrast, a lagging left-turn movement means that the two opposing left-turn movements receive green arrow indications after the through movement phase. The leading left-turn movement sequence is the most commonly used phase sequence in the state of Texas. Leading left-turn movements are usually preferred at intersections that have actuated left-turn phases. If any extra time is left over from the leading left-turn phase, it is added to the time provided for the through traffic phase which follows. If lagging left-turn movements are used, this additional time left over may not be applied where it can provide the most benefits, on the coordinated arterial.

Lead-lag left-turn movements are different from the other two phase sequences because to start the arterial street phase sequence, one left-turn movement receives the green arrow indication at the same time that its adjacent through movement receives a green ball indication. At the termination of the green arrow phase for the leading left-turn movement, the opposing through traffic also receives a green ball indication. After both through movements have received the green ball indication for some time, the through phase which began first terminates and the opposing left-turn receives a protected green arrow phase. This green arrow and the adjacent through traffic green ball indication continue for a specific amount of time, terminating simultaneously, ending the arterial street phase sequence.

Protected-Permitted Lead-Lag Left-Turn Phasing. The lead-lag phase sequence is an important left-turn phasing option. Lead-lag phasing can often improve the quality of two-way progression along a street in a coordinated traffic signal system. The option to use lead-lag phase sequences may enable traffic engineers to develop coordinated signal timing plans that result in lower system-wide delay than plans developed without lead-lag phasing. One hazard with the use of lead-lag phase sequencing and protected-permitted left-turn phasing is the "trap left-turn". This hazard occurs if a motorist is attempting a permissive left-turn, in the leading direction, when the permitted left-turn and adjacent through phases terminate. The motorist observes the yellow clearance indications on left-turn and adjacent through signal faces and assumes that the opposing through traffic is also receiving a yellow clearance indication. In this situation an aggressive driver may turn into the oncoming traffic, which actually has a green ball, and collide with an oncoming vehicle.

Because of the "trap left-turn", MUTCD phasing does not allow a lead-lag sequence with a protected-permitted left-turn movement. With MUTCD phasing, the leading side of a lead-lag signal must be protected only. In fact, the only phase sequencing options available for protected-permitted phasing with MUTCD phasing are leading left turns and lagging left turns. Another sequence option is the Dallas phasing; the Dallas phasing eliminates the "trap left-turn" because the permitted left-turn phase ends simultaneously with the opposing through phase. Therefore, when a left-turn driver receives a yellow

clearance indication, the opposing through movement also is receiving a yellow clearance indication.

The most noticeable difference between the two phase sequences occurs during the protected left-turn phases. The permitted phase of the Dallas phasing has an additional amount of permitted green time which is equal to the length of the opposing protected left-turn phase. It should be noted that even though the Dallas phasing eliminates the "trap left-turn", it can create a similar problem for the adjacent through drivers. These problems must be addressed with signal face louvers on the left-turn signal heads. Louvers are placed on the green ball and yellow ball signal faces on the left-turn signal head. These louvers prevent drivers in the adjacent through lanes from seeing a green ball on their approach during the permitted left-turn phase which occurs during the protected left-turn phase for the opposing direction. Without the louvers, a driver in an adjacent lane might see a green ball on the left-turn signal head, falsely believe he/she has the right-of-way, and enter the intersection, creating the potential for a collision with an opposing vehicle making a protected left-turn.

Left-turn Capacity Models

Basically all research performed on the left-turn capacity issue agrees that protected-permitted left-turn capacity depends upon two separate components. These components are the capacity of the protected phase and the capacity of the permitted phase. Protected left-turn capacity depends on the length of the protected left-turn phase time and the protected left-turn saturation flow rate. Permitted left-turn capacity is more difficult to estimate. Permitted capacity is dependent on the time available for turning, the left-turn saturation flow rate, the saturation flow rate of the opposing traffic, the distribution of vehicle arrivals, and the acceptable gap size and turning headway.

It is known that increased left-turn capacity results in decreased left-turn delay. Left-turn capacity is the maximum number of left-turn movements that can be made in one hour. When left-turn demand approaches or exceeds capacity, excessive delay will be incurred by the left-turning traffic. A number of different equations and procedures have been proposed to estimate left-turn capacity and delay. The Highway Capacity Manual (4) and the Australian Road Capacity Guide (5) provide empirically developed formulas for computing permitted left-turn capacity. Fambro used Drew's gap acceptance model to develop a permitted left-turn model.(6) This negative exponential model uses the critical gap, turning headway, and opposing through traffic volume to predict permitted left-turn capacity. The Texas model, a microscopic simulation model, developed at the Center for Transportation Research, models left-turns based on input values which define vehicle, driver, and intersection characteristics.(7) The Texas model is the only one of these models that attempts to account for individual driver characteristics. The following sections discuss left-turn capacity models in greater detail.

HCM Left-Turn Capacity Models. The 1985 Highway Capacity Manual presents empirical approaches to determine both protected left-turn capacity, and permitted left-turn capacity. For protected-permitted operation, the HCM recommends applying most of the left-turn volume to the protected portion, as long as the volume-to-capacity ratio for the protected left-turn phase remains less than 1.0. Any volume in excess of the protected capacity is then applied to the permitted left-turn phase. Protected left-turn capacity is a function of the left-turn saturation flow rate and the amount of time that effectively can be used to turn left. This concept is expressed in the HCM (4) as follows:

$$c_{Pr\,LT} = s_{Pr}\left(\frac{g_{Pr}}{C}\right)$$

Where:

$c_{Pr\,LT}$	=	Protected left-turn capacity, vph;
s_{Pr}	=	Protected left-turn saturation flow rate, vph;
g_{Pr}	=	Effective green during the protected phase, sec; and
C	=	Cycle length, sec.

The same methodology is used by the HCM to estimate permitted left-turn capacity. Permitted left-turn capacity is a function of the left-turn saturation flow rate during the permitted phase, and the time available for turning during the permitted phase. The difference in the procedures for calculating the two different left-turn capacities occurs because of the complexity of determining the permitted saturation flow rate. In the HCM, permitted saturation flow is a linear function of the opposing volume. The estimated permitted left-turn capacity is the maximum of:

$$c_{Pm\,LT} = (1400 - V_o)\left(\frac{g_{Pm}}{C}\right)$$

or

$$c_{Pm\,LT} = \frac{N_s\ 3600}{C}$$

Where:

$c_{Pm\,LT}$	=	Permitted left-turn capacity, vph;
V_o	=	Opposing flow rate, vph;
g_{Pm}	=	Effective green during the permitted phase, sec;
C	=	Cycle length, sec; and
N_s	=	Number of sneakers per cycle, 2 per cycle.

The HCM procedure assumes that the maximum number of permitted left-turns which can be made in one hour is 1400. This maximum value is then reduced to account for the opposing traffic flow and the available green time. If this equation calculates a permitted left-turn capacity less than 2 left-turns per cycle, the HCM recommends using 2 left-turns per cycle as the minimum permitted left-turn capacity. This minimum permitted capacity is assumed to occur during the yellow clearance interval.

The HCM methodology accounts for the effect of left-turn movements based on the manner in which they are accommodated. When protected-permitted left-turn movements are made from exclusive lanes, the HCM recommends an iterative procedure.(4) Bonneson and McCoy presented several suggestions which clarify and improve the HCM procedures for calculating protected-permitted left-turn capacity from exclusive left-turn lanes. (8)

Australian Left-Turn Capacity Model. The 1968 Australian Road Capacity Guide presents a methodology that is similar to the HCM for estimating permitted left-turn capacity. With the Australian method, left-turn capacity is determined as a function of the opposing volume. The Australian method assumes that 1200 vehicles per hour is the maximum permitted left-turn flow rate.(5) The Australian equation for permitted left-turn capacity is:

$$Q_L = 1200 * f * (G/C)$$

Where:

Q_L	=	Permitted left-turn capacity vph;
G	=	Green phase duration, sec;
C	=	Cycle length, sec; and
f	=	Left-turn equivalency factor, depending on the opposing volume.

The saturation flow of the opposing volume is represented by the 1200 value. the 1200 value is similar in the HCM, but in this model, the value is multiplied by f, a gap acceptance factor that is inversely proportional to the opposing volume. The (1200 * f) value is then reduced to a per cycle basis by multiplying by the effective green time available for turning left. Gap acceptance is represented by using the negative exponential distribution since the distribution of arrivals was assumed to follow the Poisson distribution.

The Australian Road Capacity Guide recommends a minimum permitted left capacity of 1.5 vehicles per cycle.(5) This value is an empirical value based on the number of left-turns made during the clearance interval.

Gap Acceptance Left-Turn Capacity Model. Fambro et al. developed a permitted left-turn capacity model based on permitted left-turn drivers' acceptance or rejection of gaps

in the opposing traffic flow. High opposing flow rates produce fewer acceptable size gaps in the opposing traffic stream and low opposing flows produce more acceptable size gaps in the opposing traffic stream. The left-turn capacity of an intersection is related to both the probability of gaps occurring in the opposing traffic stream and the time available during which left-turn movements can be made.(6) The equation used to express this concept is:

$$Q_L = Q_{LH}\left(\frac{T_A}{C}\right)$$

Where:

Q_L	=	Permitted left-turn capacity for an approach, vph;
Q_{LH}	=	Permitted left-turn capacity across random, free-flowing traffic, vphg;
T_A	=	Time available for turning per cycle, sec; and
C	=	Cycle length, sec.

Permitted left-turn capacity across free-flow, random traffic occurs after the opposing through queue has dissipated. All drivers are assumed to accept any gap greater than or equal to their critical gap and reject all gaps less than their critical gap. The critical gap for each individual driver will vary according to their individual driving characteristics. To simplify the modelling process, an average critical gap representative of the entire population of drivers is used.

The researchers observed that more than one vehicle may turn through an accepted gap if it is of sufficient length. The limiting factor of these multiple turns is the spacing between the successive vehicles. This spacing is defined by the turning headway, H. If a uniform arrival rate is assumed due to free-flowing traffic, the negative exponential distribution can be used to represent the probability of gap occurrence. Drew used this concept in the following equation (9):

$$Q_{LH} = Q_T\left[\frac{e^{-qT_c}}{1-e^{-qH}}\right]$$

Where:

Q_{LH}	=	Permitted left-turn capacity across random free-flow traffic, vph;
Q_T	=	Total opposing traffic (through plus right) vph;
q	=	Total opposing traffic (through plus right) vps;
T_c	=	Critical gap, sec; and
H	=	Turning headway, sec.

Field studies performed by Fambro et al. produced a recommended critical gap of 4.5 seconds, and a turning headway of 2.5 seconds. The critical gap was determined by pairing the largest rejected gap and the accepted gap for each left-turning vehicle. These data were then graphically presented as cumulative totals for rejected and accepted gaps which intersect at a value which approximates the critical gap. Left-turn headways were determined by measuring the time between the completion of the turning movement of successive vehicles through the same gap. Only gaps with successive turning vehicles were used to determine the average left-turn headway.

The researchers also found that lane distribution has a major impact on left-turn capacity (6) because the time available for left-turn movements did not begin until the longest opposing lane queue dissipated. In situations where traffic is unevenly distributed across two or more lanes, the lane that develops the longest queue will block permitted left-turns until that queue has cleared. In order to correctly a model permitted left-turn movement, the opposing through volume should be adjusted to equal an evenly distributed volume where all queues are as long as the longest queue. This adjustment will satisfy the assumption of evenly distributed traffic.

The researchers concluded that an average of 2 vehicles per cycle turn during the clearance interval.(6) This value was determined from data collected for signals with permitted-only left-turn phasing, both with and without exclusive left-turn lanes.

TEXAS Left-Turn Capacity Model. The TEXAS model (7) utilizes simulation techniques to microscopically analyze each vehicle in each lane on each intersection approach. The left-turn model used in the TEXAS model microscopically analyzes the effects of: cycle length; green splits; number of opposing lanes; multiple, exclusive or shared left-turn lanes; headway distributions; and the effects of heavy vehicles. The model uses the concepts of transparency and average left-turn processing time to determine left-turn capacity. Transparency is a method of accounting for the opposing queue dissipation and the distribution of acceptable gaps. In other words it accounts for the blockage of permitted left-turns by opposing traffic. Simulation research has shown that transparency is linearly dependent upon opposing traffic volumes for a range of 100 to 600 vph.(7) This linear relationship can be expressed as:

$$T = 0.5322 - 0.0007675\ Q_o$$

Where:

T = Transparency; and
Q_o = Opposing traffic volume, vph.

Average left-turn processing time is the other major factor used in the TEXAS model to determine left-turn capacity. The average left-turn processing time was found to be approximately 4.36 seconds for the range of opposing volumes from 100 to 500 vph.(7) This value includes both permitted left-turn movements and left-turn movements made at the end of the permissive phase of a leading left-turn movement, or "sneakers". When the opposing traffic volume approaches saturation, the average left-turn processing time decreases to 3.0 seconds. This time is assumed to be the yellow clearance interval. The average left-turn processing time is used to determine left-turn capacity using the following equation:

$$Q_L = 3600\left(\frac{T}{\bar{t}}\right)$$

Where:

Q_L	=	Left-turn capacity, vph;
T	=	Transparency; and
t	=	Average left-turn processing time, sec.

The TEXAS model assumes that the left-turn capacity during the yellow interval is approximately one left-turn per cycle when the opposing traffic is saturated. Simulation studies with the model produced a value of 5.4 seconds for the critical gap and a value of 3.6 seconds for the average left-turn headway. The turning headway estimate was obtained from a regression analysis on gap sizes and the number of left-turning vehicles accommodated.(7)

Left-Turn Delay Models

Models used to calculate left-turn delay have normally been models developed to calculate delay in general. Two types of delay, total delay and stopped delay, are presented in the literature. Total delay includes the delay incurred while decelerating or slowly moving in a queue of vehicles. Stopped delay, as the name implies, is a measurement of the delay incurred when the vehicle is physically stopped. Stopped delay is approximately equal to 67 percent of total delay.(4)

Delay calculation is based on queue-departure theory. Webster (10) produced the original delay model. The HCM (4) introduced a model that improved on Webster's original model by improving the methodology for determining random and overflow delay. The Australians also have presented their version of an improvement to the random and overflow delay term.(11) More recently, Hagen et al. have presented a model, based on queue-departure theory that calculates delay for protected-permitted left-turn movement.(12) The following sections discuss the delay models in greater detail.

Webster's Delay Model. The first model for predicting delay at signalized intersections was presented by Webster.(10) Using queue-departure theory, Webster developed the following model to predict the average delay for an approach or movement.

$$d = d_u + d_r + d_{cr}$$

Where:

d	=	Average total delay for approach or movement, sec/veh;
d_u	=	Average uniform delay for approach or movement, sec/veh;
d_r	=	Average random delay for approach or movement, sec/veh; and
d_{cr}	=	Average delay correction for approach or movement, sec/veh.

$$d = \frac{C\left[1 - \frac{g}{C}\right]^2}{2\left[1 - \frac{g}{C}X\right]} + \frac{X^2}{2q(1 - X)} - 0.65\left[X^{\left(2 + 5\frac{g}{C}\right)}\right]\sqrt[3]{\frac{C}{q^2}}$$

Where:

d	=	Average total delay for approach or movement, sec/veh;
X	=	Volume-to-capacity ratio for approach or movement;
C	=	Cycle length, sec;
q	=	Arrival rate, vps; and
g	=	Effective green time, sec.

Webster's original model consisted of only the first and second terms. The first term, known as the uniform delay term, calculates the average delay for traffic arriving at a uniform rate throughout the cycle. The second term, the random delay term, adjusts the delay to account for randomness in the arrival rate. Random arrivals account for the fact that traffic arrivals are assumed to follow a Poisson distribution. The third term, known as the correction term, was developed empirically and later added to correct the delay estimate to better fit the theory. Webster's model was limited because the model could not be used for volume-to-capacity ratios greater than 0.95. Increasing traffic volumes pushed volume-to-capacity ratios well above the limits of Webster's model, and resulted in the development of several models that can be applied with higher volume-to-capacity ratios.

HCM Delay Model. The 1985 *Highway Capacity Manual* (HCM) is one of the most widely used transportation engineering references in the United States. As illustrated in the following equation, the first term of the HCM equation is identical to Webster's first term for calculating uniform delay. The 1.33 factor merely converts the total delay to stopped

delay. This research focuses upon stopped delay, therefore, the delay model will be presented with the stopped delay factors.(4)

$$d = d_u + d_o$$

Where:

d	=	Average total delay for a lane group, sec/veh;
d_u	=	Average uniform delay for a lane group, sec/veh; and
d_o	=	Average random and overflow delay for a lane group, sec/veh.

$$d = \frac{1}{1.33} \frac{C\left[1 - \frac{g}{C}\right]^2}{2\left[1 - \frac{g}{C}X\right]} + 173X^2 \left[(X - 1) + \sqrt{(X - 1)^2 + \frac{16X}{c}} \right]$$

Where:

d	=	Average stopped delay per vehicle for a lane group, sec/veh;
C	=	Cycle length, sec;
g	=	Effective green for the lane group being considered, sec;
X	=	Volume-to-capacity ratio for the lane group; and
c	=	Capacity for the lane group, vph.

The second term of the HCM model accounts for random arrivals and overflow delay resulting from cycle failures. Cycle failures occur when the queue of vehicles does not clear during the cycle. In normal traffic flow patterns short peaks of higher than average traffic flows are common. These short peaks often oversaturate the intersection resulting in cycle failures for several cycles. It should by noted that the HCM model can be expected to produce reasonable results for volume-to-capacity ratios less than 1.2. The HCM advises that it be used with caution for volume-to-capacity ratios greater than 1.2.

Another important improvement to delay modelling provided by the HCM was the inclusion of a set of progression adjustment factors that account for the effects of the arrival time of vehicles at the intersection. It is intuitive that if a group of vehicles arrive at an intersection at the beginning of the red signal indication they will incur more delay than a group of vehicles arriving at the beginning of the green signal indication. Thus, accounting for the effects of progression is an important factor, however, it has been noted that the current methodology of applying progression adjustment factors does not always produce suitable results.(13)

Australian Delay Model. The Australian delay model predicts uniform delay with the same equation used by Webster and the HCM. The difference between the Australian and the HCM models occurs in the second, or overflow delay term. The Australian overflow delay term is based upon a time-dependent delay model which was derived by converting a steady-state delay function, which is applicable only to undersaturated conditions, to an asymptotic time-dependent function, which becomes applicable to oversaturated conditions as well.(11) Because the Australian overflow delay equation is asymptotic to the deterministic oversaturation flow line it should, in theory, provide more accurate delay estimates for volume-to-capacity ratios greater than 1.0. As noted, the first term of the Australian delay model is identical to Webster's and the HCM, it is included here for completeness:

$$d = d_u + d_o$$

Where:

- d = Average total delay per approach or movement, sec/veh;
- d_u = Average uniform delay per approach or movement, sec/veh; and
- d_o = Average overflow delay per approach or movement, sec/veh.

$$d = \frac{C\left[1 - \frac{g}{C}\right]^2}{2\left[1 - \frac{g}{C}X\right]} + \frac{T}{4}\left[(X - 1) + \sqrt{(X - 1)^2 + \frac{12\,(X - X_o)}{cT}}\right]$$

$$\text{if: } X > X_o \text{, then } X_o = 0.67 + \frac{sg}{600}$$

$$X < X_o \text{, then } d_o = 0.$$

Where:

- d = Average total delay per approach or movement, sec/veh;
- C = Cycle length, sec;
- g = Effective green for the lane group;
- X = Volume-to-capacity ratio;
- c = Capacity, vph;
- T = Flow period, hrs;
- s = Saturation flow rate, vps; and
- X_o = Volume-to-capacity ratio below which d_o equals zero.

The Australian procedure is different from the HCM or Webster equation because at low volume conditions, such as $X < X_o$, the Australian model predicts zero overflow delay, whereas the HCM and Webster methodologies for computing overflow delay predict very small overflow delays at low volumes.

III. FIELD STUDY DESIGN

This section describes the development of conceptual models for predicting delay for protected-permitted lead-lag left-turn phase sequences. In order to calibrate and validate these conceptual models, data were collected at several intersections where the Dallas phasing had been implemented. Along with a discussion of the conceptual model, this section addresses the selection of study sites and their descriptions, the data collection procedures, the validation and calibration of the conceptual model, and a summary of the analytical statistical procedures.

Conceptual Model

Modelling protected-permitted left-turn delay for the Dallas phasing follows the same queue-departure theory used by Webster to model delay at signalized intersections.(10) These modelling procedures are identical to the ones used to model protected-permitted left-turn delay using the MUTCD phasing. In order to calculate protected-permitted left-turn delay for the Dallas phasing a conceptual model was developed which incorporates the modelling techniques of the SDHPT's 1990 version of the *Progression Analysis Signal Systems Evaluation Routine* (PASSER II). The PASSER II model is a popular signal timing program which combines progression bandwidth and delay minimization to provide optimal cycle length, phase times, and offsets.(14) The model contains a feature which can be used to evaluate the Dallas phasing.

For intersection evaluation, PASSER II can be used to calculate an average total or stopped delay for each left-turn or through-plus-right movement. For protected-permitted left-turn movements, the model uses basic HCM methodology to calculate protected left-turn capacity. The model's default permitted left-turn model is Fambro's permitted left-turn capacity model. For delay calculation, the model uses basic queue-departure theory over one average cycle to calculate demand and supply functions. The integration of these two functions results in the total uniform delay for the movement. Distribution of the total delay for the movement over the left-turn volume results in an average delay per vehicle for the approach.

Factors which have been identified for inclusion in the conceptual model for predicting delay are: left-turn volume, time available for protected left-turn movements, time available for permitted left-turn movements, protected left-turn capacity, permitted left-turn capacity, left-turn arrival rates, and the left-turn phase sequence. The left-turn volume, time available for protected left-turn movements, protected left-turn capacity, left-turn arrival rate, and phase sequence can be measured in the field. The time available for permitted left-turn movements depends upon the length of the permitted phase, the opposing traffic volume, and to a lesser extent the arrival rate of the opposing traffic. The

permitted left-turn saturation flow rate is a function of the size of the critical gap, length of turning headway, opposing traffic volume, and the protected left-turn saturation flow rate.

The effects of progression on left-turn vehicles and opposing through traffic are factors in calculating delay. If the left-turn traffic arrives at the beginning of the red phase they incur more delay than if they arrive at the beginning of the protected left-turn phase. Progression of the opposing flow affects the opposing flow rate during the permitted phase, thereby increasing or decreasing the permitted left-turn capacity. Because PASSER II does not allow the user to define quality of progression, the conceptual model was used during analysis of delay in this research.

Phase sequence becomes a factor in the delay calculations because a leading protected-permitted left-turn phase incurs less delay than a lagging protected-permitted left-turn phase if all factors remain the same. This difference, as acknowledged by Hagen and Courage, occurs because the leading protected-permitted left-turn sequence functions as two separate shorter cycle lengths for moderate opposing volume conditions whereas the lagging protected-permitted left-turn sequence functions as one long cycle length for moderate opposing volume conditions.(12) This difference in delay calculation is due to the arrival and departure patterns of left-turning traffic due to fundamental differences in the queuing patterns of left-turn movements for each sequence. In order to properly accommodate the two sequences, separate modelling procedures were developed for each phase sequence.

Leading Protected-Permitted Left-Turn Model. For the leading protected-permitted left-turn model, the percentage of traffic volume in the left-turn and opposing approach, as well as the subsequent green and red times will be used to calculate arrival rates during the red and green, respectively. The modelling process will use an average cycle from a 15-minute block of data to calculate an average delay value for that data block.

The modelling process begins as vehicles arrive at either a uniform or variable rate. For simplicity in model development, uniform arrival rates are assumed, i.e., several arrival rates may occur during one cycle, but they are assumed to remain uniform for definitive periods during the cycle.

During the effective protected left-turn green phase, vehicles depart from the queue at a rate equal to the left-turn saturation flow rate. At the end of the protected green phase, left-turning vehicles are stopped while the opposing queue of vehicles blocks left-turn movements for the amount of time required to clear the opposing queue. After the opposing queue has cleared, left-turning vehicles will filter through the opposing flow which is arriving at a uniform rate. The number of left-turning vehicles in the queue grew at a uniform rate while the opposing queue cleared, i.e., the left-turning vehicles were blocked. Figure 2 provides an illustration of this process.

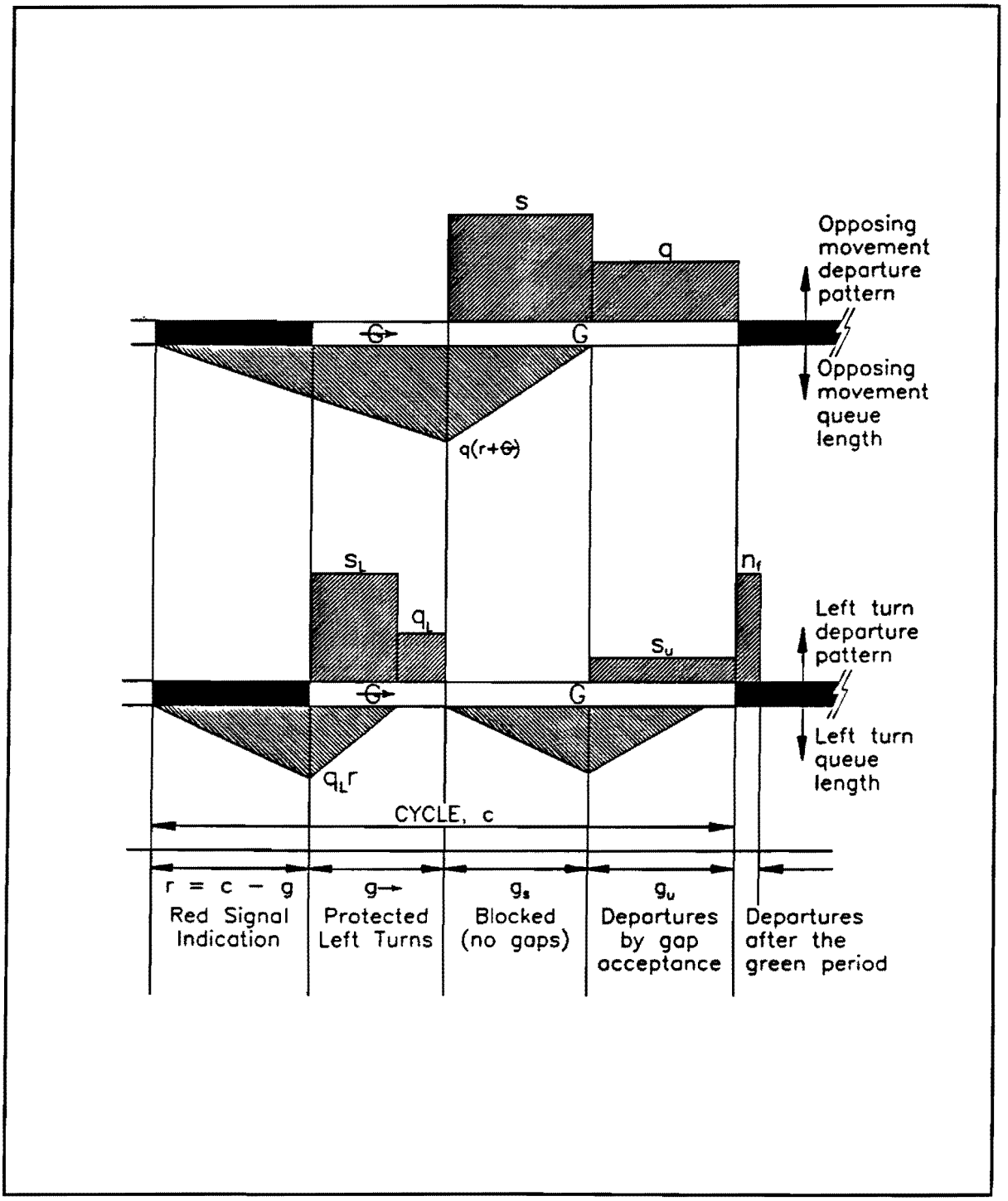

Figure 2. Leading Protected-Permitted Queue Departure Diagram

The process actually begins at the end of the preceding cycle. At this point the left-turn and opposing through queue lengths are both assumed to be zero. This assumption is valid for low to moderate volume conditions. Left-turning vehicles arrive at a uniform rate during the effective red (see Figure 2). The queue builds to a maximum length, Q_1, which occurs at the end of the effective red. The queue length at the end of the effective red, and the time required to dissipate the queue are calculated as:

$$Q_1 = r(q_L)_R$$

$$t_{1Q} = \frac{Q_1}{(s_L)_{Pr} - (q_L)_{Gr}}$$

Where:

Q_1 = Left-turn queue length at the end of the effective red, veh;
r = Left-turn effective red, sec;
$(q_L)_R$ = Left-turn arrival rate during the red, vps;
t_{1Q} = Time required to clear Q_1, sec;
$(s_L)_{Pr}$ = Left-turn saturation flow rate during the protected phase, vps; and
$(q_L)_{Gr}$ = Left-turn arrival rate during the green, vps.

At the beginning of the effective protected green, the left-turn queue begins to discharge at a departure rate equal to $(s_L)_{Pr}$. Left-turning traffic continues to arrive uniformly throughout the effective protected green at a rate of $(q_L)_{Gr}$ (see Figure 2). The left-turn queue, Q_1, will decrease in size if the departure rate, $(s_L)_{Pr}$, is greater than the arrival rate, $(q_L)_{Gr}$. The queue will completely dissipate during the protected phase if the time required to clear the queue, t_{1Q}, is less than the effective protected green, g_{Pr}. If, however, the queue does not clear during the protected phase, the length of the queue is calculated as:

$$Q_2 = Q_1 - \left[(s_L)_{Pr} - (q_L)_{Gr}\right] g_{Pr}$$

Where:

S_L = Left-turn saturation flow rate during the protected phase, vps;
Q_2 = Left-turn queue length at end of the effective protected phase, veh; and
g_{Pr} = Effective protected phase, sec.

If the queue clears during the effective green, the queue length at the end of the effective protected green, Q_2, will equal zero. The queue length at the beginning of the effective permitted green equals the queue length at the end of the protected phase. The

effective permitted green can be divided into two parts; the first, known as the saturated green time, is equal to the amount of time required to clear the queue of opposing vehicles. During the saturated green no permitted left-turn movements are made due to the blockage caused by the clearing of the opposing queue. The second part of the effective permitted green is usually known as the unsaturated effective green time. During this time left-turn traffic filters through the opposing flow. Throughout the effective permitted green, left-turn traffic arrives at a uniform arrival rate of $(q_L)_{Gr}$.

The length of the saturated green time is equal to the time required to clear the opposing queue of vehicles. The opposing queue grew at an arrival rate of $(q_{Vo})_{Red}$ during the opposing through effective red. Vehicles discharge from the queue at a rate equal to the saturation flow rate. The time required to dissipate the queue is a function of the opposing queue length, the opposing arrival rates during the red and green, and the opposing saturation flow rate. The opposing queue length at the beginning of the permitted green and the time required to clear are calculated as:

$$Q_{Vo} = (q_{Vo})_R [r + g_{Pr}]$$

Where:

Q_{Vo}	=	Opposing queue length at the beginning of the permitted phase, veh;
$(q_{Vo})_R$	=	Opposing arrival rate during opposing effective red, vps; and
$[r + g_{Pr}]$	=	Opposing effective red, sec;

and

$$t_{VoQ} = \frac{Q_{Vo}}{s_{Vo} - (q_{Vo})_{Gr}}$$

$(q_{Vo})_{Gr}$	=	Opposing arrival rate during opposing effective green, vps;
s_{Vo}	=	Opposing saturation flow rate, vps; and
t_{VoQ}	=	Time required to clear the opposing queue, sec.

If the time required to clear the opposing queue exceeds the effective permitted green time, the opposing queue will spill over into the next cycle and no permitted capacity will be available. If the time required to clear the opposing queue is less than the effective permitted green time, some permitted capacity, which occurs during the unsaturated green time, will be available.

At the beginning of the unsaturated green time, the queue of left-turn vehicles equals the queue length at the beginning of the permitted phase plus the vehicles which arrived during the saturated green time. The time required to clear the queue of left-turning vehicles is calculated as:

$$Q_3 = Q_2 + \left[g_{Sat}(q_{LT})_{Gr}\right]$$

$$t_{3Q} = \frac{Q_3}{\left[(s_{LT})_{Pm} - (q_{LT})_{Gr}\right]}$$

Where:

Q_3 = Left-turn queue length at the end of the saturated green time, veh;
t_{3Q} = Time required to clear queue, Q_3, sec;
g_{Sat} = Saturated left-turn green time, sec; and
$(s_L)_{Pm}$ = Left-turn saturation flow rate during permitted phase, vps.

The left-turn queue will continue to grow during the unsaturated green time if the left-turn arrival rate exceeds the left-turn departure rate. If the time to clear this queue exceeds the unsaturated green time a queue of vehicles will remain at the end of the unsaturated green time. This queue length is calculated as:

$$Q_4 = Q_3 + \left[g_{Unsat}(q_{LT})_{Gr}\right]$$

Where:

Q_4 = Left-turn queue length at the end of the unsaturated green time, veh;
g_{Unsat} = Unsaturated left-turn green time, sec.

The final queue length is reduced by a value less than or equal to the average number of sneakers, n_f (see Figure 2). If the queue length at the end of the unsaturated green time is less than the average number of sneakers, then adequate left-turn capacity existed and the delay estimates should be reasonable. If the left-turn queue does not clear during one cycle, the accuracy of the delay estimate will depend upon the applicability of the HCM overflow delay equation.

Delay is calculated for the cycle by summing the areas within the queue departure patterns, represented by triangles and polygons on the queue-length diagram (see Figure 2). The area under the queue length diagram is equal to the total delay incurred by all left-turning vehicles. This value is then divided by the total left-turn volume during the cycle to obtain an average left-turn delay per vehicle. This value is then reduced by 33 percent as specified by the HCM (9), to produce average stopped delay.

Lagging Protected-Permitted Left-Turn Model. The conceptual model for lagging protected-permitted left-turn delay is very similar to the model for leading protected-permitted left-turn delay. The main difference in the procedures occurs because the protected and unsaturated green times are not separated in time. This condition is illustrated in Figure 3. These two regions are separated in time by the saturated green time for leading left-turn movements (see Figure 2).

The queuing of vehicles during the effective red phase is identical to the process presented for leading left-turn movements. The queue of left-turning vehicles at the end of the effective red continues to grow during the saturated green time. The queue length at the end of the saturated permitted green time, Q_2, is calculated as:

$$Q_2 = Q_1 + \left[g_{Sat}(q_L)_{Gr}\right]$$

Where:

Q_2 = Left-turn queue length at the end of the saturated permitted green, veh;
g_{Sat} = Saturated left-turn green time, sec; and
$(q_L)_{Gr}$ = Left-turn arrival rate during the green phase, vps.

Permitted left-turn movements filter through the opposing flow during the unsaturated green time. If the queue which existed at the beginning of the unsaturated green time completely clears during the unsaturated green time, the time required to clear the queue is calculated as:

$$t_{2Q} = \frac{Q_2}{\left[(s_L)_{Pm} - (q_L)_{Gr}\right]}$$

Where:

t_{2O} = Time required to clear Q_2, sec; and
$(s_L)_{Pm}$ = Left-turn saturation flow rate during the permitted phase, vps.

If the queue does not clear before the end of the unsaturated green time, the queue length at the beginning of the protected phase, Q_3, is calculated as:

$$Q_3 = Q_2 - \left[(s_L)_{Pr} - (q_L)_{Gr}\right] g_{Unsat}$$

Where:

Q_3 = Left-turn queue length at the beginning of the protected green time, veh;
$(s_L)_{Pr}$ = Left-turn saturation flow rate during the protected phase, vps; and
g_{Unsat} = Unsaturated left-turn green time, sec.

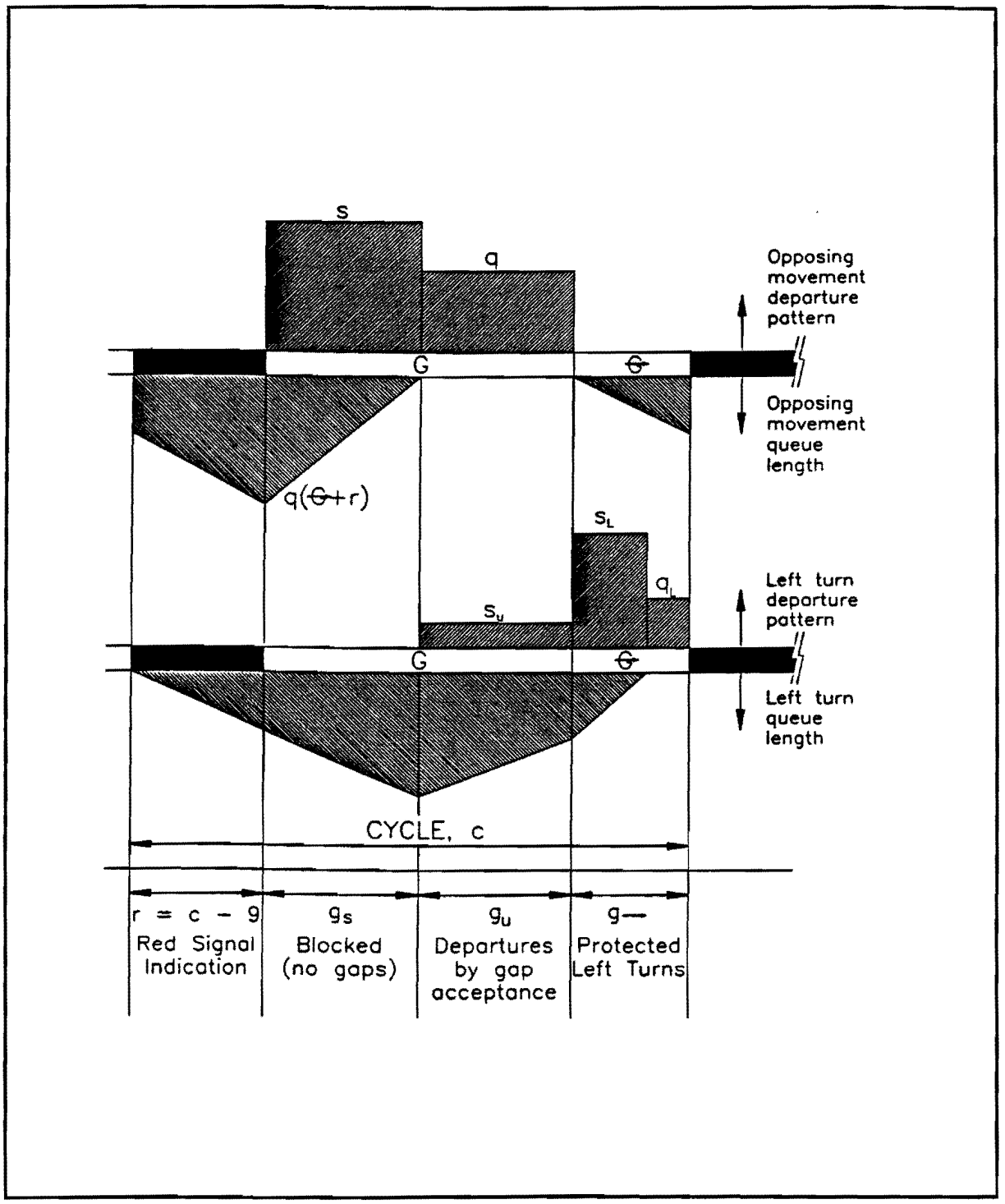

Figure 3: Lagging Protected-Permitted Queue Departure Diagram

The queue will completely clear during the effective protected green if the time required to clear the queue, Q_3, is less than the effective protected green time. The time required to clear this final queue is calculated as:

$$t_{3Q} = \frac{Q_3}{\left[(s_L)_{Prot} - (q_L)_{Gr}\right]}$$

Where:

$(q_L)_{Gr}$ = Left-turn arrival rate during green, vps.

Uniform stopped delay for the entire cycle is determined by calculating the area under the queue length diagram (see Figure 3) and reducing the value by 33 percent to convert total delay to stopped delay.

Field Study Sites

In order to validate these conceptual models, four study sites were selected for the data collection effort. Two of the sites were in Dallas, Texas and two sites were in Richardson, Texas. These cities where chosen because they have been using the Dallas phasing for several years at over 80 signalized intersections. City personnel were solicited to identify the most promising study locations. For each of the study sites identified, city personnel were asked to provide plans, signal timing data, and recent traffic volume measurements. This information was reviewed and four locations for the data collection effort were selected. Traffic volumes were analyzed to ensure that the data collection sites would provide a broad range of left-turn and opposing through volume conditions. Additional requirements for site selection included:

1. The intersection should utilize the Dallas phasing;
2. The intersection should be comprised of two arterial streets;
3. The intersection should have high type geometric features;
4. The intersection should have exclusive single left-turn lanes on the study approaches;
5. The peak hour left-turn traffic volume should be greater than or equal to 200 vehicles per hour; and
6. The opposing through plus right traffic volume should be greater than or equal to 200 vehicles per hour per lane.

In addition to the characteristics mentioned above, the study intersections had little or no pedestrian traffic. Low pedestrian traffic volumes were not a requirement, but the low volumes did ensure that pedestrians were not a factor in the data collection or the modelling

process. Locations for the four data collection sites and the corresponding data collection schedules are presented in Table 1. Intersection drawings for each of the study sites are provided in Appendix A.

Table 1: Dallas Phasing Study Locations

Intersection	Location	Date of Study	Number of Opp. Lanes
Mockingbird Lane at Inwood Road	Dallas, TX	August 21, 1989	2
Garland Road at Buckner Blvd.	Dallas, TX	August 22, 1989	3
Coit Road at Arapaho Road	Richardson, TX	August 23, 1989	3
Plano Road at Belt Line Road	Richardson, TX	August 24, 1989	3

Mockingbird Lane at Inwood Road. Mockingbird Lane is a four-lane divided arterial with an east-west orientation. Inwood Road is a six-lane divided arterial with a north-south orientation. The intersection of Mockingbird and Inwood is located approximately two-thirds of a mile west of the Dallas North Tollway in west Dallas. The arterial street grid in this area is based on a one to one-and-a-quarter mile spacings. Left-turn signals on the east and west approaches are pedestal mounted and located in the median. During the data collection effort, the temperature was hot, the streets were dry and the skies were clear.

Garland Road at Buckner Boulevard. Garland Road and Buckner Boulevard are both six-lane divided arterials in northeast Dallas. Garland Road is laid out with a northeast-to-southwest orientation. The orientation of Buckner Boulevard is perpendicular to Garland Road in a northwest-to-southeast orientation. For the purposes of this study, Garland Road is considered to be the north-south arterial and Buckner Boulevard is considered to maintain an east-west orientation. Garland Road is the major street in that it carries a higher daily volume of traffic. Left-turn signals on the north and south approaches are mounted horizontally on signal mast arms. During the data collection effort, the temperature continued to be hot, the streets remained dry, and the skies were clear.

Coit Road at Arapaho Road. Coit Road and Arapaho Road are both six-lane divided arterials in west Richardson. Coit Road is a major arterial roadway which carries a high volume of north-south traffic. Arapaho Road is a minor east-west arterial and carries a significantly lower traffic volume than Coit Road. The left-turn signal for the northbound approach is mounted vertically over the roadway on the signal mast arm. The southbound left-turn signal is pedestal mounted and located in the median. During the data collection effort, the temperature remained hot, the streets remained dry, and the skies continued to be clear.

Plano Road at Belt Line Road. Plano Road and Belt Line Road are both six-lane divided arterials in east Richardson. Plano Road and Belt Line Road are high volume roadways of similar daily traffic volumes. Plano Road maintains a north-south orientation and Belt Line Road follows an east-west orientation. Plano Road was selected as a study location because the traffic volumes during the peak periods were higher than those of any of the other potential study locations. The left-turn signal for both the northbound and southbound approaches are pedestal mounted and located in the medians. During the data collection effort the temperature remained hot. As the day progressed the partly cloudy sky became overcast which culminated in a late afternoon thundershower which brought the study to an abrupt halt. As a result of the thundershower, no pm peak data were collected.

Data Collection System

Data were collected on the opposing approaches at each of the four signalized intersections. In each case, one direction of travel operated with a leading phase sequence and the opposing direction of travel operated with a lagging phase sequence. The following data were collected for calibration of the conceptual model:

1. Signal timing information;
2. Left-turn traffic volumes;
3. Opposing through traffic volume;
4. Lane distribution of opposing traffic;
5. Base saturation flow rates;
6. Vehicle classification counts;
7. Percentage of vehicles arriving during the green signal indication;
8. Permitted left-turn accepted and rejected headways;
9. Permitted left-turn headways;
10. Number of left-turn sneakers; and
11. Left-turn stopped delay.

At each of the study sites, the traffic signal controller settings were adjusted by city personnel so that the cycle lengths and phasing sequences remained constant during each study period. This type of arrangement simulated pretimed traffic signal control. Pretimed control reduced the variability in the data and eliminated the need for collecting cycle-by-cycle signal timing information. The collection system consisted of the following three components:

1. Electronic data collection system;
2. Video data collection system; and
3. Manual data collection system.

Data were collected on a cycle-by-cycle basis throughout each study period. The data were collected in a format which facilitated reduction into fifteen minute data blocks. In

reduced format, each block of data represents an average fifteen minute period. Fifteen minute data blocks were used because previous research indicates that fifteen minutes is the smallest block for which reasonable traffic flow data can be predicted.(4) Fifteen minutes is small enough to account for fluctuations in traffic volumes and long enough for traffic flow to operate as a steady state. Smaller data blocks would have increased the variability of the data.

Electronic Data Collection System. The electronic data collection system consisted of two portable personal computers and a program which was used to collect traffic volume data. One computer and two people were used for each approach. At each computer, one person collected left-turn data while a second person collected the opposing through-plus-right traffic data. Each vehicle represented a data record which included a time stamp and a variable which indicated whether the vehicle was a left-turn or an opposing through vehicle. If the vehicle was an opposing through vehicle, the variable also described the lane in which the vehicle travelled through the intersection. Data collected with this system were reduced into fifteen minute traffic volume counts for both, left-turn and opposing through traffic, and the lane distribution of the opposing traffic.

Traffic Volumes. Traffic volumes were one of the most important variables included in the conceptual models for predicting left-turn delay. Left-turn volumes were required to distribute the delay measured in the field and also were used to predict volume-to-capacity ratios, determine arrival rates, and distribute the total stopped delay measured in the field. Opposing through traffic volumes were required to determine the opposing flow arrival rate, which directly impacts permitted left-turn capacity. A peaking factor was not used because fifteen minute volumes are considered to be the smallest amount of time for which traffic data can be effectively analyzed.

Lane Distribution. Lane distribution is important to this study because permitted left-turn models generally assume that the opposing traffic is evenly distributed across the opposing traffic lanes. The HCM model(4) and Fambro's model(6) each include lane utilization factors to account for this fact. This adjustment is necessary to accurately model permitted left-turn operation. If opposing traffic is not evenly distributed, then the lane with the longest queue will, in effect, block all left-turning vehicles. Lane utilization factors increase the opposing through traffic volume to account for uneven lane distribution. The Highway Capacity Manual recommends lane utilization factors of 1.00, 1.05, and 1.10 for one, two, and three or more opposing lanes, respectively. The lane utilization factors presented in the HCM were developed with the assumption that the most heavily used lane on a two-lane and three-lane arterial would respectively serve 52.5 and 36.7 percent of the total traffic on the approach.(4)

Video Data Collection System. The video data collection system was used to:

1. Verify the signal timing information provided by the cities;
2. Determine saturation flow headways for each location;
3. Classify vehicles on each study approach;
4. Measure the percentage of vehicles arriving during the green on each approach;
5. Collect information to determine the critical gap;
6. Measure left-turn headways; and
7. Determine the average number of sneakers.

Video data were collected with portable video cameras mounted with special brackets which could be attached to different pole diameters. Cameras were positioned to collect four different views of each study intersection. Two cameras were located to obtain a forward view, and two cameras were located to provide a rear view of the arriving traffic. The preferred forward camera location was directly in front of the approaching traffic (see "primary camera locations" in Figure 4). The forward cameras were mounted on the traffic

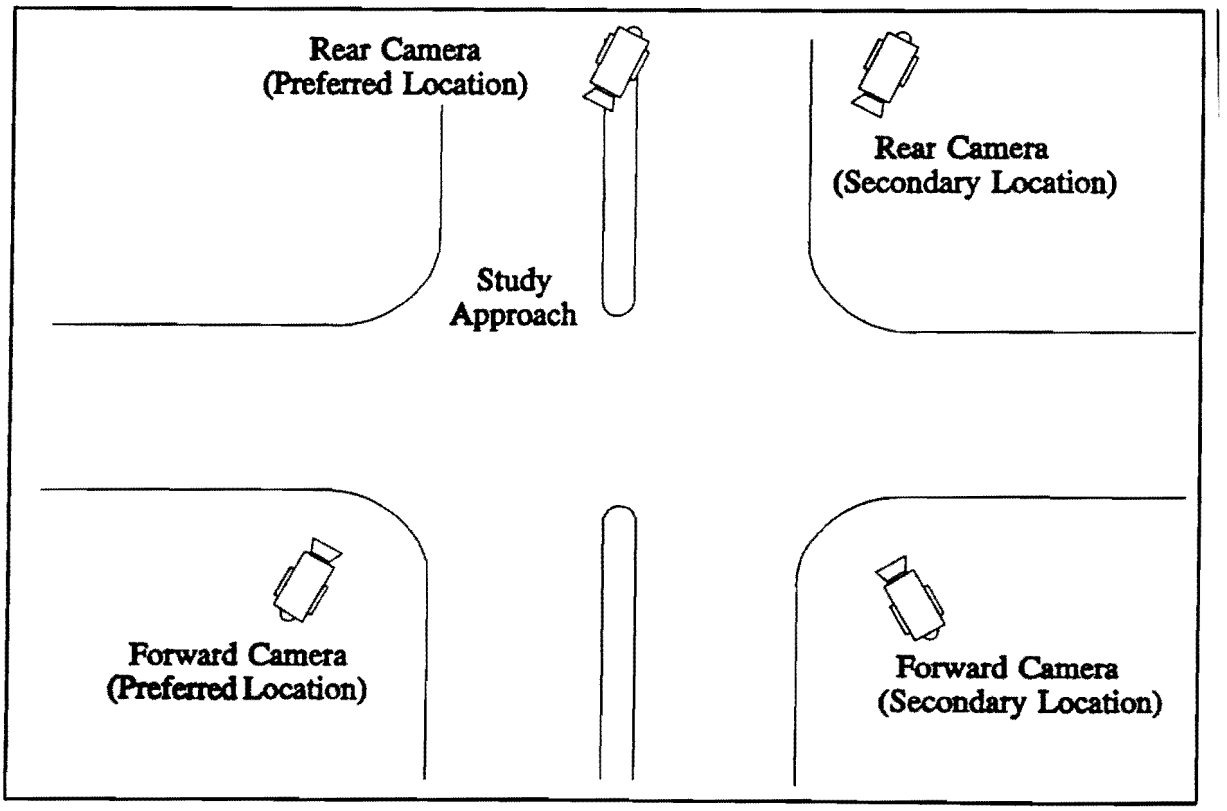

Figure 4: Camera Locations for Data Collection

signal masts located on diagonally opposite corners. These two cameras recorded a video log of the traffic movements, vehicular headways, and vehicle classification information.

The two rear cameras were located upstream of the intersection on each study approach and were used to obtain signal timing information. The cameras were mounted approximately twenty feet high on luminaire supports located in the median, or on the left-hand side of the intersection approach on a utility pole. The preferred location of the rear cameras was the luminaire supports located in the median (see "primary rear camera locations" in Figure 4). These locations were necessary to collect left-turn signal phasing data from the louvered signal heads.

Signal Timing Verification. Video data from the upstream cameras were reviewed to verify the signal timing information provided by each city. Signal timing information were verified for each of the four time periods at each study location. A stopwatch and video equipment were used to reduce and verify the signal timing information.

Saturation Flow Rates. Saturation flow rates were obtained by measuring saturation flow headways. Saturation flow rate is the number of vehicles per hour per lane that can pass through an intersection, under prevailing conditions, if the signal indication was green for a full hour(4). Saturation flow rates are calculated from saturation flow headways which are measured as the time between successive vehicles measured from the same reference point on each vehicle.

Saturation flow headway measurements are made only for vehicles which are queued at the beginning of the green signal indication. As the vehicles enter the intersection, the first four are ignored to account for start-up lost time. The start-up lost time begins at the beginning of the green phase for vehicles which have been stopped and ends when the vehicles are moving through the intersection at the saturation, or maximum, flow rate.

Saturation flow headways were determined for each study approach at each location. The equipment required for collecting saturation flow headways were a stopwatch and a video recorders. In order to accurately determine the ideal saturation flow rate, only queues consisting of automobiles were measured. Queues containing trucks, buses, stalled vehicles, or vehicles making turning or parking maneuvers were not used in the saturation flow rate analyses. Mean saturation flow rates for each approach were then determined from a weighted average of the saturation flow headways and the number of vehicles in each measured queue. Saturation flow rate adjustment factors, presented in the HCM, were used to account for heavy vehicles and turning volumes to adjust the saturation flow rates.(4)

Vehicle Classification. Fifteen minute vehicle classification counts also were collected from the video data. The fifteen minute classification counts were made with a manual

counterboard, stopwatch, and video equipment. For the purposes of this study, heavy vehicles were defined as any vehicle or vehicle combination which had more than four wheels on the pavement. This definition is fairly stringent, but it eliminated the need for judgement calls by the data collection personnel. The percentage of heavy vehicles measured were used to adjust the saturation flow rate for each movement as specified by the HCM (4).

Percent Volume on Green. The percentage of vehicles arriving on green for each approach was measured to account for the effects of progression in the collected data. These measurements were made from video data collected with the rear cameras. Using the video, a data collection person counted the number of vehicles arriving on the specific approach for the time when the through signal indications were green and red, respectively. Using these counts, the percentage of vehicles arriving during the green for each approach was determined.

The percentage of vehicles arriving during the green was used to calculated left-turn and opposing through arrival rates for green and red. For this research, the percentage of the cycle which is green for the opposing through movement is calculated directly from the signal timing parameters. The percentage of the cycle which is green for protected-permitted left-turn movements was calculated as the sum of the protected and unsaturated green times.

Critical Gap. The critical gap is defined as the gap between successive vehicles that fifty percent of the drivers accept and an equal percentage of the drivers reject. Accepted gaps are those gaps between successive opposing vehicles which are accepted by left-turning drivers as suitable for safely completing the left-turn maneuver. Rejected gaps are all of the gaps between successive opposing vehicles which left-turning drivers reject as being too short to safely execute the permitted left-turn maneuver. Accepted and rejected gap distributions were used to determine the critical gap. In this situation, a driver may reject many gaps, but can accept only one. In order to prevent these different sample sizes from biasing the data, the largest rejected gap was paired with the accepted gap.

The critical gap is determined by plotting the cumulative accepted and cumulative rejected gap distributions. The critical gap occurs where the two distributions intersect.(15) Due to the difficulty and additional effort of making time measurements associated with the front and rear bumpers of each vehicle, other researchers have previously measured vehicular headways and calculated a critical gap by subtracting the time required for a vehicle of assumed length to travel at the average vehicular speed past the observation point from the critical headway.(9) Vehicular headways are the time measurement between successive vehicles measured to the same reference point on each vehicle.

Left-Turn Headway. Permitted left-turn headways were collected concurrently with the accepted and rejected headway data. When gaps containing multiple left-turn movements occurred in the traffic stream, the headways between successive vehicles were measured with a stopwatch in a manner similar to that for collecting saturation flow headways. Left-turn headways were averaged over all successive vehicles which turned through the permitted gap.

Sneakers. A sneaker is a left-turn made during the clearance of the permissive left-turn and adjacent through phase. Sneakers cannot occur during the clearance of protected left-turn phases. Vehicles turning during the clearance of the protected phase are merely utilizing the effective green time. The number of sneakers was measured to provide a basis for comparison with other sneaker studies presented in the literature. Sneakers were quantified by viewing data collected with the rear video cameras. With these cameras, the clearance of the permitted left turn phase could be observed and vehicles turning during the clearance were counted. Sneaker measurements were made when the queue of vehicles at the beginning of the clearance interval for the permitted left-turn phase contained at least one more vehicle than the measured number of sneakers. This requirement ensured that the average number of sneakers were accurately measured.

Manual Data Collection System. A manual data collection system was used to measure stopped delay by counting the number of vehicles stopped in the left-turn lane at a regular time interval. For the purposes of this study, the "locked wheel" definition of stopped delay recommended by Reilly et al was used.(16) By this definition, vehicles are considered to be stopped, only if the wheels are not turning. This definition eliminated any problems associated with determining if and when vehicles were actually stopped.

Homogenous data samples were obtained by using regular time intervals which were not even multiples of the various cycle lengths. An even multiple of the cycle length would have introduced a cyclic bias into the data. Such a bias would be created if samples were made at the same point of each cycle throughout the study period.

Collection of stopped delay data required one person on each study approach. During this study, a computer program which provided an audible beep was used to indicate the end of each time interval. At the end of each time interval the person collecting the stopped delay data manually recorded the number of vehicles stopped in the left-turn lane on a data collection form. These data were reduced by summing the total number of vehicles stopped during each fifteen minute data block, multiplying by the time interval, and dividing by the number of left-turning vehicles during the same fifteen minute interval. The actual number of left-turning vehicles was determined from the left-turn volume data collected with the electronic data collection system.

Model Analysis

The summarized cycle lengths, green splits, traffic volumes, saturation flow rates, percentages of heavy vehicles, percentage of traffic arriving on green, critical gaps, left-turn headways, average number of sneakers, and measured stopped delay were used to calibrate the leading and lagging conceptual models. The conceptual models, explained earlier in this chapter were coded using a commercially available spreadsheet for ease and speed of calculation. After coding, the conceptual models were then validated with the PASSER II program(15) to ensure that the methodology was correctly coded.

The statistical analysis for this research consisted of a combination of univariate measures, regression analyses, multiple comparisons, and t-tests. A ninety-five percent level of confidence was maintained throughout all of the statistical comparisons of this study. Univariate measures were used to reduce the collected data.

Multiple comparisons were performed to determine if any between site variability exists in the accepted and rejected headway data, and in the left-turn headway data. These comparisons are important because previous research by Tsongos et al indicated that critical gap lengths are dependent upon night and day.(17) This research will determine if the critical gap length or average left-turn headway is dependent upon phase sequence.

Multiple regression analyses were used to compare the predictive model with measured field data. The predictive models results, the dependent variable, were compared with the measured delay using linear regression analyses. If the predictive model was able to provide an accurate prediction of the value of the measured average delay for each value of the predicted average delay, the parameter estimate resulting from the regression analysis was approximately equal one. If no delay is measured, then logically, none should be measured, therefore, the regression procedure assumes that the intercept is zero. A t-test was performed to determine whether or not the regression parameter is equal to one. The test of the parameter estimate, β, was based upon the following test hypothesis.(18)

Ho: $\beta = 1$ Model accurately predicts delay; and
Ha: $\beta \neq 1$ Model does not accurately predict delay.

Rejection Region: Reject Ho: if $|t| > t_{\alpha/2,df}$
Test Statistic:

$$t = \frac{\beta_j - 1}{s_t}$$

Where:

t	=	Calculated t value for Ho: $\beta = 1$;
β_j	=	Regression parameter estimate; and
s_t	=	Standard error of the parameter estimate.

If the absolute value of the calculated t was less than the tabulated value of $t_{\alpha/2,df}$ for $\alpha = 0.05$ and the appropriate error degrees of freedom, the null hypothesis was not rejected, i.e., the model can accurately predict delay. If the calculated value of t was greater than the tabular value, then the null hypothesis was rejected, i.e., the model cannot accurately predict delay. The level of significance of the fit of the regression will be supported by the level of significance, or p-value.

IV. FIELD STUDY RESULTS

This section of the report contains the results from the field studies and is divided into three sections -- Field Data Collected, Model Calibration, and Simulation Results. The data collected section contains summary statistics of the data collected during the field studies, and includes signal timing information, traffic characteristics, saturation flow rate measurements, and left-turn information. Reduction of these data resulted in operational information which was used to validate the conceptual models. The model calibration section describes the procedures used to validate the conceptual models with field data and compare the results to those from PASSER II. A comparison of the Dallas and conventional protected-permitted lead-lag phasing is presented in the simulation results section.

Field Data Collected

A total of twenty-five (25) hours of useable Dallas phasing data were collected (See Table 2). The amount of data is short of the study's goal of sixty-four (64) hours of data. The data collection effort was hampered by several problems which were beyond the control of the data collection team. Problems with the camera batteries, which consistently plagued the data collection effort, making it virtually impossible to collect two full hours of data for each study period. This problem was further compounded by the fact that important data were being collected by all four cameras, and when one battery failed the potential for the loss of important data was significant. Additionally, whenever two batteries failed virtually no useable delay data could be collected.

At Mockingbird Lane and Inwood Road, a total of eight (8) hours of data were collected during the off peak and pm peak time periods. Of this total, 2.5 hours of data for both the leading and lagging left-turn phase sequences were collected during the off peak time periods, and 1.5 hours of data for both the leading and lagging left-turn phase sequences were collected during the pm peak time period. No useful data were collected

Table 2: Hours of Data Collected

Hours of Data Collected	Phase Sequence		Total
	Leading	Lagging	
Peak Periods	3.25	2.75	6.00
Offpeak Periods	10.25	8.75	19.00
Total All Periods	13.50	11.50	25.00

during the am peak period. The am peak data were lost due to problems associated with mounting the video equipment. Additionally, one fifteen minute block for which data were actually collected was eliminated from the data set because of a cycle length change which occurred between 4:30 and 4:45 p.m.

At Garland Road and Buckner Boulevard, a total of six (6) hours of were collected during the off peak time periods. Of this total, 2.75 hours of data for the leading left-turn phase sequence and 3.25 hours of data for the lagging left-turn phase sequence were collected. No data were collected at this intersection during the am peak period because condensation inside the cameras rendered them inoperable during the am peak study period. No data were collected during the pm peak time period because the signal timing plan included both leading and lagging protected left-turn indications on the same approach. Because this phasing was inconsistent with the study's objectives, the data for both approaches were discarded.

At Coit Road and Arapaho Road, a total of 8.5 hours of useable data were collected during the off peak and pm peak time periods. Of this total, 3.0 hours of data for the leading and lagging left-turn phasing sequences were collected during the off peak time periods, and another 1.25 hours of data for each phasing sequence were collected during the pm peak period. No useable data were collected during the am peak period because the signal timing plan during that time period consisted of dual left turns leading on both the north and south approaches to the intersection. Because vehicles making permitted left-turn movements never faced an opposing traffic stream which included a protected left-turn movement, this data was discarded.

At Plano Road and Belt Line Road, a total of 2.5 hours of useable data were collected during the off peak and am peak time periods. Of this total, two (2) hours of data for the leading left-turn phasing sequence were collected during the off peak time period, and 0.5 hours of data for the leading left-turn phase sequence were collected during the am peak time period. Only two 15-minute blocks of data were collected during the am peak period because problems with camera batteries. Another problem with this location was that a recent traffic accident had damaged the intersection wiring thereby preventing the use of the Dallas phasing on the northbound approach. For this reason the southbound data was eliminated from the data set, and the northbound data, which was considered to be suspect, was eliminated from the regression analyses.

The resulting data set contained 100 15-minute blocks of data, 54 blocks of data for the leading left-turn phasing sequence and 46 blocks of data for the lagging left-turn phasing sequence. Each block of data represents the average condition for 15-minutes of data, and corresponds to one data point in the delay analyses presented later in this chapter. A complete copy of leading and lagging left-turn data sets are presented in Appendix B.

Signal Timing Data. Signal timing characteristics observed during the field study included a range of cycle lengths from 90 to 180 seconds. As illustrated in Figure 5, the majority of the data (19 hours or 76 percent) were collected for off peak cycle lengths of 90 and 100 seconds. The remaining 6 hours of data (24 percent) were collected during the peak periods at cycle lengths ranging from 150 to 180 seconds. Thus, although most of the data were collected at the shorter cycle lengths, the entire data set represents a wide range of cycle lengths.

Green times for protected and permitted left-turn phases during each of the study periods are presented in Table 3. As illustrated, green times for the protected portion of the leading left-turn phase sequence ranged from 10.5 seconds at Coit Road during the off peak time period to 28 seconds at Plano Road during the am peak time period. Green times for the permitted portion of the leading left-turn phase sequence ranged from 26 seconds at Mockingbird Lane to 73 seconds at Coit Road. Green times for the protected portion of the lagging left-turn phase sequence ranged from 11.5 at Coit Road to 17 seconds at Mockingbird Lane, and green times for the permitted portion of the lagging left-turn phase sequence ranged from 28 seconds at Mockingbird Lane to 83 seconds at Coit Road.

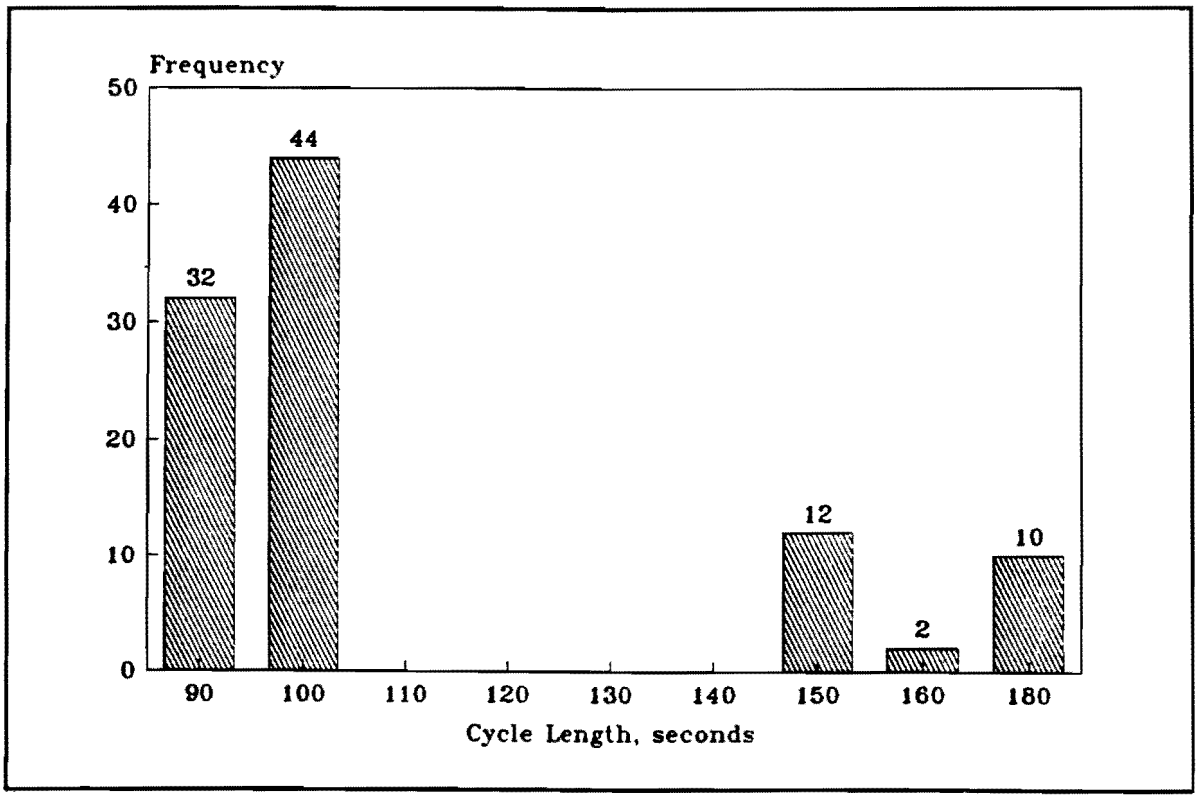

Figure 5: Cycle Length Frequency

Table 3: Cycle Lengths and Green Times for Each Study Period

Intersection	Time	Cycle	Lead Dir	Leading		Lagging	
				Prot	Perm	Prot	Perm
Mockingbird	Peak (7-9)	-	-	-	-	-	-
	Off-Peak (10-12)	100	WB	15	26	13	28
	Off-Peak (1-3)	100	WB	15	26	13	28
	Peak (4-4:30)	150	EB	20	48	17	51
	(4:30-6)	150	EB	26	47	16	57
Garland	Peak (7-9)	-	-	-	-	-	-
	Off-Peak (10-12)	100	SB	13	43.5	20	36.5
	Off-peak (1-3)	100	SB	13	43.5	20	36.5
	Peak (4-6)	-	-	-	-	-	-
Coit	Peak (7-9)	-	-	-	-	-	-
	OFF-Peak (10-12)	90	NB	10.5	39	11.5	38
	Off-Peak (1-3)	90	NB	10.5	39	11.5	38
	Peak (4-6)	180	NB	27.5	73	17.5	83
Plano	Peak (7-9)	160	SB	28	47	-	-
	Off-peak (10-12)	90	SB	14	35	-	-
	Off-peak (1-3)	90	SB	14	35	-	-
	Peak (4-6)	-	-	-	-	-	-

Traffic Data.

Turning Movements Counts. The relative frequencies of measured left-turn flow rates are presented in Figure 6. As shown, the majority (63 percent) of observed left-turn flow rates were in the range from 150 to 200 vehicles per hour. The distribution of left-turn flow rates appear to be positively skewed which is not surprising considering the majority of data being collected during the off peak time periods. The actual left-turn flow rates that were measured are listed in Appendix B and ranged from 88 to 332 vehicles per hour.

Opposing traffic flow rates were grouped using cell frequency widths of one-hundred vehicles. The resulting relative frequency distribution is presented in Figure 7 and shows that the majority of the observed opposing flow rates volumes fell within the range of 600 to 1100 vehicles per hour. The actual opposing flow rates that were observed ranged from 191 vehicles per hour per lane at Plano Road to 737 vehicles per hour per lane at Coit Road. Each of the individual observations are listed in Appendix B.

Permitted Left-Turns Percentages. The relative frequencies of the percentage of the total left-turn movements made during the permitted phase are illustrated in Figure 8. This percentage averaged 34 percent with a range from 0 to 79 percent. The majority of the observed permitted left-turn percentages (90 percent) were between 10 and 60 percent of the total left-turn volume. A complete listing of the percentages of total left-turning vehicles within the permitted phase for each location and type of phase sequence are presented in Appendix B.

Lane Distribution. Uneven lane distributions were observed at all of the study locations. Lane distributions on a per cycle basis were measured throughout each study period at both Mockingbird Lane and Coit Road. The inability to use the secondary data collection locations at Garland and Buckner prevented the continuous measurements of lane distribution. At this location sample measurements were obtained from the video data. Measured lane distributions for each location are presented in Appendix C. The range of measured values appear to correlate with the values presented in the HCM.(9)

One area where measured data does not support the HCM deals with the effect of increasing volume to capacity ratios. HCM reports that when the volume-to-capacity ratio of a lane group approaches one, the lanes tend to be more equally utilized. Results of the lane distribution analyses for this research do not support this position. For example, the northbound traffic at Coit Road during the pm peak time period was near capacity and a distinct distribution of traffic was observed. Conversely, at both Coit Road and Mockingbird Lane, an even distribution of traffic across all lanes of traffic was measured during the off peak time periods when traffic was relatively light.

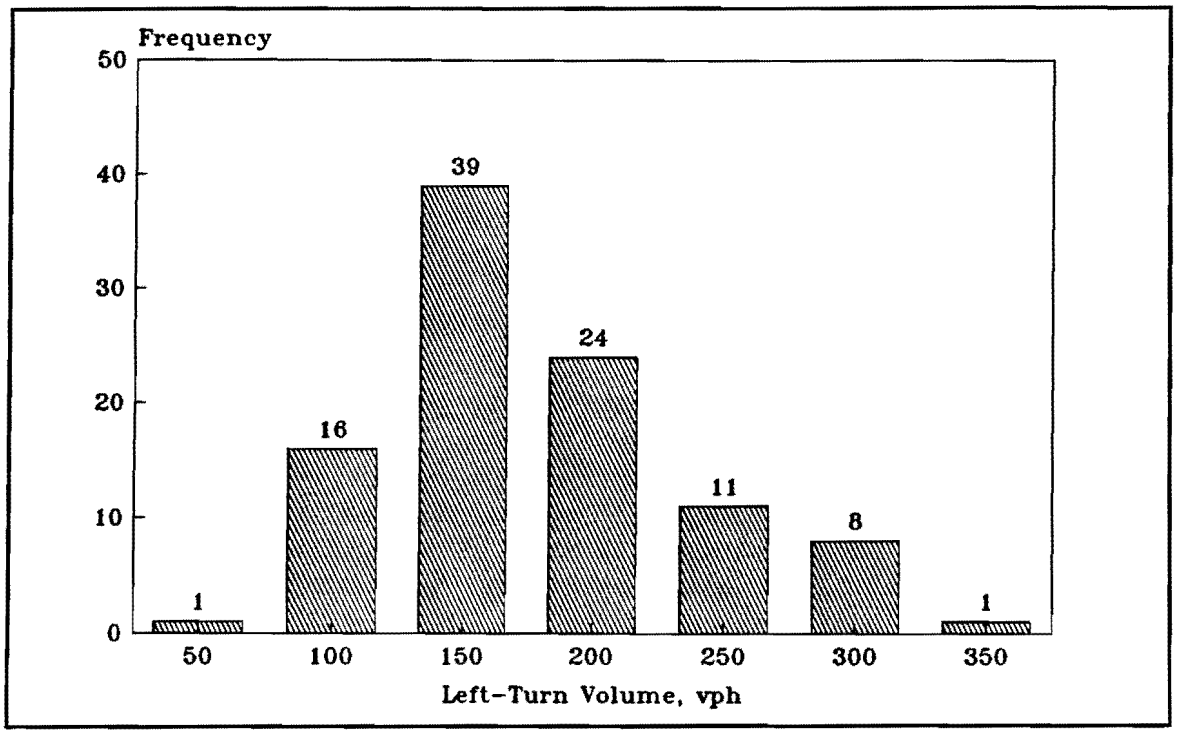

Figure 6: Range of Left-Turn Flow Rates Observed

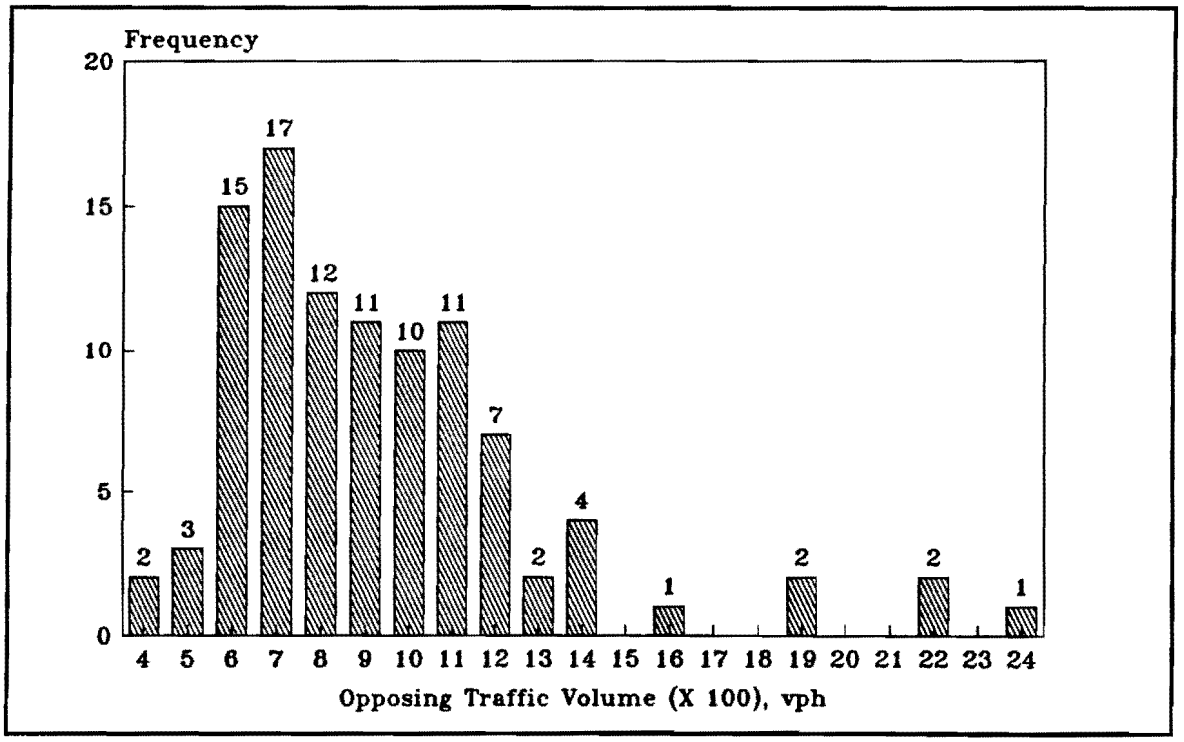

Figure 7: Range of Opposing Traffic Flow Rates Observed

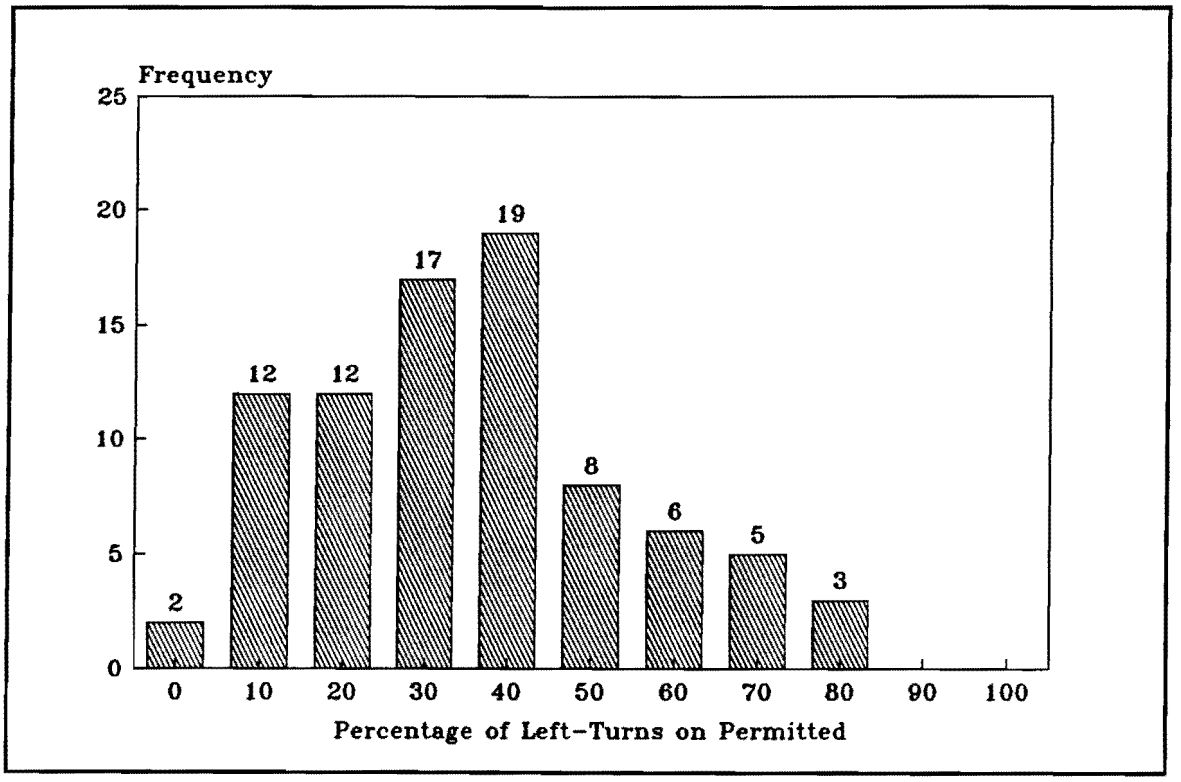

Figure 8: Percentage of Total Left-Turns During the Permitted Phase

Percent Volume Arriving on Green. The percentage of vehicles arriving on green and red were measured for each study approach on a per cycle basis. These measurements were used to account for the effects of progression on the stopped delay values measured in the field. Vehicles were measured as arriving on green if they arrived at the stop line or back of queue during the time the through signal indication was green. Conversely, vehicles were counted as arriving on red if they arrived at the stop line, or back of queue during the time the through signal indication was red. This procedure did not attempt to differentiate between the arrivals during the protected and permitted left-turn phases.

The volumes arriving on green and red were used to calculate vehicle arrival rates on both the green and red phases. Calculation of arrival rates for red and green depended upon the number of vehicles per hour, the percentage of the volume on red or green, and the amount of red or green time available per hour. The per cycle percentages were aggregated into fifteen minute intervals and the resultant 15-minute averages are presented in Appendix B. Relative frequency distributions for the percentage of left-turn and opposing traffic arriving on green are grouped and presented in Figure 9. The percentage of vehicles arriving on green for the two types of movements are almost identical because the adjacent traffic for one left-turn movement is the opposing traffic for the opposing left-turn movement.

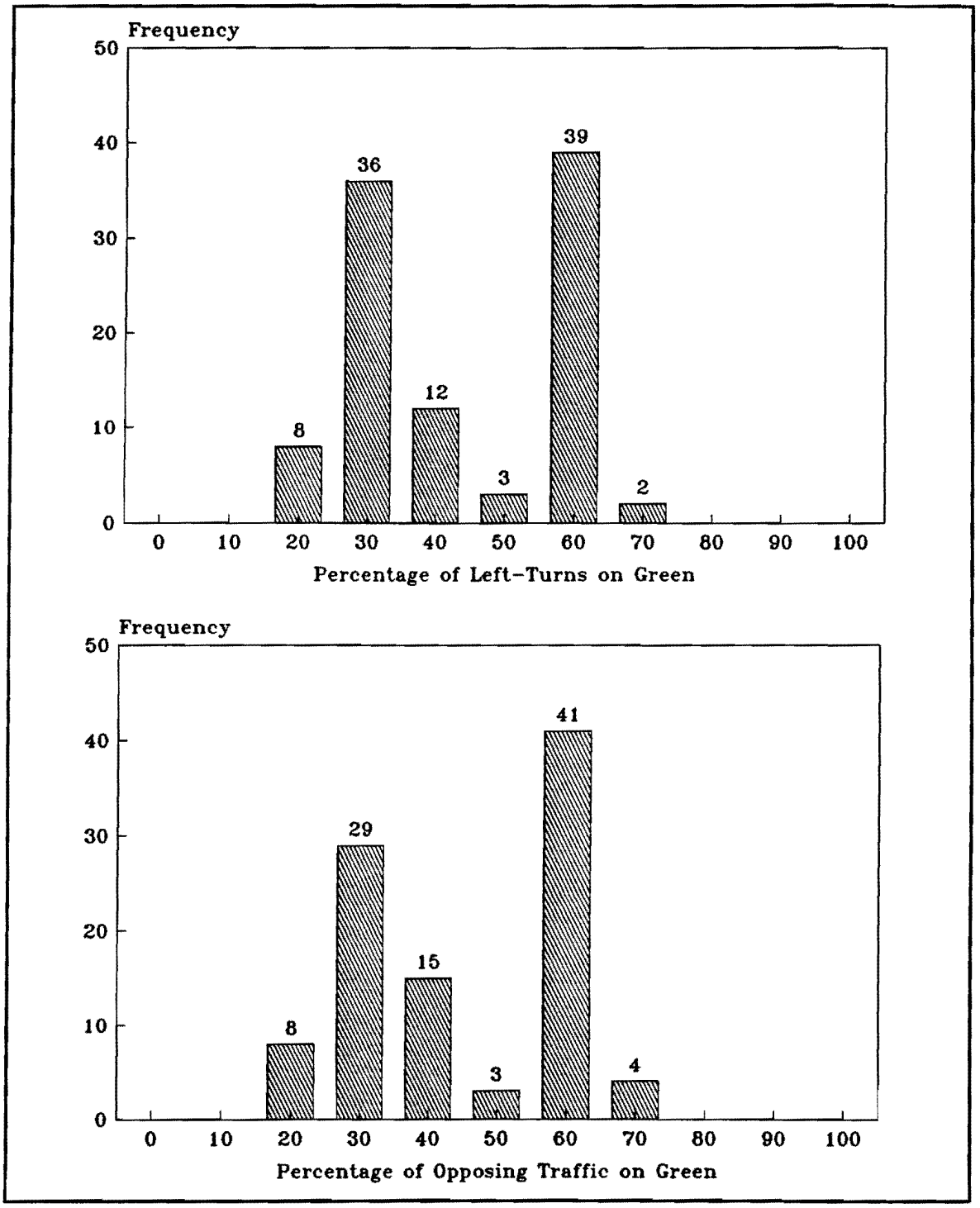

Figure 9: Percentage Volume Arriving on Green

Saturation Flow Data

Saturation Flow Rates. Saturation flow headways for at least two time periods were collected at each of the study locations. During several of the off peak periods studied, low traffic volumes resulted in very few queue lengths in excess of four vehicles which is the minimum queue size recommended by the HCM, to account for start-up lost time.(4) This requirement resulted in several very small sample sizes being collected during some of the off peak periods. Saturation flow data at each study location were collected for both study directions using the video data that was available.

Detailed results of the saturation flow rate analysis for each location are presented in Appendix C. At each location the saturation flow rate measured for the peak direction of travel appeared to be higher that the saturation flow rate for the off peak direction of travel. This observation led to a detailed analysis of the effects of the peak direction of travel on the saturation flow rate. The results of these analyses, which are presented in Appendix D, revealed that the observed differences were not statistically significant.

The combined saturation flow rate measurements appear to be normally distributed, see Figure 10. Measured saturation flow rates ranged from a low of 1610 vehicles per hour per lane at Garland Road to a high of 2126 vehicles per hour per lane at Coit Road. The average saturation flow rate for all of the locations combined was 1910 vehicles per hour per lane. This number is significantly higher than the 1800 vehicles per hour per lane recommended by the HCM.(4)

Vehicle Classification. Vehicle classification counts were performed to determine the percentage of heavy vehicles in the traffic stream. Actual fifteen minute measurements were used to adjust the saturation flow rate for each block of data. The HCM recommends the use of two (2) percent heavy vehicles if the actual distribution is not known.(4) Based upon the data collected for this study, the recommended value of two (2) percent heavy vehicles should result in a conservative estimate for most time periods.

With peak period traffic, however, it would seem that a more appropriate value would be one (1) percent heavy vehicles. This value seems to be justified with the limited amount of peak period data collected. This value also seems logical because during the peak periods the volume of passenger cars is expected to increase and the number of heavy vehicles should remain constant.

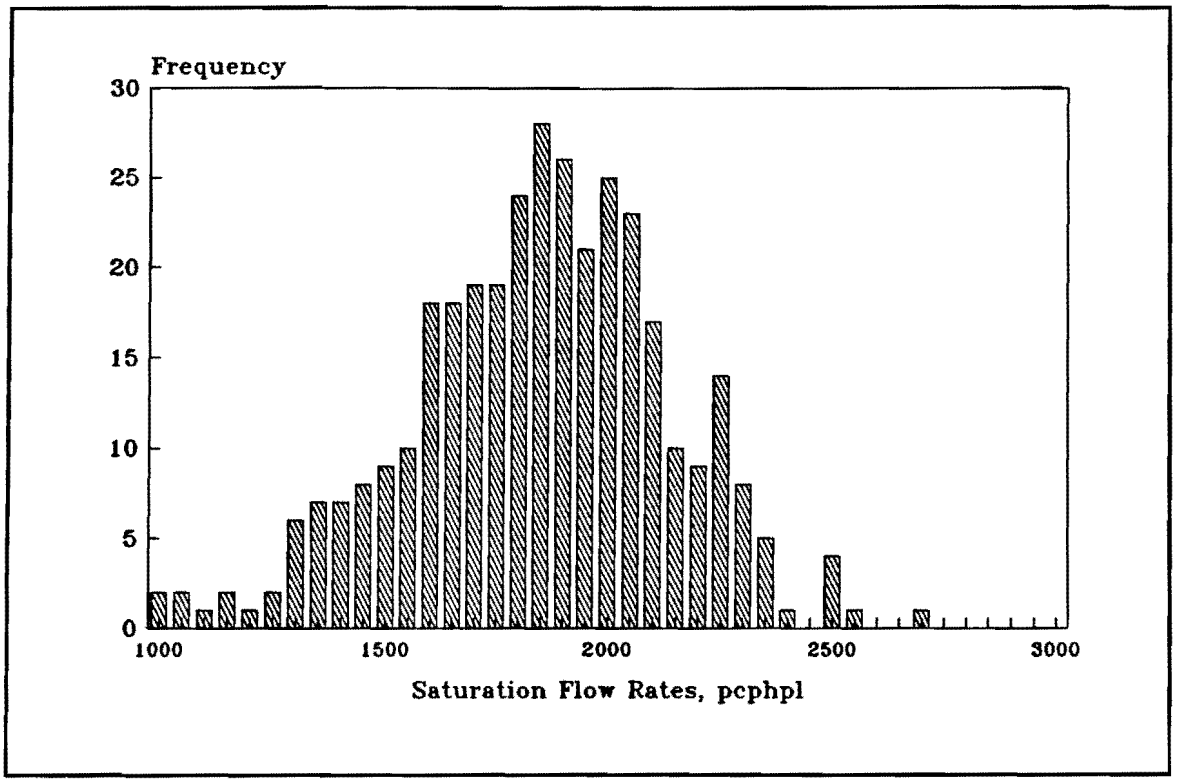

Figure 10: Measured Saturation Flow Rates

Left-Turn Data

Critical Gaps. Critical gap data for permissive left-turns through opposing traffic were collected for three of the intersections studied. Critical gap measurements were made at Mockingbird Lane, Garland Road, and Coit Road. To simplify the data collection process, the critical gap was determined from the critical headway. Headway measurements were collected for vehicles which make permissive left-turns after first rejecting at least one gap. In the subsequent critical gap analysis, the largest headway rejected by the driver was paired with the headway eventually accepted by the driver. Relative cumulative frequencies for both the accepted and the rejected headways were developed from this data. Cell frequencies were calculated using one-half second increments. As shown in Table 4, very small differences between the mean observed headways of the Mockingbird, Garland, and Coit data were detected.

In order to use the paired headways to determine the critical headways, plots containing the relative cumulative frequencies of the rejected and the one minus the accepted headways were developed. A graphical curve fitting process was used to determine the best fit curves for the data. Attempts to fit the Erlang, negative exponential, shifted negative exponential, and lognormal distributions to the relative cumulative frequency data produced unsatisfactory results, in that, none of the distributions consistently fit the data at a 95 percent level of confidence. Goodness-of-fit was measured using the Chi-squared test.

Table 4: Accepted and Rejected Headway Analysis

Location	Accepted Headways		Rejected Headways	
	Mean	Standard Deviation	Mean	Standard Deviation
Mockingbird	8.73	4.38	3.63	2.14
Garland	8.96	4.31	3.48	2.16
Coit	8.87	4.70	3.86	2.46
All Sites	8.85	4.48	3.66	3.27

In order to actually determine the critical headway, which in turn would yield the critical gap, the paired data points (i.e., paired data being the largest rejected and the accepted headways for each left-turning vehicle) were plotted as cumulative frequency distributions. These plots were generated for headways between zero and ten seconds. The ten second range was selected to provide more detail in the expected area of interest. The length of headway at the intersection of the two distributions is the headway which fifty percent of the drivers will accept as suitable to safely make a permitted left-turn. This measurement is defined as the critical headway.

Critical headways, determined by the graphical curve fitting process for each individual location, and all the locations combined are presented in Table 5 and Figure 11. Individual figures are presented in Appendix D for Mockingbird Lane, Garland Road, and Coit Road. The critical headway values for all three locations combined was 5.4 seconds. Critical headways for the individual locations ranged from 5.3 seconds at Coit Road to 5.6 seconds at Garland Road.

By using an average speed of 40 mph and assuming an average car length of 20 feet, critical gaps were determined from the measured critical headways. As shown in Table 5, the combined headway from all sites resulted in a average critical gap of 5.1 seconds with a range from 5.0 seconds to 5.3 seconds. All of the individual measurements were within the limits of 3.8 to 5.8 seconds presented in the literature. Fambro et al., used cumulative accepted and rejected gaps to determine a critical gap of 4.5 seconds.(6) This value was developed from data collected at three two-lane intersections operating with permitted-only phasing.

Lin et al, recommended a critical headway of 5.4 seconds. The researchers, using an average speed of 30 mph and an assumed average length of 20 feet, determined that a critical headway of 5.4 seconds was equivalent to a critical gap of 5.0 seconds.(7) These values were developed from data collected with simulation research. It should be noted that these researchers also relied on a graphical fit of the accepted and rejected headway data.

Table 5: Critical Gap Analysis

Location	Critical Headway (sec)	Number of Paired Headways	Critical Gap (sec)
Mockingbird	5.5	112	5.2
Garland	5.6	118	5.3
Coit	5.3	129	5.0
All Sites	5.4	359	5.1

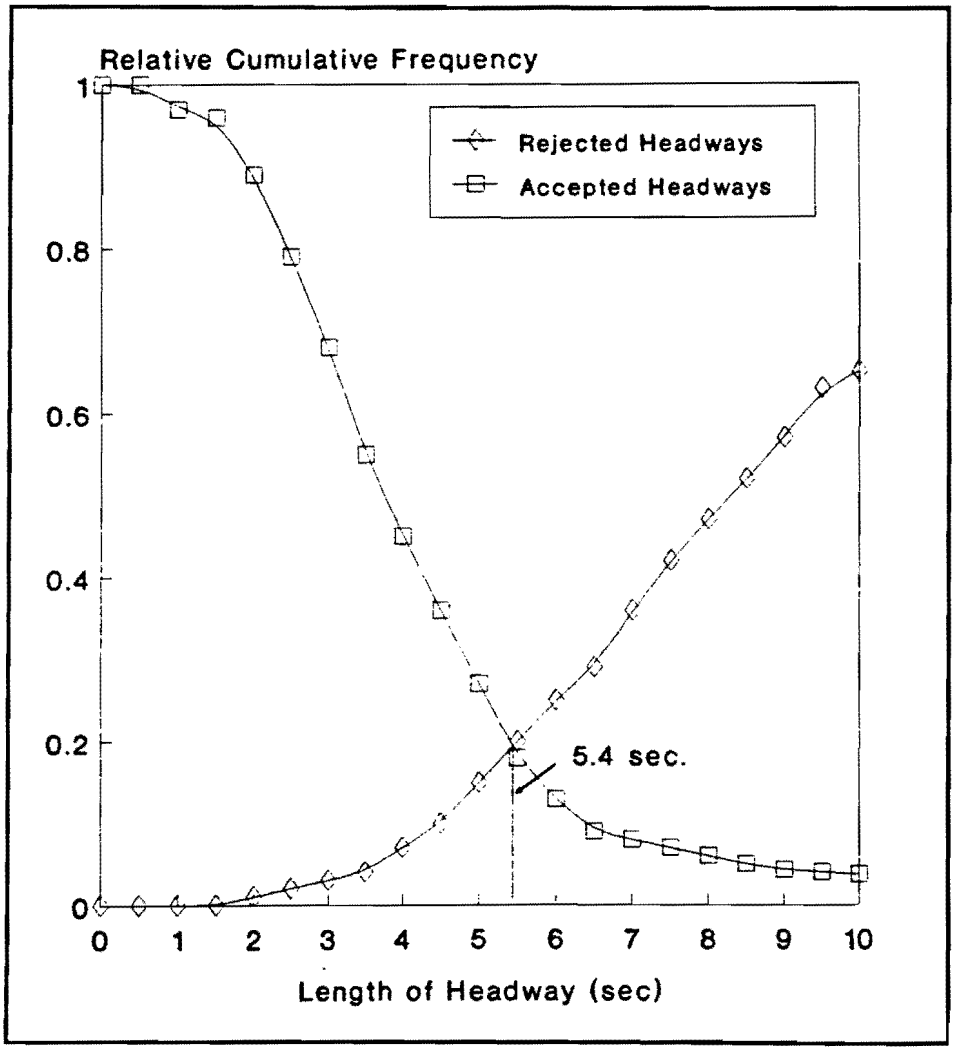

Figure 11: Critical Headway Analysis - All Locations Combined

Headway data were analyzed to determine if any of the study locations produced significantly different accepted and rejected headways. This procedure was used to determine if driver behavior was significantly different between different locations and different traffic flow conditions. Accepted and rejected headways for leading and lagging left-turns were compared to determine whether or not drivers required a different critical gap for lagging protected-permitted left-turns than for leading protected-permitted left-turns.

Scheffe's multiple comparison procedure was used in all of the comparisons, however, no between site differences were identified. Scheffe's procedure was also used to check for differences by groups in the following: number of lanes, time of day, and left-turn phase sequence. All comparisons were performed at a 95 percent level of confidence. Some differences were identified by making pair-wise comparisons of leading versus lagging and peak versus off peak data at Mockingbird Lane.

This difference was attributed to an extremely small off peak leading left-turn data set. At this location, it is hypothesized that the off peak data were biased by the lack of an adequate sample of the driving population. Left-turn volumes at the intersection during the off peak periods were light, such that several vehicles did not use the same gap. Results of the comparative analysis are presented in Appendix D.

Turning Headways. Data were collected for two and three opposing lanes at two locations. Mockingbird Lane was used to collect two lane turning headway data. Three lane data turning headway data was collected at Coit Road. Small samples of data collected with the electronic data collection system were used in this analysis. In order to collect this data, a queue of left-turning vehicles had to be present, suitable gaps in the opposing traffic stream also had to exist so that at least two vehicles could turn consecutively. During the permissive phase, left-turn vehicles were marked whenever they crossed the curb line at the end of the permitted left-turn. Measurements were recorded for vehicles which were in a standing queue when the permissive gap occurred. Left-turn headways from the data collected at Mockingbird Lane and Coit Road were used in the analysis. Data from Garland Road was discarded because of the poor location of the video data collection equipment.

The measured values appear to correlate with other studies reported in the literature. The average left-turn headways measured at Mockingbird Lane were equal for both directions of travel, see Table 6. A directional difference was detected in the Coit Road and Arapaho Road data, however, the difference is unexplained. The Mockingbird Lane measurements are low, but are near the shortest headways reported by Messer and Fambro.(6) The values reported by Messer and Fambro were collected for two-lane arterials with separate left-turn lanes and permitted-only phasing. This research appears to substantiate the results from previous field studies, but does not substantiate the results of simulation research reported by Lin et al (7).

Table 6: Left-Turn Headway Data

	Sample Size	Mean Left-turn Headway (sec)
Two Opposing Lanes		
Mockingbird Westbound	52	2.24
Mockingbird Eastbound	61	2.24
Mockingbird All	113	2.24
Three Opposing Lanes		
Coit Northbound	46	2.36
Coit Southbound	69	2.71
Coit All	115	2.57

Scheffe's multiple comparison procedure was used to compare the leading and lagging left-turn headways for the two locations. This analysis found no significant difference in turning headways between the leading 3-lane, lagging 3-lane, leading 2-lane, and lagging 2-lane data.

Sneakers. Sneakers, or the number of left-turns made during the clearance interval were measured at Mockingbird Lane, Garland Road, and Coit Road. At Mockingbird Lane, the am peak time period was used as the study period. The pm peak time period was used at Coit Road. Sneaker counts for Garland Road were made during the off peak time periods. For reference, the directions for which the sneaker counts were made were the peak direction of travel at Mockingbird Lane and also at Coit Road.

The number of sneakers that were observed ranged from zero to three sneakers per cycle with most of the observations (73 percent) in the zero and one sneaker per cycle categories. As shown in Table 7, the average number of sneakers was approximately one per cycle. These findings are significantly different from those presented in the literature. The HCM recommends that the minimum protected-permitted capacity (or number of sneakers) is two per cycle.

Table 7: Average Number of Left-Turn Sneakers

Location	Sample Size	Average Number of Sneakers	Standard Deviation
Mockingbird	50	0.82	0.86
Garland	26	1.04	0.90
Coit	23	0.83	0.76
All Locations	99	0.88	0.86

It is possible that the two sneakers per cycle was developed from the fact that adequate time may exist for two vehicles per cycle to turn during the clearance. If drivers were forced to wait for a long period of time, they might actually utilize the extra time during the clearance interval or that the two per cycle was developed for intersections without any protected left-turn phasing. At these intersections, left-turn drivers will probably incur more delay and as a result, may use the clearance time more effectively. Results from this study indicate that the average number of sneakers for protected-permitted phasing may be less than the average of sneakers for permitted-only phasing.

Operational Data (Stopped Delay)

Stopped delay measurements were made for each location and time period for which the left-turn queues did not experience overflow delay. Overflow delay occurred when the left-turn or adjacent through queues became so long that an observer could not distinguish between the left-turn and adjacent through vehicles. This situation occurred in the peak direction during the pm peak time period at both Coit Road and also at Garland Road. In these instances, it became impossible to accurately measure the stopped delay of left-turning vehicles.

A broad range of stopped delay observations were collected. As shown in Table 8, the measured delay ranged from a low of 7.4 seconds per vehicle to a high of 79.6 seconds per vehicle. The average and median measurements were 32.2 and 27.8 seconds per vehicle, respectively. The frequency distribution of the measured delay is presented in Figure 12. As illustrated, the majority of the observations (77 percent) ranged from 15 to 40 seconds per vehicle.

Table 8: Observed Left-Turn Delay Measurements

	Leading	Lagging
Range	7.7 to 74.7	16.0 to 79.6
Average	16.0	36.3
Median	25.0	32.5

* Note: All delay measurements reported in units of seconds per vehicle.

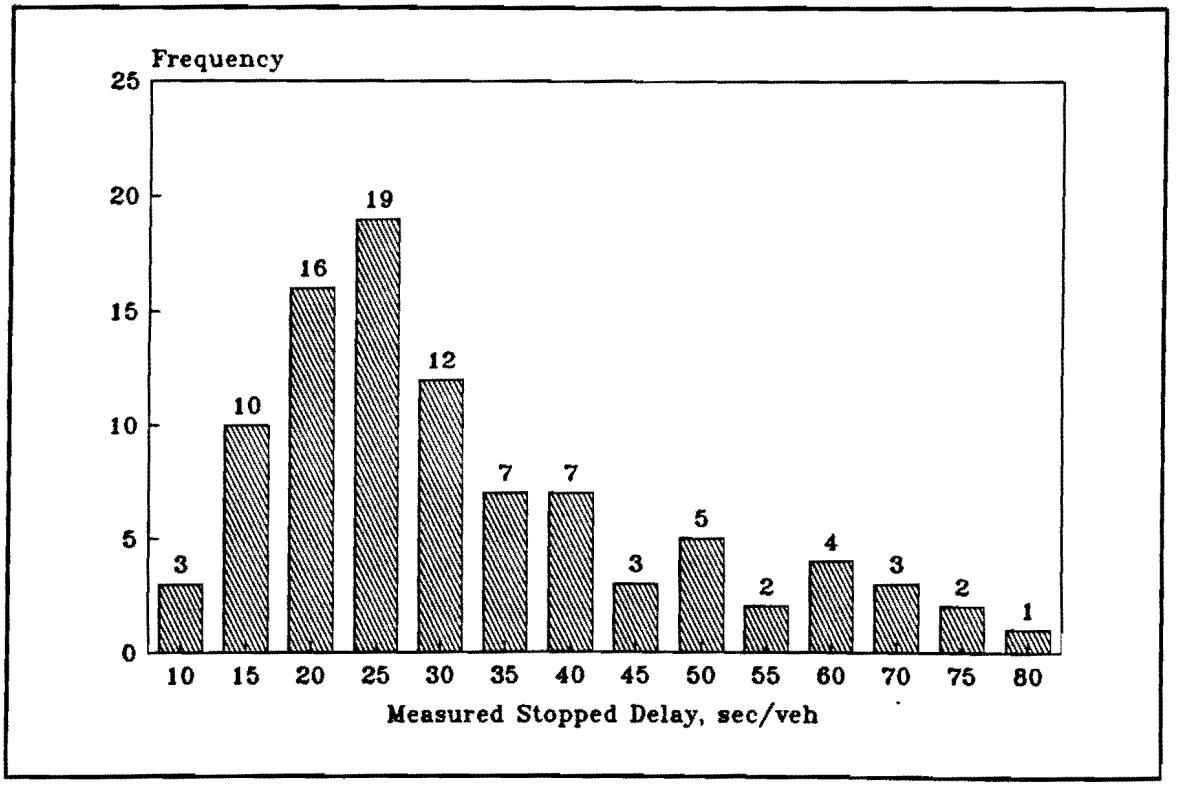

Figure 12: Range of Left-Turn Delays Observed

An analysis of the delay observations based on phasing sequence seems to provide support of research by Hagen and Courage (12), who noted that the delay values for a lagging-protected-permitted left-turn would be higher than the delay experienced by a leading protected-permitted left-turn, when all other factors remain constant. Figure 13 provides support for this statement presenting the results of regression analyses of measured delay on the independent variable volume-to-capacity ratio. As indicated by the slopes of the slopes of the regression lines, leading protected-permitted left-turns do seem to experience less delay than lagging protected-permitted left-turns.

Model Calibration

Before the conceptual models could be used for a comparison with the field data, it was first validated with an established model -- PASSER II. The PASSER II-90 program, the latest version of the SDHPT's *Progression Analysis Signal System Evaluation Routine* was selected because it also relies on queue-departure theory for delay calculation.

The leading and lagging predictive models were both compared to the delay values predicted by the PASSER II-90 program. In order to compare to PASSER II delay calculations with those of the conceptual models, vehicle arrival rates were assumed to be uniform throughout the cycle. Since the conceptual model calculates delay for only cycle, the number of sneakers in the PASSER II program was set to zero. This change was accomplished by circumventing the program's menu system and error checking routine by modifying the data set directly with an ASCI text editor.

Due to minor differences in modelling methodology, such as the amount and location of lost-time, the conceptual models were validated using a two part process. The first part consisted of validation of the protected portion of the left-turn phase. This is the simplest segment of the left-turn modelling process, in that it follows the modelling process which would also be used for predicting through traffic delay. The more complex issue of modelling protected and permitted left-turns in the same cycle was addressed in the second part of the validation process. The results of these validation processes are described in more detail in the following sections.

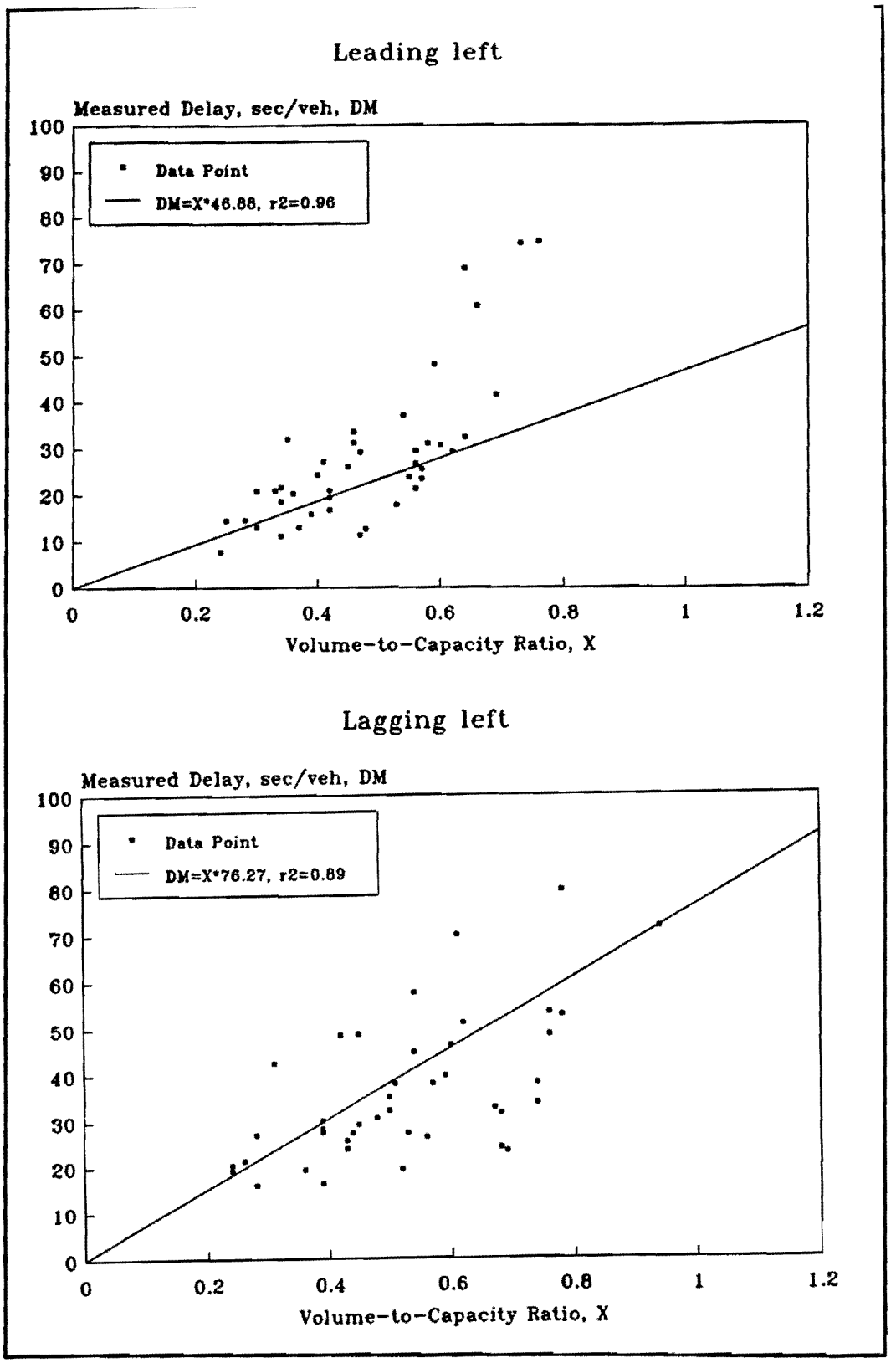

Figure 13: Regression Analysis of Measured and Predicted Delay

Model Validation

Delay values for protected-only left-turns were predicted using the PASSER II program and the conceptual model for a range of left-turning volumes. In order to model protected-only left-turns with the conceptual model, the length of the permitted phase, and input, was set to zero. All model parameters remained constant between the PASSER II and conceptual model for each left-turn volume condition. A plot of the predicted volume-to-capacity ratios and stopped delay values from PASSER II and the conceptual model indicated close agreement between the two methodologies, and it was decided to proceed to Step 2.

The protected-permitted validation also was conducted over a range of left-turn and opposing through traffic volumes. One comparison was performed for the leading left-turn phase sequence and another was performed for the lagging left-turn phase sequence. The opposing traffic volume was maintained at a constant rate throughout the analysis process. The results of the leading and lagging left-turn phase comparisons are presented in Figures 14.

As illustrated by the symbols used to identify the PASSER II and conceptual model data points, the two models are predicting slightly different volume-to-capacity ratios for the different left-turn volume conditions. The delay values predicted by the two models, however, are approximately equal. Following the previously mentioned work of Hagen and Courage (12), the conceptual model also predicts lower delay values for the leading left-turn phase sequence. Based on these results, it was concluded that the conceptual model produces results very similar to the PASSER II program, and it was decided to proceed to Step 3.

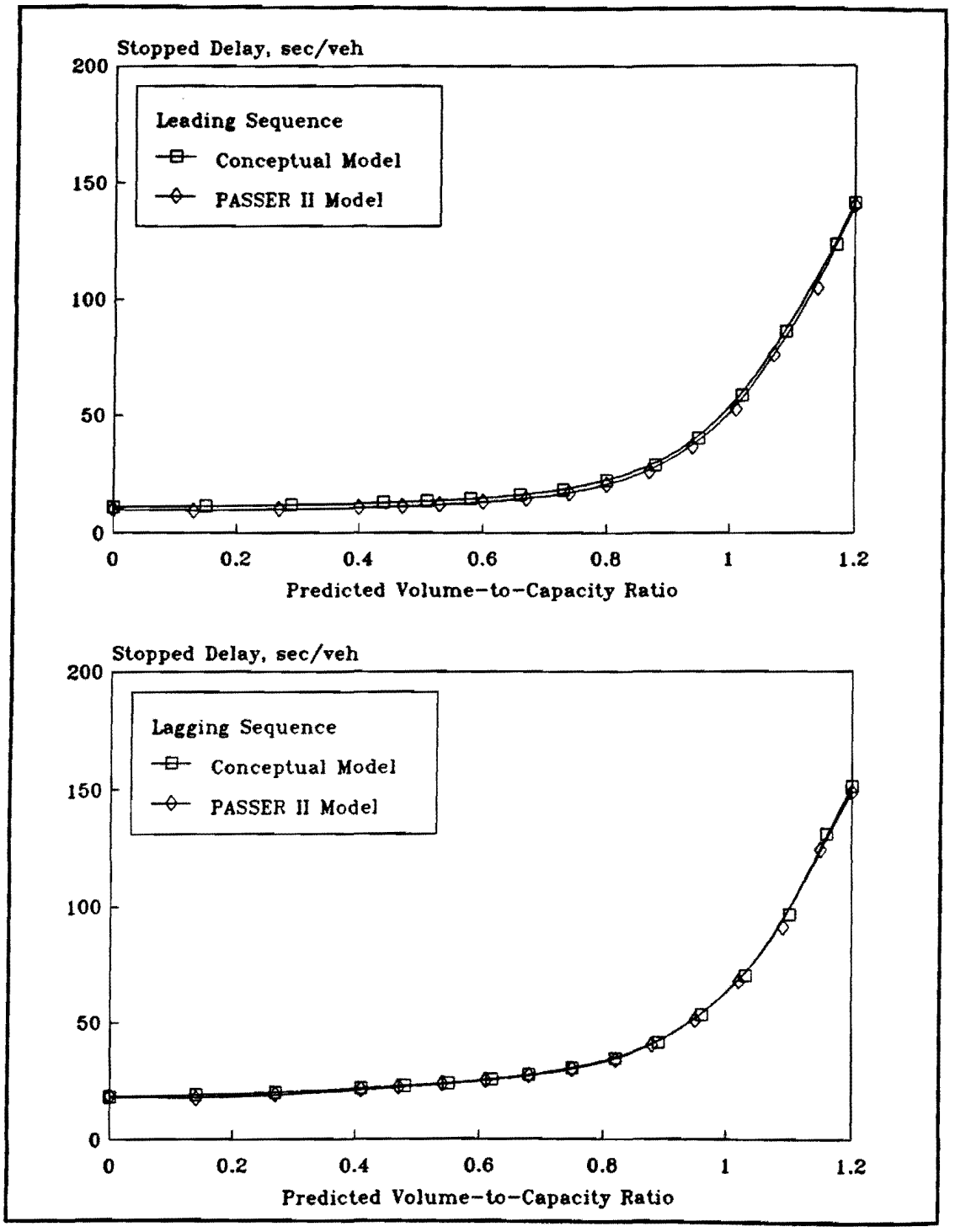

Figure 14: Comparison of Protected-Permitted Delay Values

Uniform Arrivals

After comparing the delay values predicted by the conceptual model with the delay values predicted by the PASSER II program and finding close agreement, a comparison of the predicted and observed stopped delay values was performed. Signal timing and traffic data corresponding to 94 of the 15-minute blocks of data were used as model inputs. First, the models were used to predict delay based in the assumption that vehicle arrival rates were random, or uniformly distributed throughout the cycle. In other words, the effects of progression were ignored. Once delay values had been predicted for both the leading and lagging phase sequences, a comparison between the predicted and measured delay values was made. Data from Mockingbird Lane, Garland Road, and Coit Road were included in the analysis.

As illustrated in Table 9 and Figure 15, the conceptual model does not accurately predict delay at a 95 percent level of confidence. In each case, the regression analysis reveals that the predicted results do not accurately reflect the measured value; i.e., the parameter estimate for the slope of the regression line is significantly less than 1.0 It was hypothesized that the effects of progression could be the cause of this lack of prediction capability. In order to test this hypothesis, arrival rates during the green and red phases for the left-turn and opposing through movements were included in the calculation procedure. Results of the analysis of progressed arrivals are presented in the next section.

Table 9: Delay Analysis - Uniform Arrivals

Phase Sequence	Degrees of Freedom	Parameter Estimate β	Standard Error s_e	t for Ho: $\beta = 1$	$t_{\alpha/2,df}$	Ho: $\beta = 1$	Level of Significance
Leading	38	0.5872	0.0370	-11.1464	2.025	Reject	< 0.001
Lagging	14	0.6995	0.0338	-8.8788	2.021	Reject	< 0.001

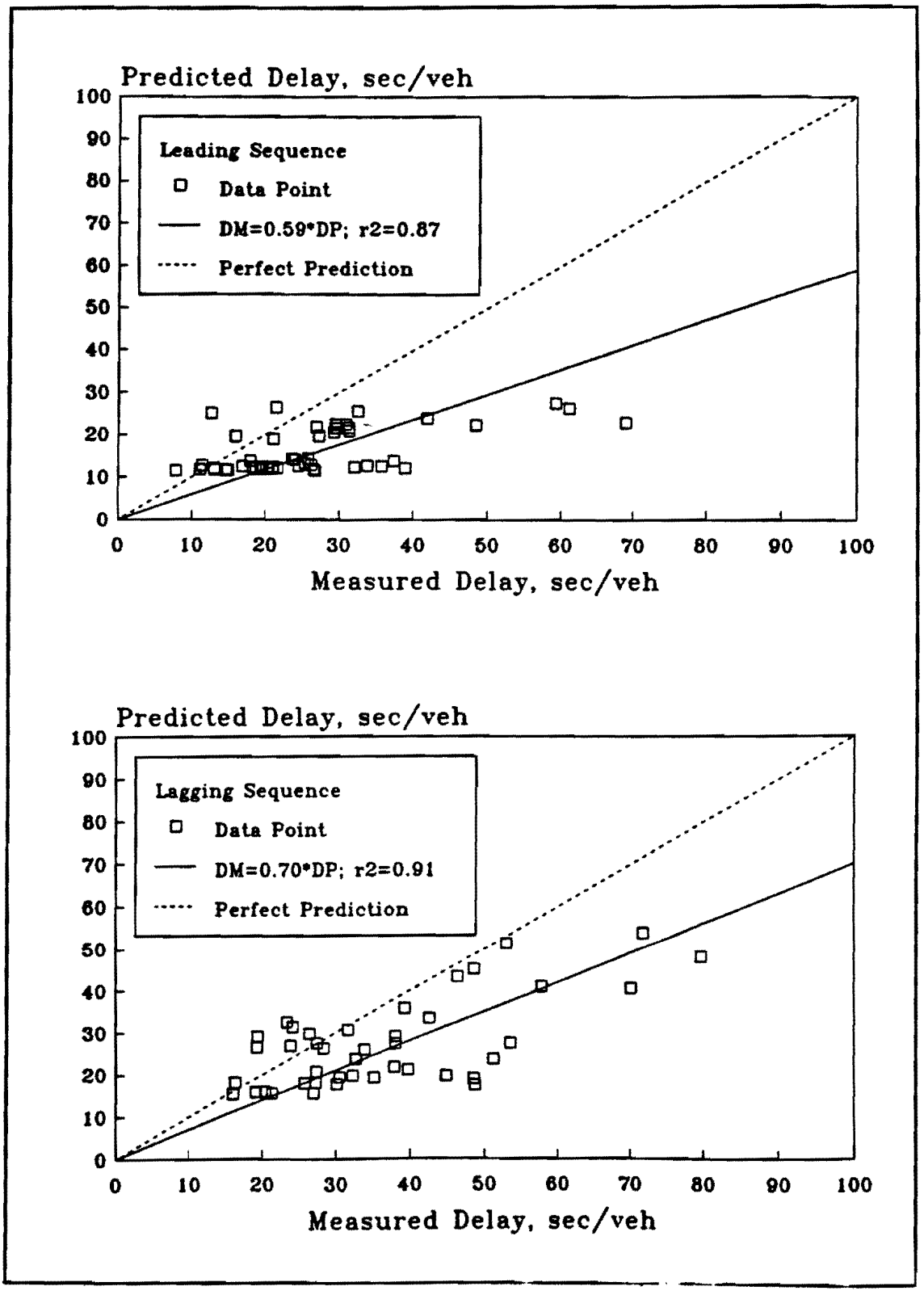

Figure 15: Delay Analysis - Uniform Arrivals

Progressed Arrivals

Progression effects (i.e., proportion of the total volume arriving on green) were included in the conceptual models and an analysis of the predicted and measured delay values was performed. As before, the data were separated by phase sequence. The results of these regression analysis are presented in tabular form in Table 10 and graphically in Figures 16.

As illustrated by the results presented in Table 10, the inclusion of an estimate of the quality of progression greatly improves the estimation capabilities of the conceptual models. Based on these results, it can be stated that the conceptual model accurately predicts delay for the lagging left-turn phase sequence, but does not accurately predict delay for the lagging left-turn sequence. A comparison of Table 9 and Figure 15 to Table 10 and Figure 16, however, shows that when the effects of progression are included in the calculation procedure, the model does a much better job of predicting delay. For example, the addition of the effects of progression for the leading protected left-turn sequence changes the slope of the regression line from 0.59 to 0.77.

Based on these results, the conceptual model can predict delay accurately for the lagging left-turn sequence when the effects of progression are included in the calculation procedures. The conceptual model does not, however, accurately predict delay for the leading left-turn sequence, although it does a better job of predicting delay for this sequence when the effects of progression are included in the calculation procedure.

Table 10: Delay Analysis - Progressed Arrivals

v/c	Degrees of Freedom	Parameter Estimate β	Standard Error s_e	t for Ho: $\beta = 1$	$t_{\alpha/2,df}$	Ho: $\beta = 1$	Level of Significance
Leading	38	0.7675	0.0491	-4.7328	2.025	Reject	< 0.001
Lagging	41	0.9767	0.0419	-0.5565	2.021	Accept	> 0.10

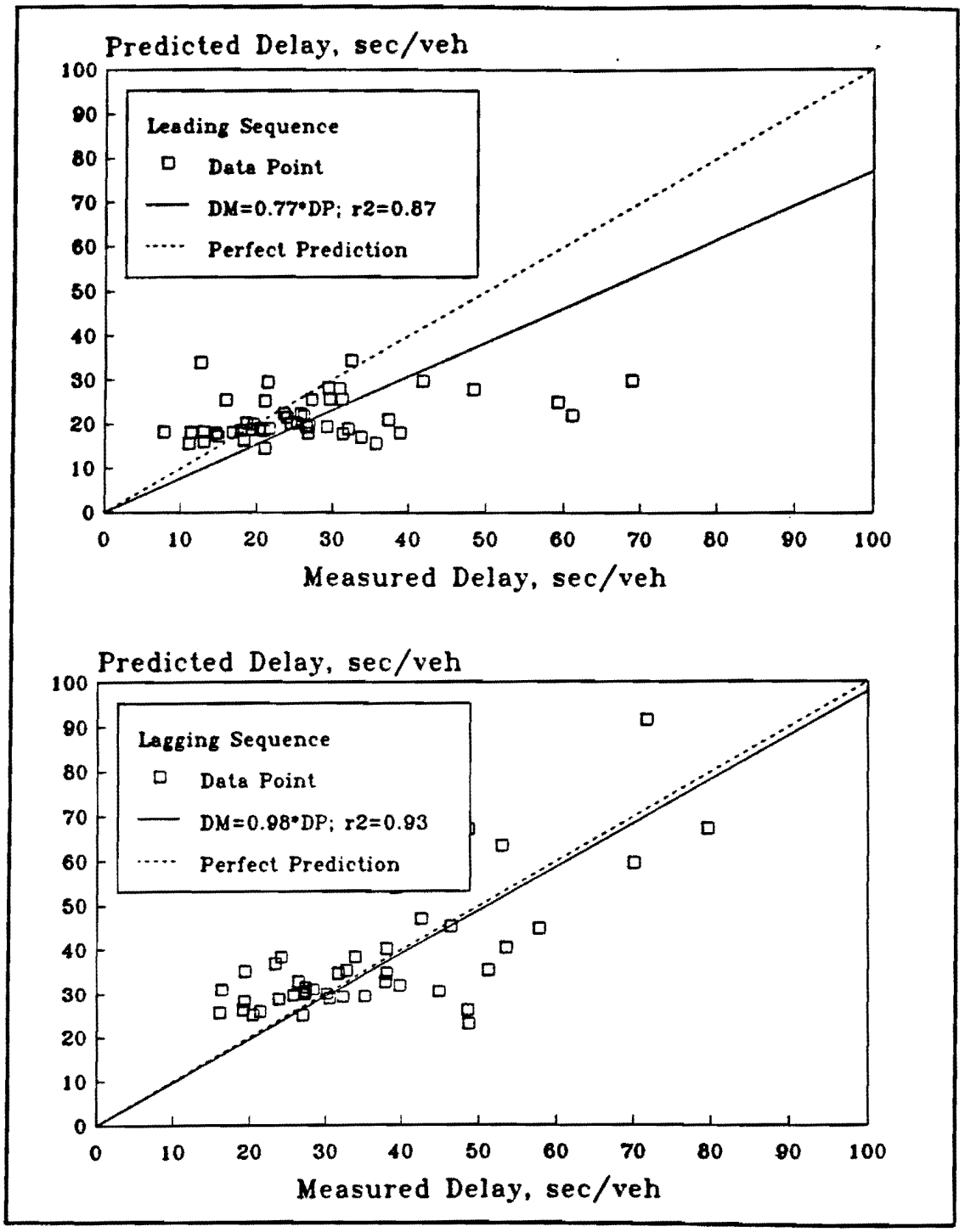

Figure 16: Delay Analysis - Progressed Arrivals

Early and Late Arrivals

Research reported by Fambro et al(20), indicates that the effects of progression on delay extend even farther than the simple inclusion of the proportion of vehicles arriving on green. The researchers concluded that the inclusion of the proportion of vehicles arriving on green is important, but the flow during the green and red phases needs to be further defined to account for the peaking characteristics of platoons of vehicles.

They noted that delay observations for a given value of the proportion of the total volume arriving on green will be less than predicted delay whenever the front of the platoon of vehicles arrives before the start of green and the rear of the platoon arrives before the start of red (early arrivals). Conversely, the observed delay, for the same value of proportion of the total volume on green, will be greater than the predicted delay whenever the front of the platoon arrives at the end of the green (late arrivals).(20)

The researchers quantified the effect of early and late arrivals and provide factors to be used to adjust predicted delay values to account for early and late arrivals. These factors, 0.85 for early arrivals and 1.30 for late arrivals, are used to adjust predicted delay values to account for the peaking characteristics of platoon flow. If both the front and back of a platoon arrive during the green or red phase, then no adjustment is required, or the factor equals 1.0. The effects of early and late arrivals on the predicted delay values were analyzed to determine if the factors would improve the delay prediction capability of the conceptual model. For the purposes of analysis, the data were again separated by phase sequence, and the adjusted predicted delay values were compared with the observed delay values with regression analyses. The results of the analyses are presented in tabular form in Table 11 and graphically in Figure 17.

Table 11: Delay Analysis - Early and Late Arrivals

v/c	Degrees of Freedom	Parameter Estimate β	Standard Error s_e	t for Ho: $\beta = 1$	$t_{\alpha/2,df}$	Ho: $\beta = 1$	Level of Significance
Leading	38	0.8869	0.0402	-2.8146	2.025	Reject	= 0.004
Lagging	41	1.0404	0.0446	0.9067	2.021	Accept	> 0.10

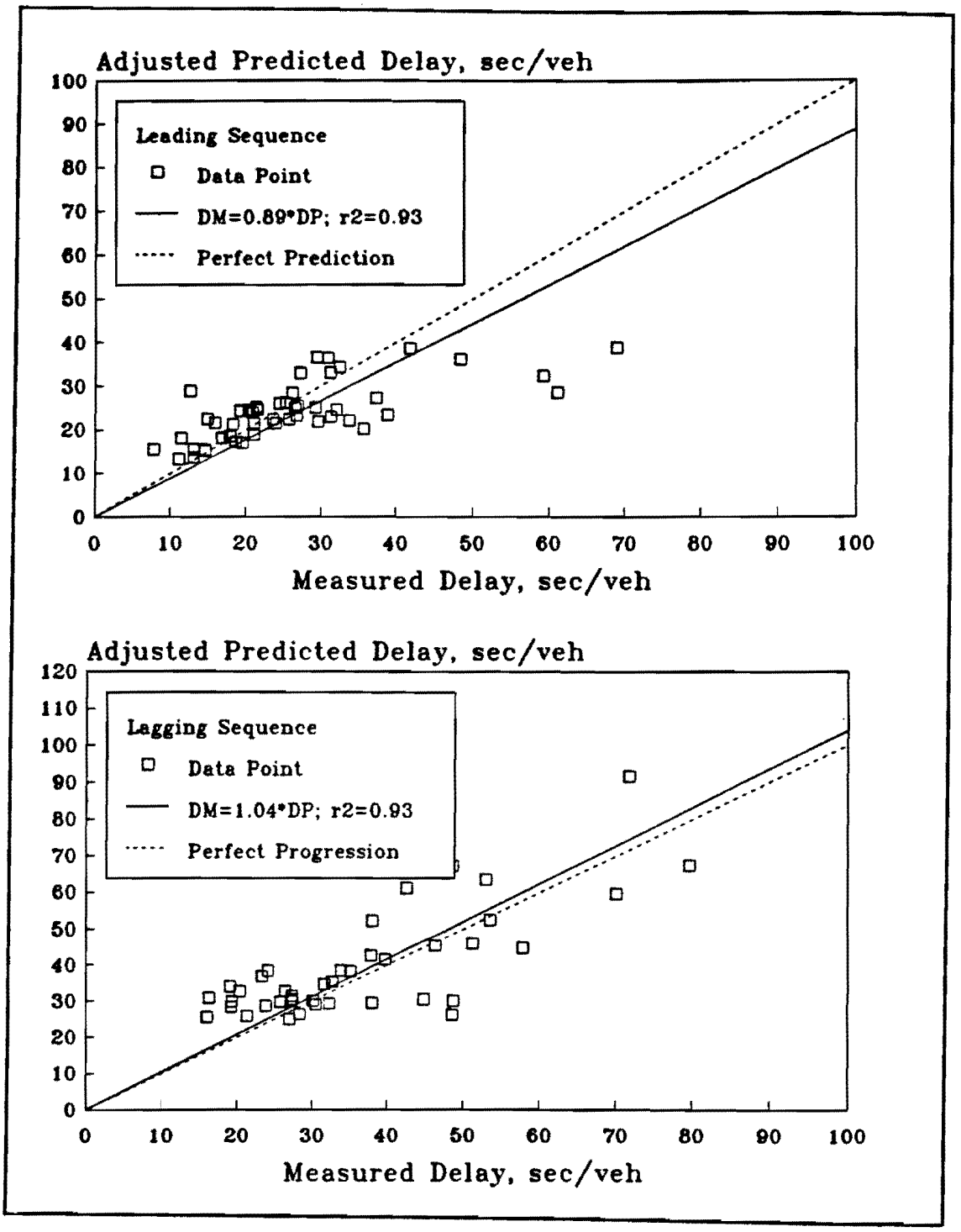

Figure 17: Delay Analysis - Early and Late Arrivals

Based upon these results, the conceptual model continues to accurately predict delay values for the lagging left-turn phase sequence. As illustrated in Tables 11 and 12, the parameter estimate improves from 0.77 to 0.89, but is not statistically equal to 1.0; therefore, the conceptual model does not accurately predict delay for this set of data. Analysis of the error sum of squares for the leading left-turn phase sequence for the progressed arrivals and early and late arrivals reveals that the inclusion of a factor to account for early and late arrivals reduces the error sum of squares; i.e., the model does a better job of predicting delay. This statement is supported by the level of significance reported in Table 11 and in the scatter of data points presented in Figure 17.

Simulation Studies

Study Design. In order to compare the differences between the Dallas and conventional protected-permitted lead-lag left-turn phasing, a wide range of operating conditions was desirable. Two cycle lengths (90 and 120 seconds), three green time to cycle lengths ratios (0.4, 0.5, and 0.6), two types of left-turn phasing (protected only lead-lag left-turns, MUTCD protected-permitted lead-lag left-turns, and Dallas protected-permitted lead-lag left-turns), five left-turn volumes (100 to 300 vehicles per hour in steps of 50), and six opposing through volumes (300 to 800 vehicles per hour per lane in steps of 100) were studied. This design resulted in 360 different combinations of traffic conditions being evaluated by PASSER II. The resultant predicted delays for each of these combinations are contained in Appendix E.

Results. For all conditions evaluated, protected-permitted lead-lag left-turn phasing resulted in less delay than did protected-only lead-lag left-turn phasing. Reductions resulting from the change in phasing ranged from 20 to 50 percent (from 10 to 20 seconds per left-turn vehicle). Interestingly, delay reductions were greater for the left-turn movement with the leading protected phase. For this situation, the protected phase is being used to clear the queue of left-turning vehicles, the first portion of the permitted phase is effectively red because of the dissipation of the opposing queue, and the remainder of the permitted phase is being used to clear the left-turning vehicles that arrived during green. Thus, the protected portion of the phase occurs when the left-turn demand is the heaviest.

For the opposite situation (i.e., lagging protected phase), the first portion of the permitted phase is effectively red because of the dissipation of the opposing queue, the remainder of the permitted phase is being used to clear the waiting queue of left-turning vehicles, and the protected phase is being used to clear the remainder of the queued vehicles and those left-turning vehicles that arrived during green. In this case, the permitted portion of the phase occurs when the left-turn demand is the heaviest.

When comparing the Dallas to MUTCD protected-permitted lead-lag left-turn phasing, the Dallas phasing generally resulted in less delay. There were no conditions for which the Dallas phasing was worse than MUTCD protected-permitted phasing. Reductions in delay resulting from the change to the Dallas phasing range from 10 to 50 percent in most cases. As with the previous comparison, delay reductions were greater for the left-turn movement with the leading protected phase. This difference is a result of the additional time for the permitted movement with the lagging protected phase being added during eh time the opposing queue is dissipating.

V. CONCLUSIONS AND RECOMMENDATIONS

The objectives of this research were to validate that existing left-turn modeling methodology could be used to model the Dallas phasing and to compare the Dallas phasing to conventional or MUTCD protected-permitted left-turn phasing. Predicted and measured left-turn delays were the primary measures used in this comparison. As a result of the findings from of this study, several conclusions and recommendations concerning the Dallas protected-permitted lead-lag left-turn phasing can be drawn. Each of these findings are discussed in the following sections.

Comparison of Dallas and Conventional (MUTCD) Phasing

1. The Dallas protected-permitted lead-lag left-turn phasing resulted in similar behavior by left-turning vehicles when compared to behavior during other types of permitted left-turn phasing; i.e., critical gaps, turning headway, and saturation flow rates were consistent to those reported in the literature.

2. The Dallas protected-permitted lead-lag left-turn phasing results in less delay for both the left-turning and through movements than MUTCD protected-permitted lead-lag left-turn phasing. This saving is slightly higher for the case where the protected phase leads the permitted phase than it is for the case where the protected phase lags the permitted phase.

3. At high volume intersections where protected-permitted left-turn phasing is beneficial from a capacity standpoint, and lead-lag left-turn phasing is necessary from a progression standpoint, Dallas left-turn phasing offers an operationally efficient alternative.

Protected-Permitted Left-Turn Model Parameters

1. The conceptual model developed in this research can accurately model protected-permitted operations. Based on the close agreement between the delays predicted by the conceptual model with those delays predicted by the PASSER II program, it can be stated that the PASSER II program also can accurately model protected-permitted left-turn operations.

2. Several permitted left-turn model parameter values for critical gap, left-turn headway, and number of sneakers were measured and compared to results from previous studies. The parameter values measured in this study should be considered representative for all leading-left, lagging-left, or lead-lag phase

sequences used with protected-permitted left-turn phasing on major arterial streets.

a. Critical gap measurements at Mockingbird Lane, Garland Road, and Coit Road ranged from 5.0 to 5.3 seconds, an average of 5.1 seconds. Analysis of the critical gap data that was collected indicated that the critical gap size was the same for both two and three opposing lanes.

b. Permitted left-turn headway measurements ranged from 2.2 seconds at Mockingbird Lane to 2.7 seconds at Coit Road. The average headway for both sites was 2.5 seconds.

c. Sneaker measurements at Mockingbird Lane, Garland Road, and Coit Road ranged from zero to three sneakers per cycle. The average for the three site was approximately one left-turn sneaker per cycle. It should be noted, however, that when modeling the Dallas phasing, sneakers should only be applied to the leading protected left-turn phase sequence.

3. Leading protected-permitted left-turns, in general, incur less delay than lagging protected-permitted left-turns. This difference is caused by a fundamental difference in the operation of the two phase sequences, as illustrated by the queue departure diagrams that were presented previously. Because of this difference, which has been documented with field data and the PASSER II program, it is recommended that separate modeling procedures be used for leading and lagging left-turn phase sequences.

4. Based on the comparisons of measured and predicted delays for uniform arrivals, progressed arrivals, and early and late arrivals, it is apparent that the effects of progression cannot be ignored when attempting to predict delay at signalized intersections. The quality of progression for left-turning vehicles appears to have a larger impact on delay calculations for protected-permitted left-turns than does the quality of progression for the opposing traffic. This effect is intuitive in that the progression of opposing traffic can only affect permitted left-turns, but the quality of progression of left-turning traffic affects the delay incurred by all left-turning vehicles.

Recommendations

1. Because of its operational benefits, it is recommended that Dallas protected-permitted lead-lag left-turn phasing be considered as a viable phasing alternative for intersections with moderate to high left-turn volumes that also are a part of a coordinated arterial street system. It should be noted,

however, that this study only evaluated the operational benefits of the Dallas phasing. A thorough safety analysis should be performed at all locations where protected-permitted left-turn phasing is being considered.

2. Because leading protected left-turn phase sequences generally result in more capacity and less delay for left-turning vehicles, it is normally advantageous to allow the heavier left-turn movement to lead. This decision, however, is subject to arterial progression considerations and the availability of left-turn storage.

3. It is recommended that the following left-turn model parameter values be used when modeling protected-permitted left-turns on high type arterial streets with two and three opposing lanes.

   a. Critical gap = 5.1 seconds;

   b. Left-turn headway = 2.5 seconds; and

   c. Number of sneakers = 1 per cycle.

4. The quality of progression should always be determined for all traffic movements when modeling traffic flow at signalized intersections. It is recommended that further research be conducted on the effects of the quality of progression of the opposing traffic flow on permitted left-turn capacity.

REFERENCES

1. *Manual on Uniform Traffic Control Devices for Streets and Highways.* Washington D.C.: Federal Highway Administration, U.S. Department of Transportation, 1988.

2. *FM 2818 Left-Turn Study, Protected Only vs. Protected/Permissive Left Turns.* College Station Texas: City of College Station, Traffic Engineering Section, 1988.

3. R. Collins. *A Comparative Analysis of Left-Turn Delay Associated with Two Different Lead Lag Phasing Arrangements*, Masters Thesis, Austin, Texas: The University of Texas at Austin, 1988.

4. *Highway Capacity Manual - 1985.* TRB, Special Report 209, Washington, D.C.: Transportation Research Board, National Research Council, 1985.

5. *Australian Road Capacity Guide: Provisional Introduction and Signalized Intersections,* Australian Research Board, Bulletin 4, 1968.

6. D.B. Fambro, C.J. Messer, and D.A. Anderson. *Estimation of Unprotected Left-Turn Capacity at Signalized Intersections.* Transportation Research Record 644, Washington, D.C.: Transportation Research Board, National Research Council, 1977, pp. 113-119.

7. H.J. Lin, R.B. Machemehl, C.E. Lee, and R. Herman. *Guidelines for Use of Left-Turn Lanes and Signal Phases.* Research Report 258-1, Center for Transportation Research, The University of Texas at Austin, 1984.

8. J.A. Bonneson and P.T. McCoy. *Operational Analysis of Exclusive Left-Turn Lanes with Protected/Permitted Phasing.* Transportation Research Record 1114, Washington, D.C.: Transportation Research Board, National Research Council, 1987, pp. 74-85.

9. D.R. Drew. *Traffic Flow Theory and Control.* New York, New York: McGraw-Hill Publishing Co., 1968.

10. F.V. Webster. *Traffic Signal Settings.* Road Research Technical Paper No. 39, London, England: Her Majesty's Stationary Office, 1958.

11 R. Akcelik. *The Highway Capacity Manual Delay Formula for Signalized Intersections.* ITE Journal. Vol. 58, No. 3, March 1988, pp. 23-27.

12. L.T. Hagen and K.G. Courage. *Comparison of Macroscopic Models for Signalized Intersection Analysis.* Transportation Research Record 1225, Washington, D.C.: Transportation Research Board, National Research Council, 1989, pp. 33-44.

13. F. Lin. *Application of 1985 Highway Capacity Manual for Estimating Delays at Signalized Intersections.* Transportation Research Record 1225, Washington D.C.: Transportation Research Board, National Research Council, 1989, pp. 18-22.

14. E.C.P. Chang and C.J. Messer. *Passer II: A User's Manual,* TTI Research Report 467-3F, College Station, Texas: Texas Transportation Institute, Texas A&M University System, 1988.

15. D.L. Gerlough and M.J. Huber. *Traffic Flow Theory - A Monograph,* TRB, Special Report 165, Washington, D.C.: Transportation Research Board, National Research Council, 1975.

16. W.R. Reilly, C.C. Gardner, and J.H. Kell. *A Technique for Measurement of Delay at Intersections.* Report No. FHWA-RD-76-137, Washington, D.C.: Federal Highway Administration, U.S. Department of Transportation, 1976.

17. N.G. Tsongos and S. Weiner. *Comparison of Day and Night Gap-Acceptance Probabilities.* Public Roads. Vol. 35, 1969.

18. L. Ott. *An Introduction to Statistical Methods and Data Analysis.* Boston, Massachusetts: PWS-Kent Publishing Co., 1988.

19. E.C.P. Chang and C.J. Messer. *Arterial Signal Timing Optimization Using PASSER II-90.* Research Report 467-2F, College Station, Texas: Texas Transportation Institute, Texas A&M University System, June 1991.

20. D.B. Fambro, E.C.P. Chang, and C.J. Messer. *Effects of the Quality of Traffic Signal Progression on Delay.* NCHRP Report 339, Washington, D.C.: Transportation Research Board, National Research Council, December 1990.

APPENDIX A

STUDY SITE DRAWINGS

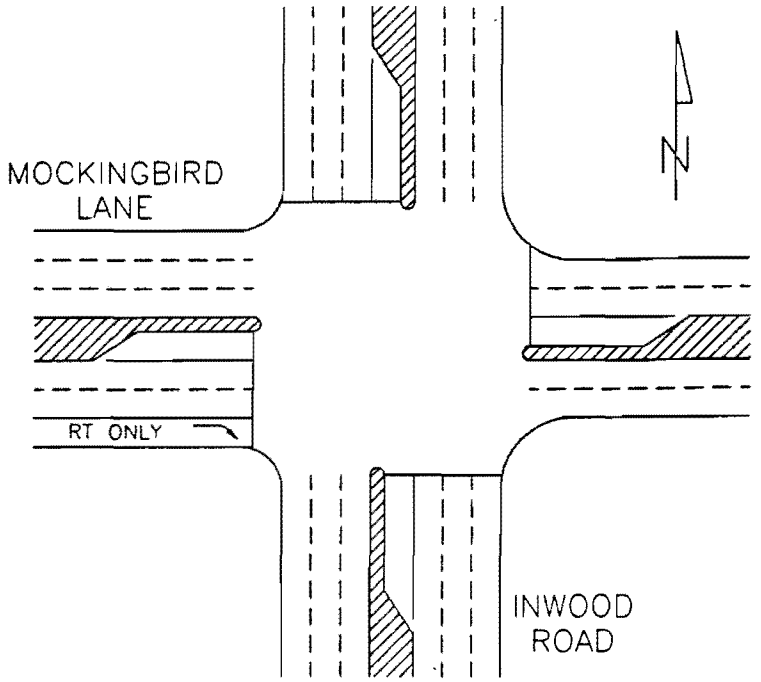

Figure A-1: Mockingbird Lane and Inwood Road, Dallas TX.

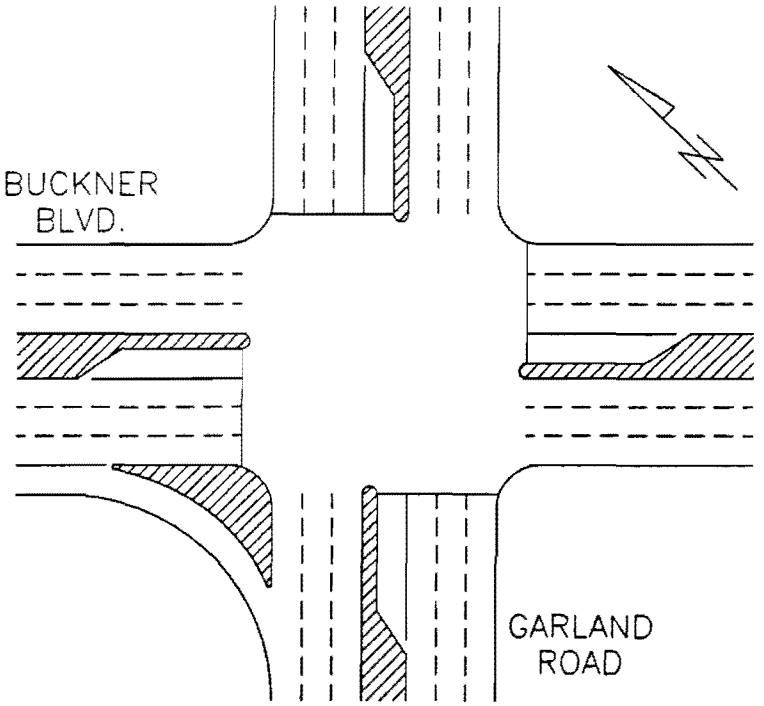

Figure A-2: Garland Road and Buckner Boulevard, Dallas TX.

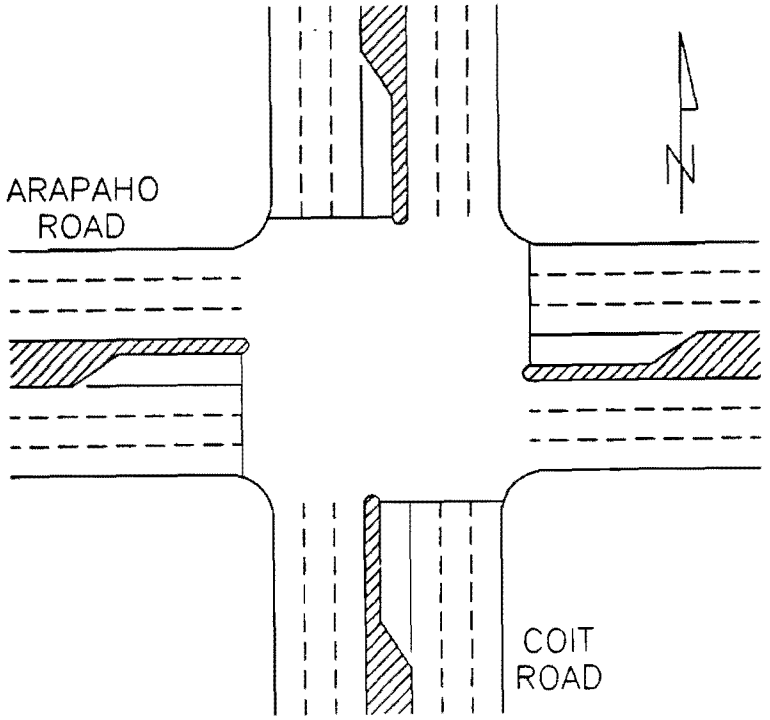

Figure A-3: Coit Road and Arapaho Road, Richardson TX.

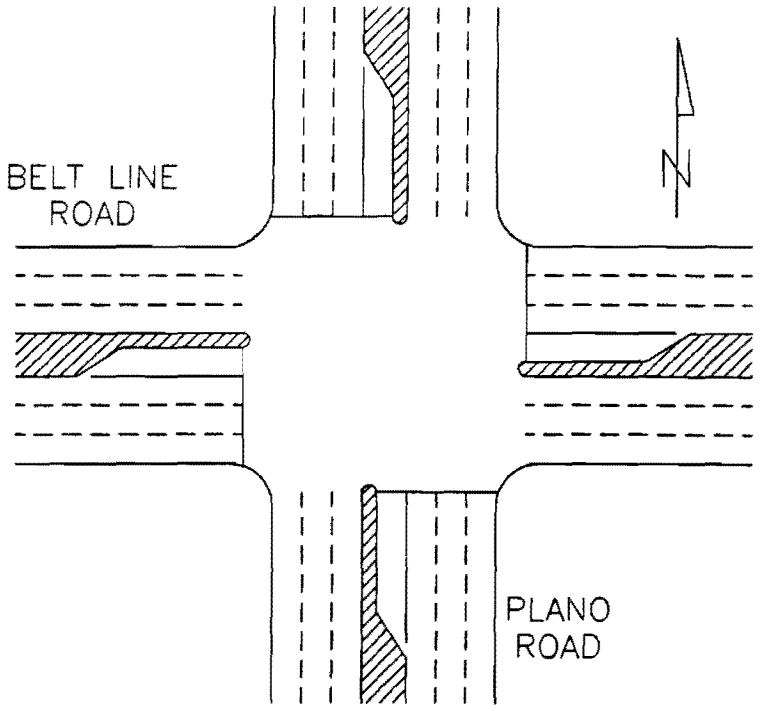

Figure A-4: Plano Road and Belt Line Road, Richardson TX.

APPENDIX B

DATA SUMMARIES

Table B-1: Leading Left-Turn Data

Loc	Time	Lane	Dir	Cyc	Gprot	Gperm	Vlt	Vlr	LTpvg	Vopvg	LTvs	Vovs	%Perm	LT X	Rp LT	Rp Vo	HCM Arr LT	HCM Arr Vo	DM	DPU	DPP
M	10:15	2	W	100	15.0	26.0	148	437	23.3	60.0	0.07	0.12	25.6	0.39	0.69	0.58	2	2	15.9	19.4	25.3
M	10:30	2	W	100	15.0	26.0	124	416	21.9	60.0	0.06	0.12	9.4	0.33	0.61	1.28	2	4	21.0	18.9	25.1
M	10:45	2	W	100	15.0	26.0	180	567	28.8	60.0	0.09	0.16	14.0	0.56	0.90	1.30	3	4	29.6	21.4	25.4
M	1:00	2	W	100	15.0	26.0	228	533	26.0	60.0	0.12	0.15	21.4	0.69	0.77	1.50	2	4	41.8	23.8	29.6
M	1:15	2	W	100	15.0	26.0	196	592	20.9	60.0	0.10	0.17	12.0	0.64	0.66	1.50	2	4	68.9	22.9	29.8
M	1:30	2	W	100	15.0	26.0	196	571	24.5	60.0	0.10	0.16	25.0	0.62	0.75	1.50	2	4	29.4	22.3	28.0
M	1:45	2	W	100	15.0	26.0	192	538	29.8	60.0	0.10	0.15	14.9	0.58	0.89	1.50	3	4	31.2	21.5	25.4
M	2:00	2	W	100	15.0	26.0	140	517	23.2	60.0	0.07	0.14	35.3	0.41	0.68	1.50	2	4	27.2	19.6	25.3
M	2:15	2	W	100	15.0	26.0	176	622	23.9	60.0	0.09	0.18	14.6	0.60	0.78	1.50	2	4	30.9	22.3	27.9
M	2:30	2	W	100	15.0	26.0	168	655	23.9	60.0	0.09	0.18	11.9	0.59	0.80	1.50	2	4	48.3	22.2	27.7
M	4:00	2	E	150	20.0	48.0	220	596	25.0	60.0	0.12	0.16	34.0	0.56	1.12	0.78	3	2	21.4	26.2	29.4
M	4:15	2	E	150	20.0	48.0	196	559	26.6	60.0	0.10	0.15	25.5	0.48	0.72	0.83	2	2	12.6	24.9	33.8
M	4:45	2	E	150	26.0	47.0	276	596	36.4	60.0	0.15	0.16	31.3	0.64	0.78	1.16	2	4	32.5	25.4	34.2
M	5:00	2	E	150	26.0	47.0	324	638	33.6	60.0	0.17	0.17	23.8	0.76	0.80	1.07	2	3	74.7	29.5	40.1
M	5:15	2	E	150	26.0	47.0	308	651	24.8	60.0	0.16	0.17	21.3	0.73	0.80	1.11	2	3	74.4	28.1	37.8
M	5:30	2	E	150	26.0	47.0	284	643	27.4	60.0	0.15	0.17	27.1	0.66	0.82	0.87	2	3	60.9	26.2	34.7
G	10:00	3	S	100	13.0	43.5	124	669	32.2	60.0	0.07	0.12	77.4	0.24	0.63	0.81	2	2	7.7	11.4	18.1
G	10:15	3	S	100	13.0	43.5	132	818	34.6	60.0	0.07	0.15	60.6	0.28	0.71	0.87	2	3	14.6	11.6	17.7
G	10:30	3	S	100	13.0	43.5	128	691	33.3	60.0	0.07	0.13	64.7	0.25	0.66	0.83	2	2	14.5	11.4	17.9
G	10:45	3	S	100	13.0	43.5	148	717	33.9	60.0	0.08	0.13	60.0	0.30	0.67	0.83	2	2	13.0	11.7	18.1
G	11:00	3	S	100	13.0	43.5	152	880	28.5	60.0	0.08	0.16	52.8	0.34	0.60	0.83	2	2	18.6	12.0	20.0
G	1:00	3	S	100	13.0	43.5	148	972	30.0	60.0	0.08	0.18	40.5	0.35	0.72	0.83	2	2	32.0	12.2	18.7
G	1:15	3	S	100	13.0	43.5	172	950	30.0	60.0	0.10	0.18	51.3	0.40	0.71	0.83	2	2	24.4	12.5	19.9
G	1:45	3	S	100	13.0	43.5	220	761	30.0	60.0	0.12	0.14	38.1	0.45	0.66	0.83	2	2	26.2	12.8	21.7
G	2:00	3	S	100	13.0	43.5	164	792	30.0	60.0	0.09	0.15	47.6	0.34	0.67	0.83	2	2	21.6	12.0	18.8
G	2:15	3	S	100	13.0	43.5	144	783	30.0	60.0	0.08	0.14	51.2	0.30	0.67	0.83	2	2	20.8	11.7	18.3
G	2:30	3	S	100	13.0	43.5	156	933	30.0	60.0	0.09	0.17	48.6	0.36	0.70	0.83	2	2	20.4	12.2	18.8

Table B-1: continued

Loc	Time	Lane	Dir	Cyc	Gprot	Gperm	Vlt	Vlr	LTpvg	Vopvg	LTvs	Vovs	%Perm	LT X	Rp LT	Rp Vo	HCM Arr LT	HCM Arr Vo	DM	DPU	DPP
C	10:15	3	N	90	10.5	39.0	164	937	40.1	31.9	0.08	0.18	23.7	0.37	0.88	0.74	3	2	13.0	11.8	15.9
C	10:30	3	N	90	10.5	39.0	152	946	40.5	34.6	0.07	0.18	38.2	0.34	0.88	0.80	3	2	11.1	11.7	15.5
C	10:45	3	N	90	10.5	39.0	172	1065	31.7	34.3	0.09	0.20	38.6	0.42	0.72	0.79	2	2	19.5	12.3	19.8
C	11:00	3	N	90	10.5	39.0	204	1201	36.1	33.7	0.10	0.22	37.5	0.54	0.86	0.78	3	2	37.3	13.7	20.9
C	11:15	3	N	90	10.5	39.0	176	1052	47.1	33.1	0.09	0.19	46.0	0.42	1.06	0.76	3	2	21.0	12.3	14.4
C	11:30	3	N	90	10.5	39.0	176	1153	40.6	49.3	0.09	0.21	42.9	0.46	0.90	1.14	3	3	33.7	12.7	16.8
C	1:15	3	N	90	10.5	39.0	216	1157	32.9	45.7	0.11	0.21	28.3	0.57	0.73	1.05	2	3	23.6	14.1	22.2
C	1:30	3	N	90	10.5	39.0	196	1298	33.6	38.4	0.10	0.24	15.2	0.57	0.83	0.89	2	3	25.7	14.3	22.2
C	1:45	3	N	90	10.5	39.0	220	1109	35.3	38.0	0.11	0.20	39.2	0.55	0.80	0.88	2	3	23.9	14.0	21.3
C	2:00	3	N	90	10.5	39.0	216	1100	42.1	38.0	0.11	0.20	35.3	0.53	0.95	0.88	3	3	17.9	13.6	18.4
C	2:15	3	N	90	10.5	39.0	188	1104	39.5	38.0	0.09	0.20	30.0	0.47	0.89	0.88	3	3	11.3	12.7	17.9
C	2:30	3	N	90	10.5	39.0	160	1197	35.0	38.0	0.08	0.22	30.0	0.42	0.82	0.88	2	3	16.8	12.4	17.9
C	4:30	3	N	180	27.5	73.0	204	1258	61.5	64.5	0.10	0.23	39.2	0.46	1.30	1.59	4	5	31.3	20.8	17.6
C	4:45	3	N	180	27.5	73.0	220	1135	57.1	68.3	0.11	0.21	40.0	0.47	1.15	1.68	3	5	29.3	20.5	19.2
C	5:00	3	N	180	27.5	73.0	252	1210	59.3	67.3	0.13	0.22	42.9	0.56	1.21	1.66	4	5	26.9	21.6	19.4
C	5:15	3	N	180	27.5	73.0	244	1364	57.7	62.7	0.13	0.25	.	0.58	1.26	1.55	4	5	.	22.4	20.9
C	5:30	3	N	180	27.5	73.0	224	1360	56.4	62.9	0.12	0.25	.	0.53	1.23	1.55	4	5	.	21.8	20.8
P	7:30	3	S	160	28.0	47.0	88	1386	59.9	41.4	0.05	0.26	.	0.33	2.36	1.41	5	4	61.1	26.2	21.8
P	7:45	3	S	160	28.0	47.0	52	1646	56.5	31.6	0.03	0.31	.	0.20	2.83	1.08	5	3	59.2	27.4	24.8
P	10:15	3	S	90	14.0	35.0	172	629	30.0	60.0	0.09	0.12	.	0.33	0.63	0.35	2	1	19.2	11.8	18.6
P	10:30	3	S	90	14.0	35.0	128	686	30.0	60.0	0.06	0.13	.	0.25	0.64	0.39	2	1	26.7	11.3	17.8
P	1:15	3	S	90	14.0	35.0	208	981	29.5	62.7	0.11	0.18	.	0.51	0.60	1.61	2	5	25.3	13.2	20.0
P	1:30	3	S	90	14.0	35.0	132	1065	36.6	62.5	0.07	0.20	.	0.34	0.77	1.61	2	5	18.2	12.1	16.2
P	1:45	3	S	90	14.0	35.0	196	854	42.7	67.1	0.10	0.16	.	0.45	0.83	1.72	2	5	35.7	12.5	15.4
P	2:00	3	S	90	14.0	35.0	160	889	31.4	68.7	0.08	0.17	.	0.37	0.61	1.77	2	5	38.9	12.0	17.9
P	2:15	3	S	90	14.0	35.0	132	726	31.9	61.8	0.07	0.14	.	0.28	0.61	1.59	2	5	14.9	11.4	17.1
P	2:30	3	S	90	14.0	35.0	152	805	26.4	63.6	0.08	0.15	.	0.34	0.51	1.64	2	5	26.5	11.8	19.1

Table B-2: Lagging Left-Turn Data

Loc	Time	Lane	Dir	Cyc	Gprot	Gperm	Vlt	Vtr	LTpvg	Vopvg	LTvs	Vovs	%Perm	LT X	Rp LT	Rp Vo	HCM Arr LT	HCM Arr Vo	DM	DPU	DPP
M	10:15	2	E	100	13.0	28.0	120	697	55.5	23.3	0.07	0.18	12.0	0.52	1.38	1.20	4	4	19.3	29.0	35.0
M	10:30	2	E	100	13.0	28.0	120	676	55.5	21.9	0.07	0.18	18.2	0.51	1.34	1.19	4	4	37.9	28.8	34.5
M	10:45	2	E	100	13.0	28.0	104	596	55.5	28.8	0.06	0.15	22.2	0.39	1.23	1.21	4	4	28.3	26.2	30.8
M	1:00	2	E	100	13.0	28.0	144	739	55.5	26.0	0.08	0.19	8.6	0.68	1.66	1.39	5	4	24.1	31.2	38.2
M	1:15	2	E	100	13.0	28.0	168	672	55.5	20.9	0.09	0.17	17.8	0.69	1.50	1.39	4	4	23.3	32.3	36.7
M	1:30	2	E	100	13.0	28.0	136	659	55.5	24.5	0.08	0.17	24.1	0.56	1.49	1.39	4	4	26.4	29.6	32.6
M	1:45	2	E	100	13.0	28.0	96	605	55.5	29.8	0.05	0.16	25.0	0.36	1.40	1.39	4	4	19.3	26.4	28.2
M	2:00	2	E	100	13.0	28.0	120	575	55.5	23.2	0.08	0.15	33.3	0.43	1.36	1.39	4	4	23.8	26.8	28.6
M	2:15	2	E	100	13.0	28.0	88	697	55.5	23.9	0.05	0.18	41.4	0.39	1.56	1.39	5	4	27.4	27.4	30.3
M	2:30	2	E	100	13.0	28.0	188	575	55.5	23.9	0.10	0.15	14.0	0.68	1.37	1.39	4	4	31.6	30.4	34.5
M	4:00	2	W	150	16.0	57.0	140	815	55.5	25.0	0.07	0.23	46.9	0.45	0.85	1.01	2	3	39.2	35.6	54.0
M	4:15	2	W	150	17.0	51.0	112	617	55.5	26.6	0.06	0.17	58.1	0.31	0.89	0.76	3	2	42.5	33.2	46.9
M	4:45	2	W	150	17.0	51.0	176	1008	55.5	36.4	0.10	0.28	15.6	0.94	2.09	0.88	5	3	71.6	53.6	91.5
M	5:00	2	W	150	16.0	57.0	164	1046	55.5	33.6	0.09	0.29	7.3	0.76	1.62	0.79	5	2	48.5	45.0	67.1
M	5:15	2	W	150	16.0	57.0	176	1025	55.5	24.8	0.09	0.28	0.0	0.78	1.63	0.79	5	2	79.6	47.9	67.2
M	5:30	2	W	150	16.0	57.0	164	899	55.5	27.4	0.09	0.25	27.9	0.61	1.07	0.79	3	2	70.0	40.4	59.5
G	10:00	3	N	100	20.0	36.5	268	673	55.5	32.2	0.14	0.13	42.6	0.54	0.78	0.88	2	3	44.8	19.5	30.3
G	10:15	3	N	100	20.0	36.5	244	735	55.5	34.6	0.13	0.15	44.8	0.50	0.86	0.95	3	3	32.2	19.6	29.1
G	10:30	3	N	100	20.0	36.5	316	796	55.5	33.3	0.17	0.16	35.2	0.67	0.85	0.91	2	3	32.7	23.5	35.0
G	10:45	3	N	100	20.0	36.5	244	792	55.5	33.9	0.13	0.16	40.4	0.53	0.85	0.93	2	3	27.3	20.5	31.3
G	11:00	3	N	100	20.0	36.5	332	840	55.5	28.5	0.18	0.17	32.1	0.74	0.88	0.78	3	2	33.8	25.8	38.2
G	11:15	3	N	100	20.0	36.5	244	783	55.5	26.4	0.13	0.16	.	0.52	0.86	0.72	3	2	.	20.4	31.4
G	11:30	3	N	100	20.0	36.5	268	792	55.5	28.0	0.15	0.16	.	0.58	0.85	0.90	2	3	.	21.4	32.5
G	1:00	3	N	100	20.0	36.5	260	827	55.5	28.0	0.14	0.16	34.3	0.57	0.86	0.90	3	3	37.9	21.6	32.6
G	1:15	3	N	100	20.0	36.5	264	933	55.5	28.0	0.15	0.19	17.6	0.62	0.91	0.90	3	3	51.1	23.6	35.2
G	1:30	3	N	100	20.0	36.5	308	977	55.5	28.0	0.17	0.19	24.6	0.74	0.93	0.90	3	3	38.0	27.1	40.0
G	1:45	3	N	100	20.0	36.5	320	955	55.5	28.0	0.18	0.19	30.3	0.76	0.92	0.90	3	3	53.4	27.3	40.3

Table B-2: continued

Loc	Time	Lane	Dir	Cyc	Gprot	Gperm	Vlt	Vlr	LTpvg	Vopvg	LTvs	Vovs	%Perm	LT X	Rp LT	Rp Vo	HCM Arr LT	HCM Arr Vo	DM	DPU	DPP
G	2:00	3	N	100	20.0	36.5	292	713	55.5	28.0	0.16	0.14	31.4	0.59	0.82	0.90	2	3	39.7	20.9	31.8
G	2:15	3	N	100	20.0	36.5	248	686	55.5	28.0	0.13	0.14	32.0	0.50	0.81	0.90	2	3	35.1	19.0	29.3
C	10:15	3	S	90	11.5	38.0	100	915	31.9	40.1	0.05	0.17	66.7	0.26	0.76	0.95	2	3	21.3	15.4	25.7
C	10:30	3	S	90	11.5	38.0	108	906	34.6	40.5	0.05	0.17	72.4	0.28	0.82	0.96	2	3	27.0	15.4	24.9
C	10:45	3	S	90	11.5	38.0	112	880	34.3	31.7	0.06	0.16	78.8	0.28	0.83	0.75	2	2	16.0	15.2	25.5
C	11:00	3	S	90	11.5	38.0	88	1012	33.7	36.1	0.04	0.19	66.7	0.24	0.85	0.85	2	2	19.1	15.7	26.1
C	11:15	3	S	90	11.5	38.0	88	986	33.1	47.1	0.04	0.18	75.0	0.24	0.79	1.12	2	3	20.4	15.8	25.0
C	11:30	3	S	90	11.5	38.0	160	1052	49.3	40.6	0.08	0.20	39.0	0.45	1.25	0.96	4	3	48.7	17.3	22.9
C	1:15	3	S	90	11.5	38.0	136	1355	45.7	32.9	0.07	0.25	51.4	0.48	1.43	0.78	4	2	30.5	19.2	28.8
C	1:30	3	S	90	11.5	38.0	156	1175	38.4	33.6	0.08	0.21	44.4	0.42	0.94	0.80	3	2	48.5	18.8	26.0
C	1:45	3	S	90	11.5	38.0	132	1140	33.0	35.3	0.07	0.21	68.8	0.39	0.89	0.84	3	2	30.1	17.6	29.9
C	2:00	3	S	90	11.5	38.0	148	1109	33.0	42.1	0.08	0.20	56.1	0.43	0.84	1.00	2	3	25.7	17.8	29.5
C	2:15	3	S	90	11.5	38.0	152	1096	33.0	42.1	0.08	0.20	60.0	0.44	0.85	1.00	2	3	27.3	18.0	29.8
C	2:30	3	S	90	11.5	38.0	124	1219	33.0	35.0	0.06	0.22	66.7	0.39	0.93	0.83	3	2	16.3	17.9	30.8
C	4:30	3	S	180	17.5	83.0	132	1896	64.5	61.5	0.06	0.35	6.5	0.54	2.18	1.33	5	4	57.7	40.9	44.7
C	4:45	3	S	180	17.5	83.0	144	1945	68.3	57.1	0.07	0.35	8.7	0.60	2.47	1.24	5	4	46.3	43.1	45.2
C	5:00	3	S	180	17.5	83.0	144	2235	67.3	59.3	0.07	0.41	3.1	0.78	3.59	1.29	5	4	52.9	51.2	63.3
C	5:15	3	S	180	17.5	83.0	160	2165	62.7	57.7	0.08	0.39	.	0.79	2.90	1.25	5	4	.	51.4	65.9
C	5:30	3	S	180	17.5	83.0	168	2433	62.9	56.4	0.08	0.45	.	1.12	5.27	1.22	5	4	.	65.3	163.8

APPENDIX C

TRAFFIC DATA

Table C-1: Mockingbird Lane Saturation Flow Analysis.

Time Period/Direction	Sample Size	Saturation Flow Headway (sec)	Standard Deviation	Saturation Flow Rate (vphgpl)
Off-Peak				
EB	38	1.95	0.16	1843
WB	76	1.87	0.29	1925
Peak				
EB	50	2.01	0.21	1788
WB	105	1.90	0.27	1899
Peak Direction Analysis				
Westbound				
AM Peak (Peak Direction)	39	1.75	0.13	2058
PM Peak (Off-Peak Direction)	66	1.98	0.29	1815

Table C-2: Garland Road Saturation Flow Analysis.

Time Period/Direction	Sample Size	Saturation Flow Headway (sec)	Standard Deviation	Saturation Flow Rate (vphgpl)
Off-Peak				
NB	38	2.05	0.33	1758
SB	58	2.24	0.41	1610
Peak				
NB	46	1.97	0.34	1830
SB	59	2.12	0.26	1702
Peak Direction Analysis				
Northbound				
AM Peak (Off-Peak Direction)	19	2.17	0.29	1655
PM Peak (Peak Direction)	27	1.82	0.31	1976

Table C-3: Coit Road Saturation Flow Analysis.

Time Period/Direction	Sample Size	Saturation Flow Headway (sec)	Standard Deviation	Saturation Flow Rate (vphgpl)
AM Peak Northbound (Off-Peak Direction)	505	1.94	0.35	1852
AM Peak Southbound (Peak Direction)	291	1.69	0.10	2126
PM Peak Southbound (Off-Peak Direction)	372	1.94	0.39	1859

Table C-4: Plano Road Saturation Flow Analysis.

Time Period/Direction	Sample Size	Saturation Flow Headway (sec)	Standard Deviation	Saturation Flow Rate (vphgpl)
Southbound				
Off-Peak	10	1.91	0.31	1888
AM Peak	323	1.97	0.37	1824

Table C-5: Mockingbird Lane - Lane Distribution Summary.

Direction/Lane	AM Peak (%)	AM Off-Peak (%)	PM Off-Peak (%)	PM Peak (%)	Daily Total (%)
Eastbound					
Median	40.3	43.0	43.4	40.3	41.5
Center	51.2	49.7	49.2	49.9	49.8
Excl. Right	8.5	7.3	7.4	9.8	8.7
Westbound					
Median	47.0	51.8	51.5	47.4	49.4
Right	53.0	48.2	48.5	52.6	50.6

Table C-6: Coit Road - Lane Distribution Summary.

Direction/Lane	AM Peak (%)	AM Off-Peak (%)	PM Off-Peak (%)	PM Peak (%)	Daily Total (%)
Northbound					
Median	29.1	28.9	29.8	23.8	30.4
Center	37.0	36.9	34.7	35.2	35.8
Right	33.9	34.2	35.5	32.0	33.7
Southbound					
Median	33.3	33.8	31.5	33.5	33.0
Center	37.6	33.7	35.3	37.2	36.2
Right	29.1	32.6	32.2	29.3	30.8

Table C-7: Plano Road - Lane Distribution Summary

Direction/Lane	AM Peak (%)	AM Off-Peak (%)	PM Off-Peak (%)	PM Peak (%)	Daily Total (%)
Northbound					
Median	31.3	24.7	28.7	N/A	30.4
Center	38.9	35.6	35.9	N/A	35.8
Right	29.8	39.7	35.4	N/A	33.7
Southbound					
Median	27.6	26.2	27.8	N/A	33.0
Center	34.0	33.3	32.8	N/A	36.2
Right	38.4	40.5	39.4	N/A	30.8

APPENDIX D

LEFT-TURN DATA

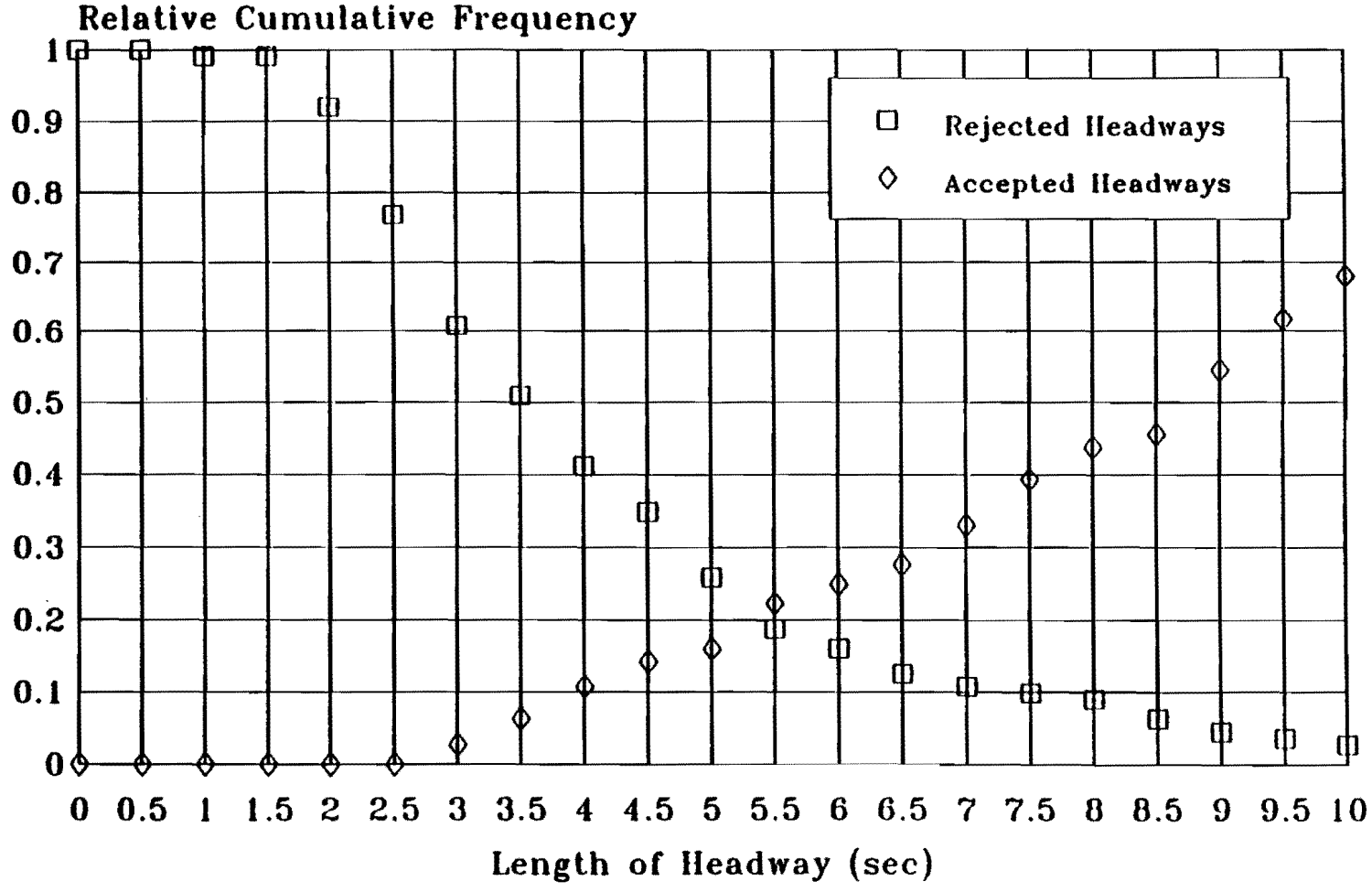

Figure D-1: Critical Headway - Mockingbird Lane and Inwood Road

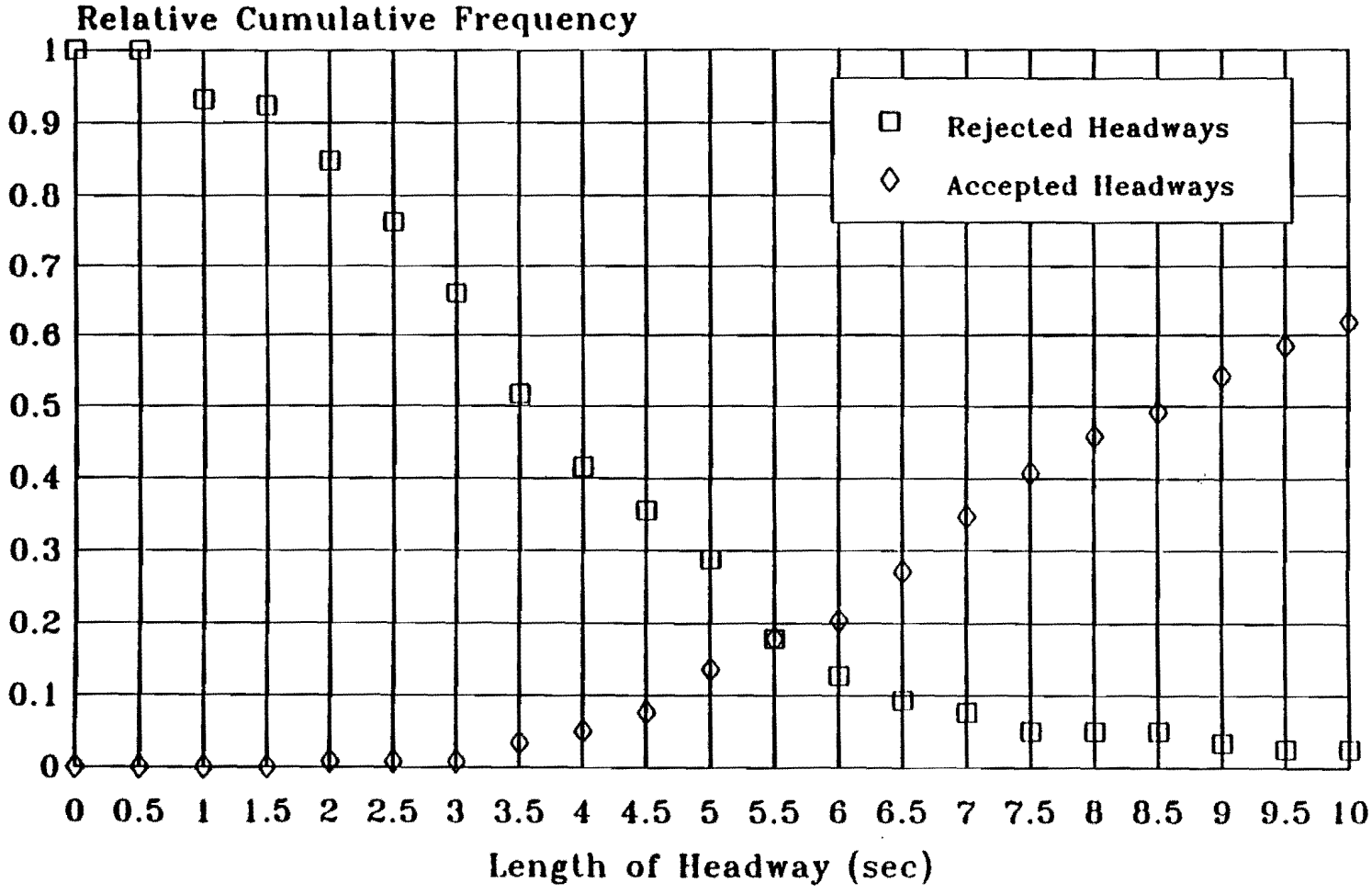

Figure D-2: Critical Headway - Garland Road and Buckner Boulevard

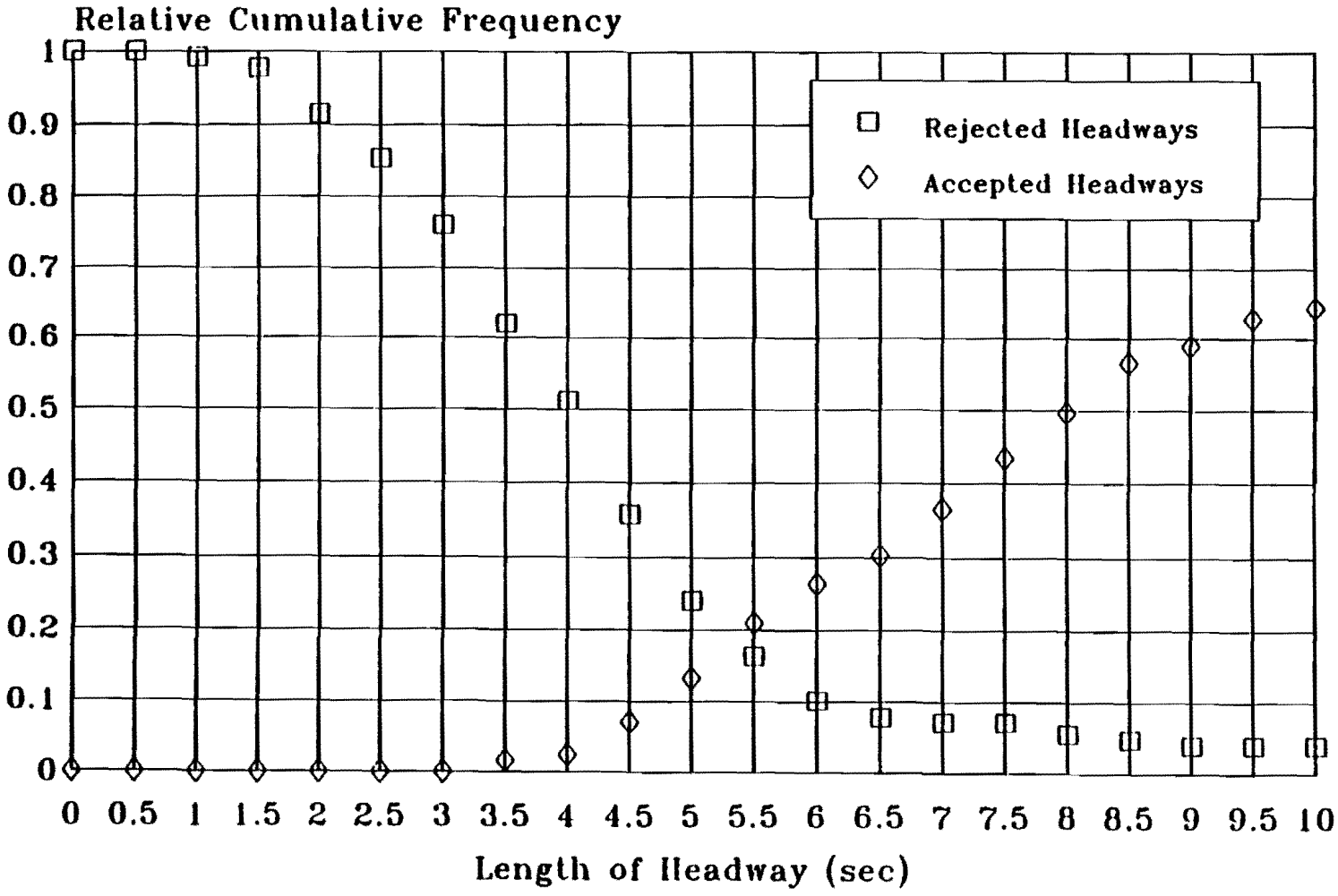

Figure D-3: Critical Headway - Coit Road and Arapaho Road

Table D-1: Results of Multiple Comparison of Accepted Headways.

	Sample Size	Scheffe Grouping
Mockingbird		
Peak Time Period	72	Significantly
Off-Peak Time Period	40	Different
Leading Left Turn	48	Significantly
Lagging Left Turn	64	Different
Garland		
Peak Time Period	6	No
Off-Peak Time Period	112	Difference
Leading Left Turn	66	No
Lagging Left Turn	52	Difference
Coit		
Peak Time Period	73	No
Off-Peak Time Period	56	Difference
Leading Left Turn	76	No
Lagging Left Turn	53	Difference

Table D-2: Results of Multiple Comparison of Rejected Headways.

	Sample Size	Scheffe Grouping
Mockingbird		
Peak Time Period	72	No
Off-Peak Time Period	40	Difference
Leading Left Period	48	Significantly
Lagging Left Turn	64	Different
Garland		
Peak Time Period	6	No
Off-Peak Time Period	112	Difference
Leading Left Turn	66	No
Lagging Left Turn	52	Difference
Coit		
Peak Time Period	73	No
Off-Peak Time Period	56	Difference
Leading Left Turn	76	No
Lagging Left Turn	53	Difference

APPENDIX E

SIMULATION DATA

Table E-1: Predicted Left-Turn Delay for Alternate Phasing (g/C=0.4)

Opposing Volume	Left Turn Volume	Cycle Length	Leading Left			Lagging Left		
			Delay		Percent	Delay		Percent
			MUTCD	Dallas	Reduction	MUTCD	Dallas	Reduction
300	100	90	22.1	19.1	13.6	29.9	25.6	14.4
300	150	90	33.1	19.8	40.2	34.5	27.3	20.9
300	200	90	37.5	20.9	44.3	40.1	29.5	26.4
300	250	90	44.5	22.3	49.9	43.3	32.0	26.1
300	300	90	58.5	24.4	58.3	50.1	35.7	28.7
300	100	120	27.1	24.9	8.1	38.2	32.8	14.1
300	150	120	39.2	25.8	34.2	44.0	35.0	20.5
300	200	120	43.2	27.1	37.3	50.5	37.6	25.5
300	250	120	49.1	28.6	41.8	53.6	40.2	25.0
300	300	120	59.2	30.8	48.0	59.0	43.5	26.3
400	100	90	23.6	19.4	17.8	29.0	27.7	4.5
400	150	90	42.8	20.3	52.6	33.8	30.1	10.9
400	200	90	53.2	21.6	59.3	40.3	33.1	17.9
400	250	90	70.1	23.6	66.3	57.5	37.1	35.5
400	300	90	99.1	26.8	73.0	73.4	44.5	39.4
400	100	120	28.1	25.2	10.3	37.0	35.5	4.1
400	150	120	48.3	26.3	45.5	42.9	38.3	10.7
400	200	120	56.3	27.9	50.4	49.4	41.6	15.8
400	250	120	68.1	30.0	55.9	62.8	45.0	28.3
400	300	120	91.0	33.4	63.3	80.2	51.4	35.9
500	100	90	31.4	19.6	37.6	30.3	30.3	0.0
500	150	90	58.3	21.0	64.0	33.6	33.6	0.0
500	200	90	78.4	22.8	70.9	40.6	37.8	6.9
500	250	90	111.1	26.0	76.6	57.8	45.8	20.8
500	300	90	160.5	31.7	80.2	109.2	64.2	41.2
500	100	120	30.0	25.7	14.3	38.6	38.6	0.0
500	150	120	61.6	27.1	56.0	42.5	42.4	0.2
500	200	120	75.8	29.2	61.5	49.4	46.6	5.7
500	250	120	101.3	32.4	68.0	62.5	53.0	15.2
500	300	120	140.6	38.3	72.8	101.3	65.8	35.0
600	100	90	40.9	20.4	50.1	33.4	33.4	0.0
600	150	90	80.8	22.0	72.8	38.1	38.1	0.0
600	200	90	120.2	24.9	79.3	46.5	46.5	0.0
600	250	90	168.1	30.2	82.0	65.8	65.8	0.0
600	300	90	234.9	41.0	82.5	114.8	110.9	3.4
600	100	120	34.5	26.5	23.2	42.3	42.3	0.0
600	150	120	83.0	28.3	65.9	47.3	47.3	0.0
600	200	120	111.9	31.4	71.9	54.1	54.1	0.0
600	250	120	151.5	37.0	75.6	67.4	67.4	0.0
600	300	120	211.1	48.1	77.2	104.0	98.5	5.3

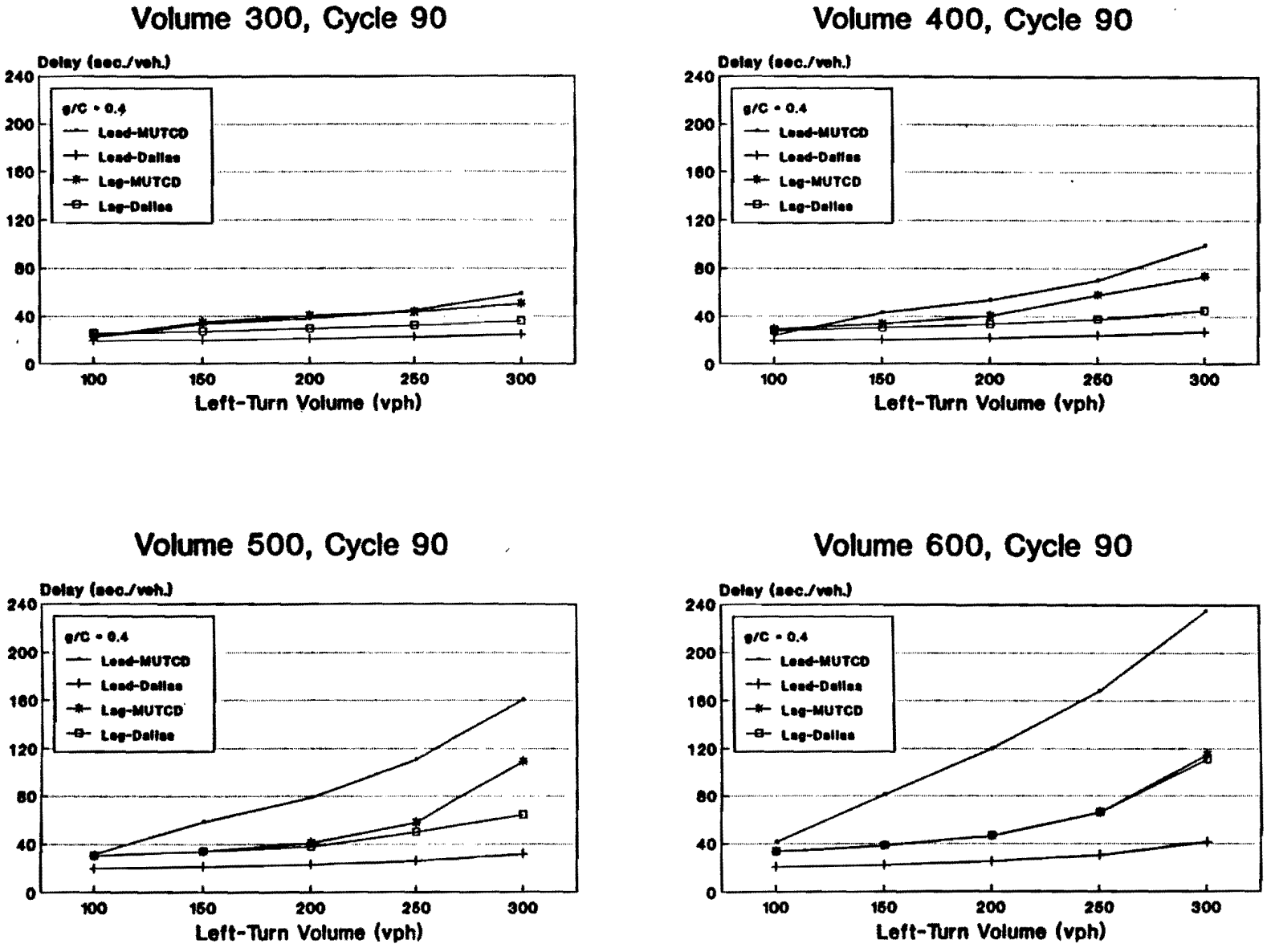

Figure E-1: Predicted Delay vs Left-Turn volumes (g/C=0.4, Cycle=90 sec.)

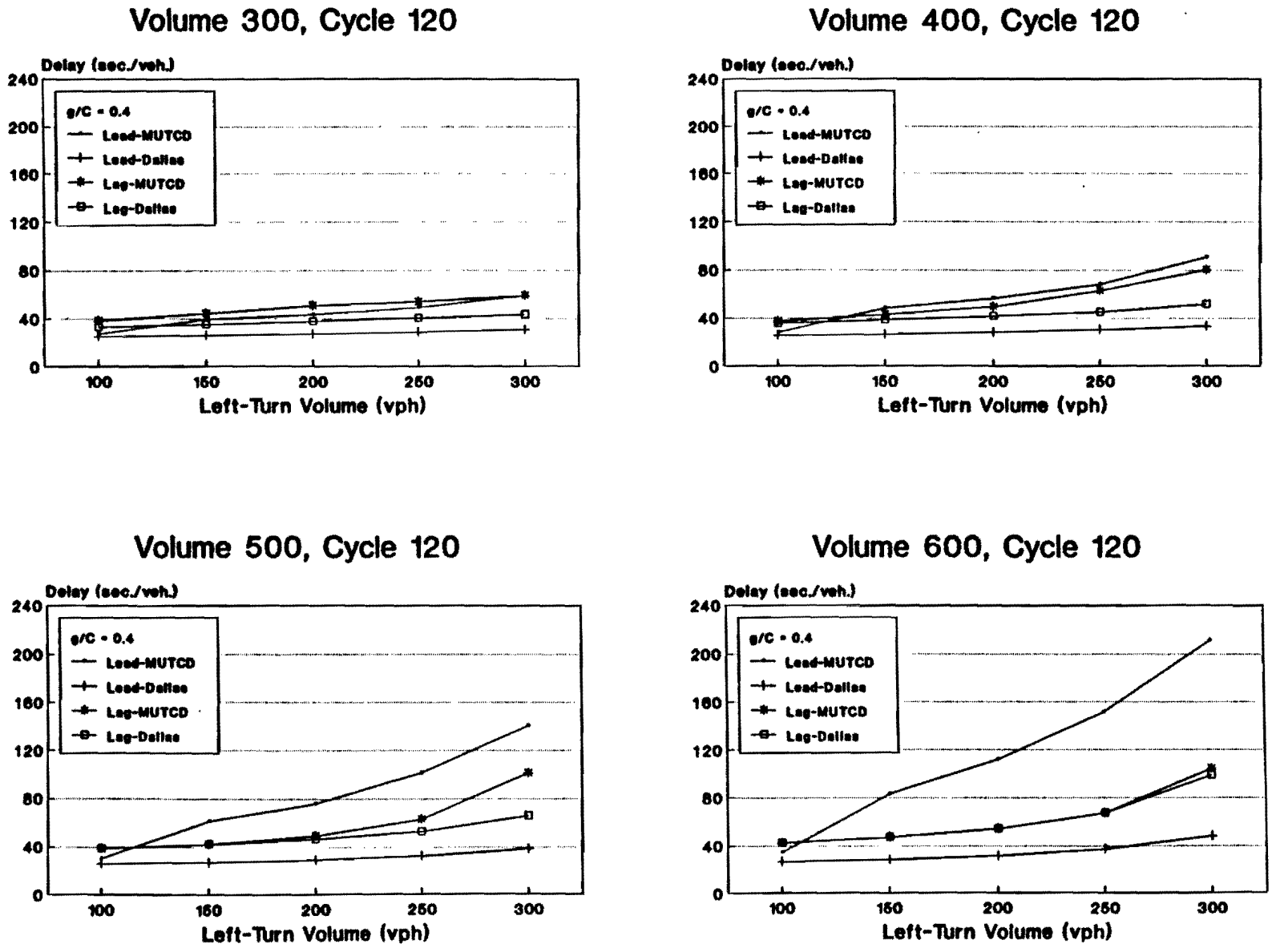

Figure E-2: Predicted Delay vs Left-Turn volumes (g/C=0.4, Cycle=120 sec.)

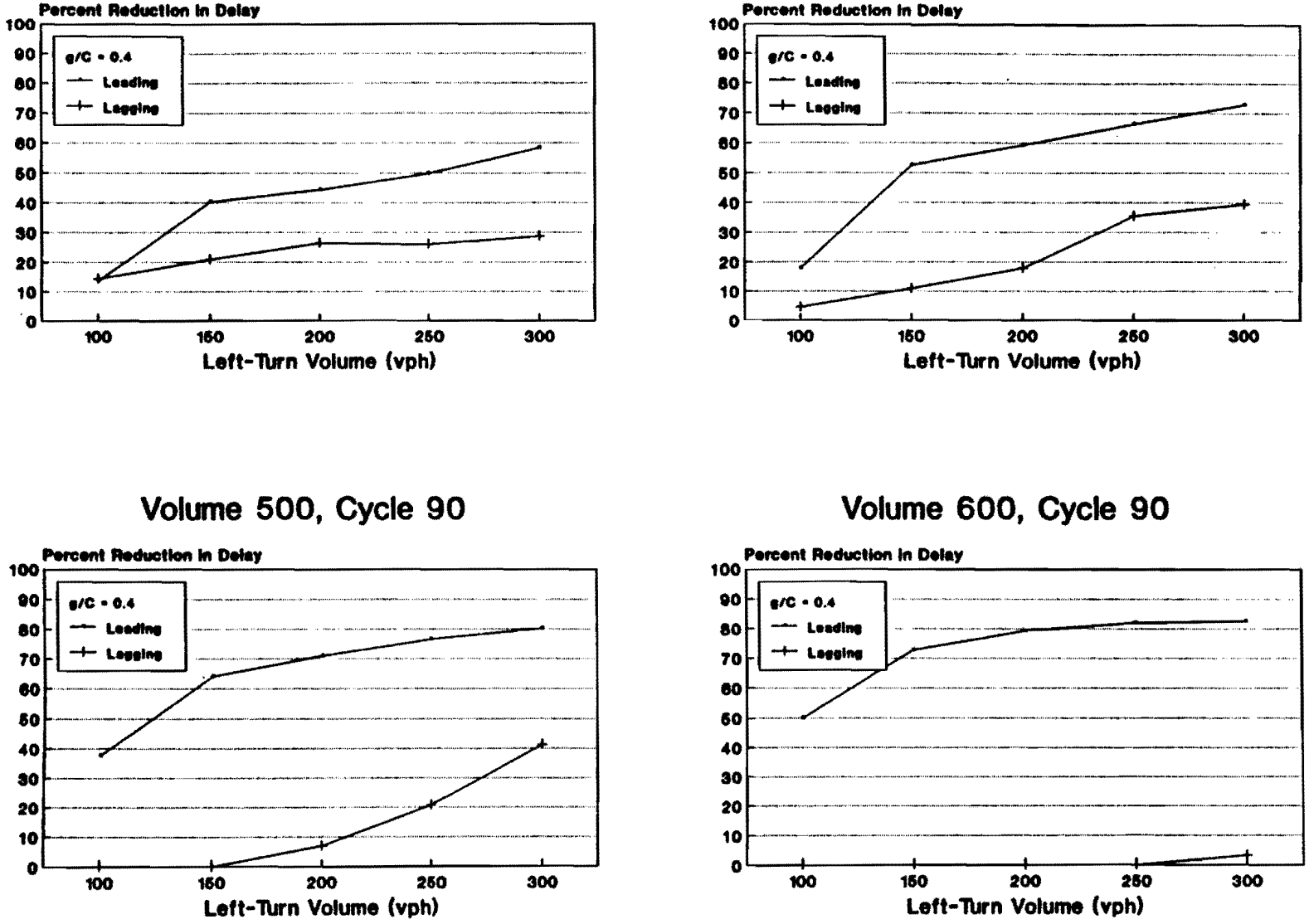

Figure E3: Reduction In Delay vs Left-Turn Volumes (g/C=0.4, Cycle=90 sec.)

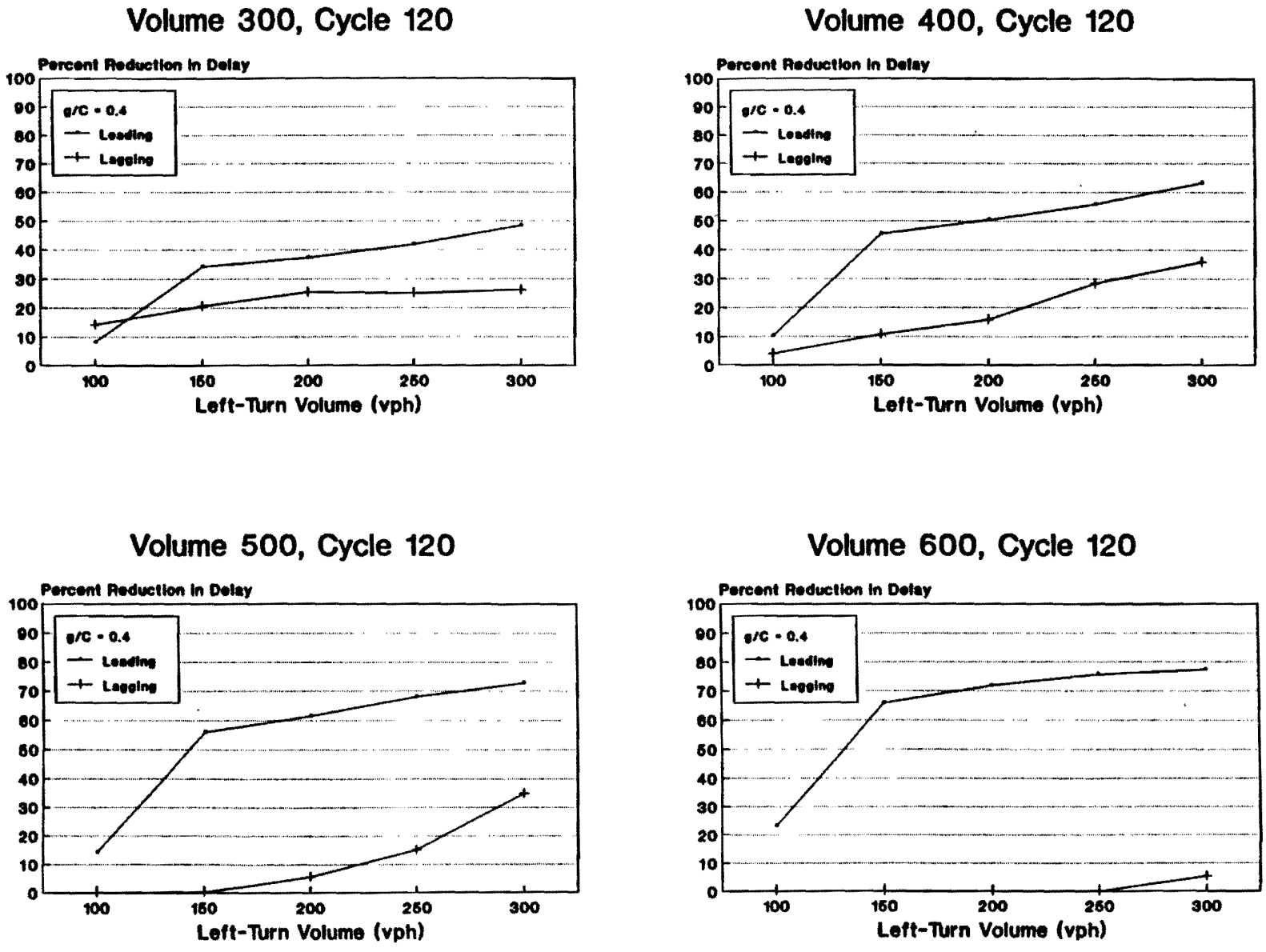

Figure E4: Reduction In Delay vs Left-Turn Volumes (g/C=0.4, Cycle=120 sec.)

Table E-2: Predicted Left-Turn Delay for Alternate Phasing (g/C=0.5)

Opposing Volume	Left Turn Volume	Cycle Length	Leading Left			Lagging Left		
			Delay		Percent	Delay		Percent
			MUTCD	Dallas	Reduction	MUTCD	Dallas	Reduction
300	100	90	14.8	13.4	9.5	25.0	18.5	26.0
300	150	90	21.2	11.9	34.4	29.0	19.6	32.4
300	200	90	22.9	14.5	36.7	32.4	21.1	34.9
300	250	90	24.8	15.2	38.7	32.6	22.6	30.7
300	300	90	27.6	16.1	41.7	33.5	24.2	27.8
300	100	120	18.7	17.5	6.4	31.7	23.5	25.9
300	150	120	24.4	18.1	25.8	37.3	25.1	32.7
300	200	120	27.9	18.8	32.6	41.5	26.8	35.4
300	250	120	30.0	19.7	34.3	42.3	28.9	31.7
300	300	120	32.5	20.7	36.3	42.6	30.7	27.9
400	100	90	15.2	13.7	9.9	23.8	20.0	16.0
400	150	90	19.5	14.2	27.2	27.8	21.5	22.7
400	200	90	26.7	14.9	44.2	31.6	23.3	26.3
400	250	90	30.0	15.7	47.7	36.0	25.3	29.7
400	300	90	34.4	16.8	51.2	38.9	27.2	30.1
400	100	120	19.1	17.7	7.3	30.1	25.5	15.3
400	150	120	21.0	18.4	12.4	35.6	27.5	22.8
400	200	120	31.9	19.3	39.5	40.3	29.7	26.3
400	250	120	34.8	20.3	41.7	45.0	32.1	28.7
400	300	120	39.1	21.5	45.0	48.8	34.4	29.5
500	100	90	15.7	14.0	10.8	23.2	21.7	6.5
500	150	90	21.5	14.6	32.1	27.3	23.6	13.6
500	200	90	31.4	15.4	51.0	31.4	26.1	16.9
500	250	90	37.0	16.4	55.7	35.8	28.4	20.7
500	300	90	45.4	17.8	60.8	44.1	30.8	30.2
500	100	120	19.6	18.1	7.7	29.4	27.7	5.8
500	150	120	22.1	18.9	14.5	34.6	30.1	13.0
500	200	120	36.7	19.9	45.8	39.9	33.0	17.3
500	250	120	41.5	21.1	49.2	44.6	35.8	19.7
500	300	120	48.3	22.6	53.2	51.9	38.4	26.0
600	100	90	16.4	14.4	12.2	23.7	23.7	0.0
600	150	90	26.4	15.1	42.8	27.0	26.2	3.0
600	200	90	37.8	16.1	57.4	31.4	29.0	7.6
600	250	90	47.0	17.5	62.8	36.2	31.8	12.2
600	300	90	61.1	19.4	68.2	44.7	35.5	20.6
600	100	120	20.3	18.6	8.4	30.2	30.2	0.0
600	150	120	23.9	19.5	18.4	34.2	33.2	2.9
600	200	120	43.9	20.7	52.8	39.7	36.8	7.3
600	250	120	51.4	22.3	56.6	44.8	39.9	10.9
600	300	120	62.9	24.3	61.4	52.4	43.5	17.0

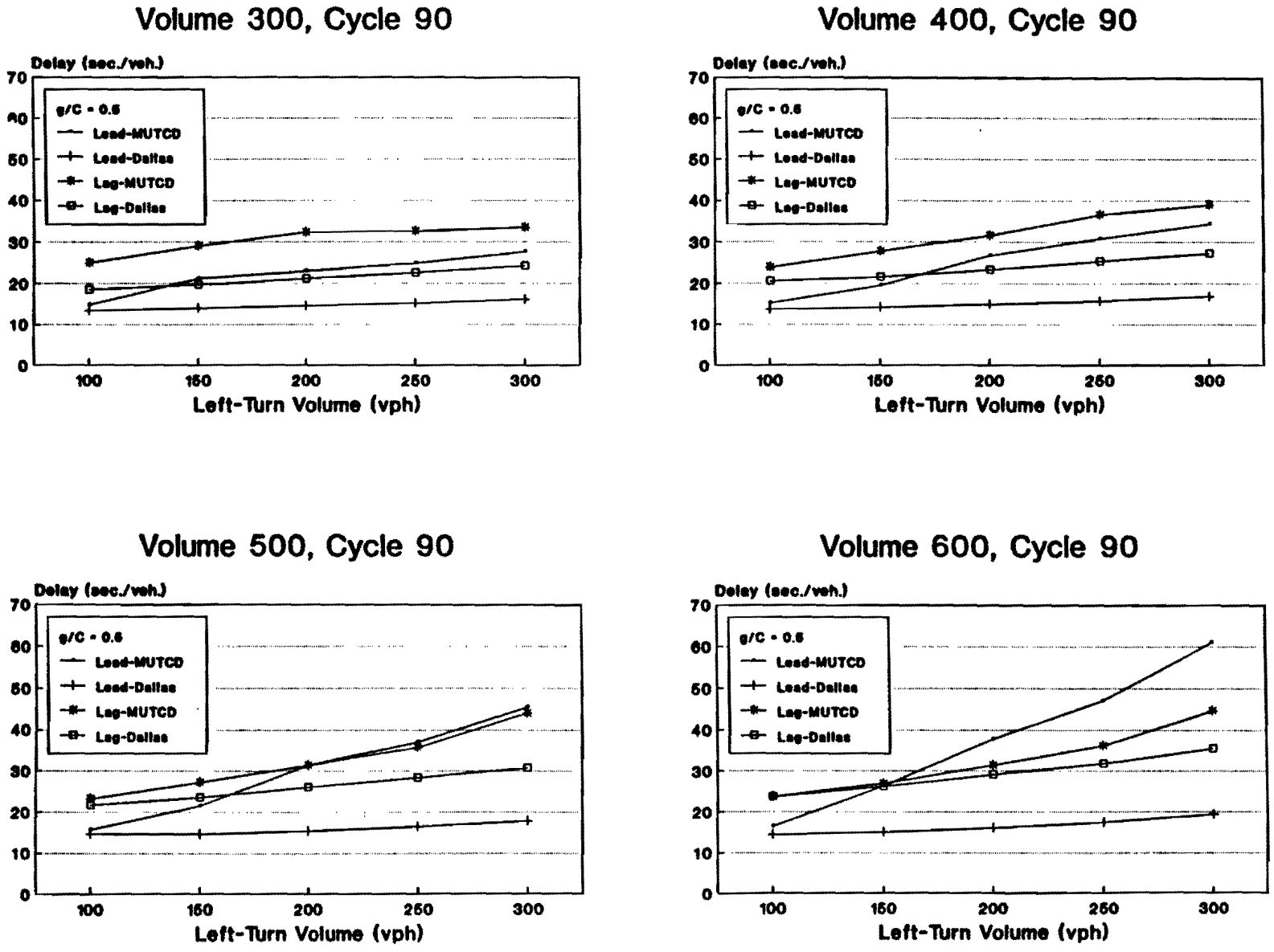

Figure E-5: Predicted Delay vs Left-Turn Volumes (g/C=0.5, Cycle=90 sec.)

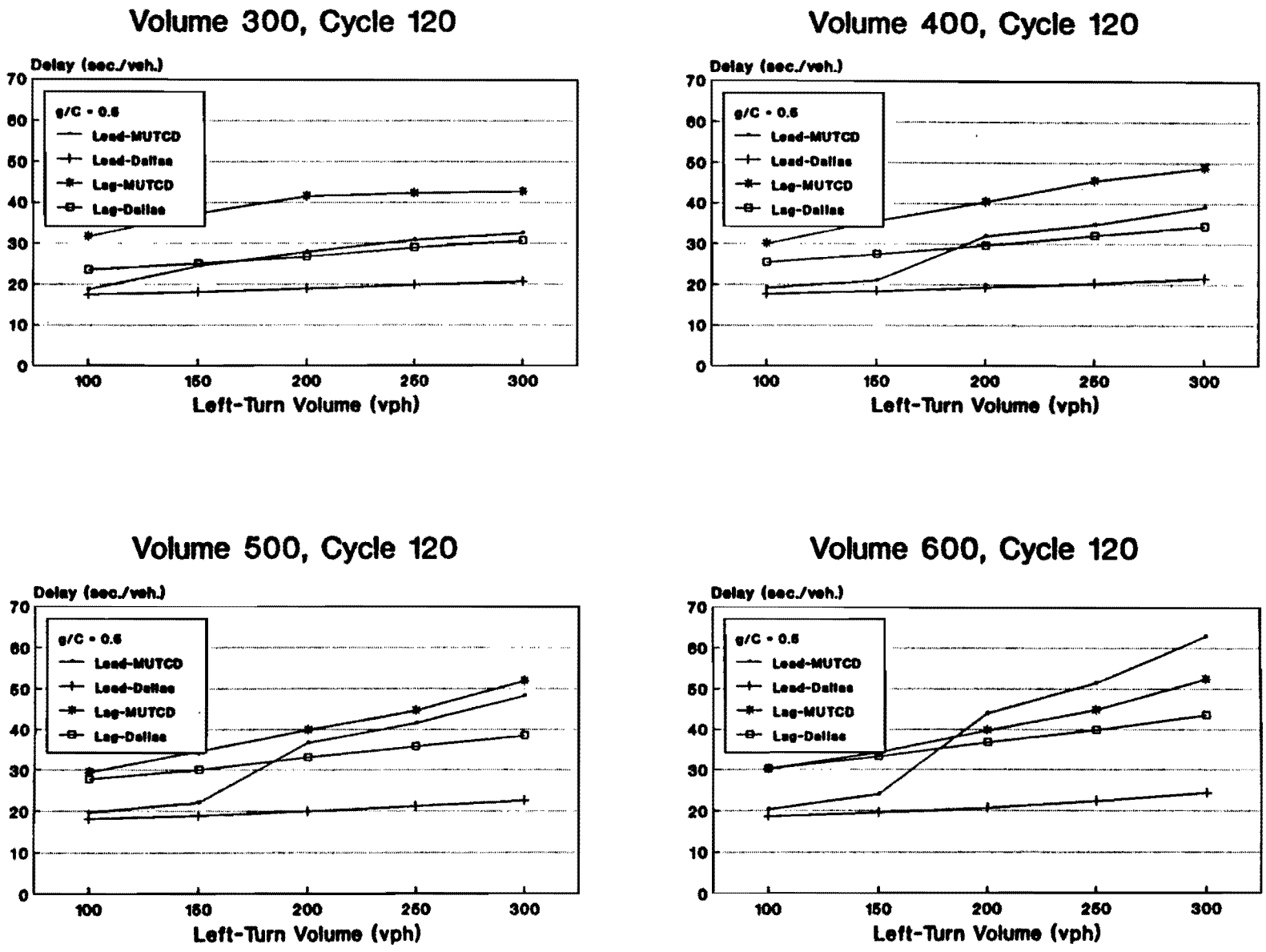

Figure E-6: Predicted Delay vs Left-Turn Volumes (g/C=0.5, Cycle=120 sec.)

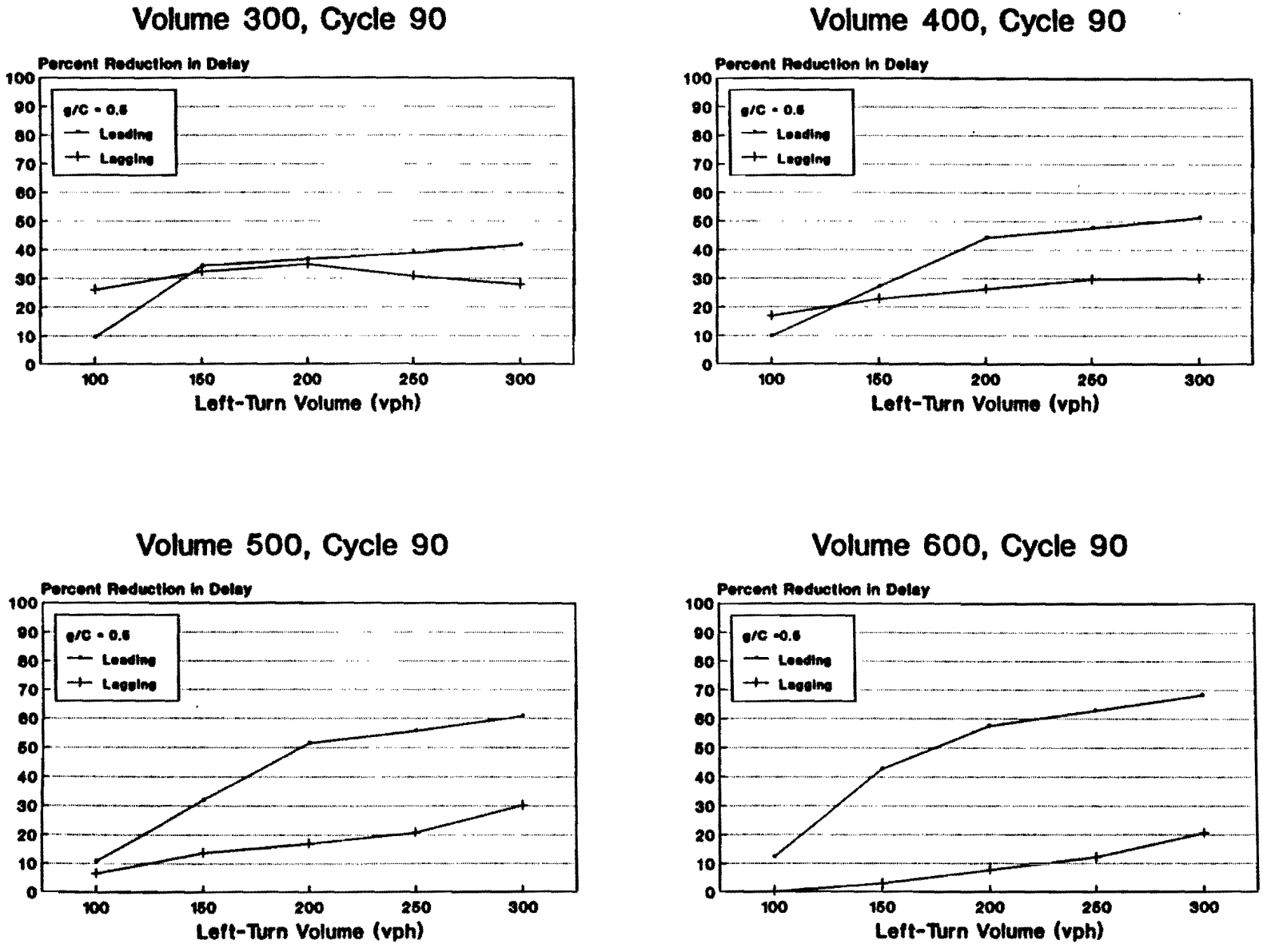

Figure E-7: Predicted Delay vs Left-Turn Volumes (g/C=0.5, Cycle=90 sec.)

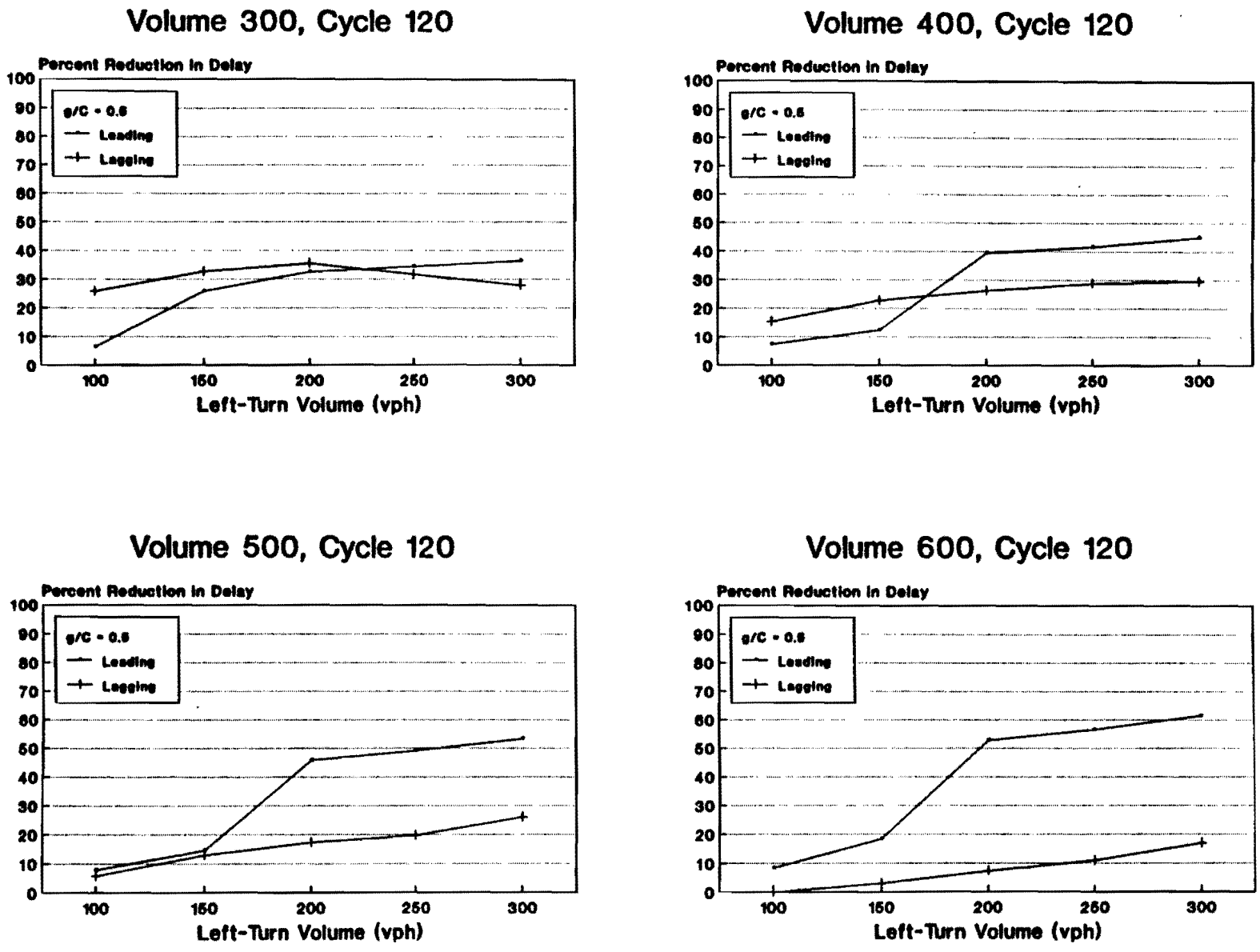

Figure E-8: Reduction In 'Delay vs Left-Turn Volumes (g/C=0.5, cycle=120 sec.)

Table E-3: Predicted Left-Turn Delay for Alternate Phasing (g/C=0.6)

Opposing Volume	Left Turn Volume	Cycle Length	Leading Left			Lagging Left		
			Delay		Percent	Delay		Percent
			MUTCD	Dallas	Reduction	MUTCD	Dallas	Reduction
300	100	90	9.9	8.9	10.1	20.1	13.7	31.8
300	150	90	10.4	9.2	11.5	24.2	14.7	39.3
300	200	90	15.3	9.6	37.3	28.3	15.8	44.2
300	250	90	16.3	10.0	38.7	31.5	17.1	45.7
300	300	90	17.5	10.5	40.0	31.7	18.6	41.3
300	100	120	12.4	11.5	7.3	25.4	17.3	31.9
300	150	120	13.0	11.9	8.5	31.1	18.6	40.2
300	200	120	18.3	12.4	32.2	36.4	20.0	45.1
300	250	120	19.9	12.9	35.2	40.5	21.6	46.7
300	300	120	21.1	13.5	36.0	40.6	23.5	42.1
400	100	90	10.1	9.1	9.9	18.8	15.3	18.6
400	150	90	10.7	9.4	12.1	22.6	16.6	26.5
400	200	90	11.9	9.9	16.8	26.9	18.0	33.1
400	250	90	18.6	10.4	44.1	30.6	19.8	35.3
400	300	90	20.3	11.0	45.8	35.2	21.8	38.1
400	100	120	12.6	11.7	7.1	23.6	19.3	18.2
400	150	120	13.3	12.2	8.3	28.9	21.0	27.3
400	200	120	14.4	12.7	11.8	34.3	22.8	33.5
400	250	120	22.4	13.3	40.6	39.0	25.0	35.9
400	300	120	24.1	14.0	41.9	43.8	27.4	37.4
500	100	90	11.6	10.5	9.5	19.4	16.6	14.4
500	150	90	11.6	10.0	13.8	22.2	16.6	25.2
500	200	90	18.1	10.2	43.6	25.8	17.8	31.0
500	250	90	21.5	10.8	49.8	28.8	19.7	31.6
500	300	90	23.9	11.5	51.9	32.2	21.6	32.9
500	100	120	14.7	13.6	7.5	24.7	21.3	13.8
500	150	120	14.3	12.9	9.8	28.2	21.3	24.5
500	200	120	17.8	13.1	26.4	33.0	22.6	31.5
500	250	120	25.4	13.8	45.7	36.9	24.8	32.8
500	300	120	27.8	14.7	47.1	40.4	27.2	32.7
600	100	90	12.3	11.0	10.6	19.3	18.6	3.6
600	150	90	12.8	10.7	16.4	22.0	18.9	14.1
600	200	90	18.9	10.7	43.4	25.4	20.0	21.3
600	250	90	25.1	11.4	54.6	28.1	22.3	20.6
600	300	90	28.6	12.3	57.0	32.3	24.3	24.8
600	100	120	15.6	14.4	7.7	24.4	23.7	2.9
600	150	120	15.7	13.9	11.5	28.0	24.3	13.2
600	200	120	17.8	13.7	23.0	32.2	25.2	21.7
600	250	120	29.2	14.5	50.3	36.6	28.1	23.2
600	300	120	32.4	15.6	51.9	40.5	30.6	24.4

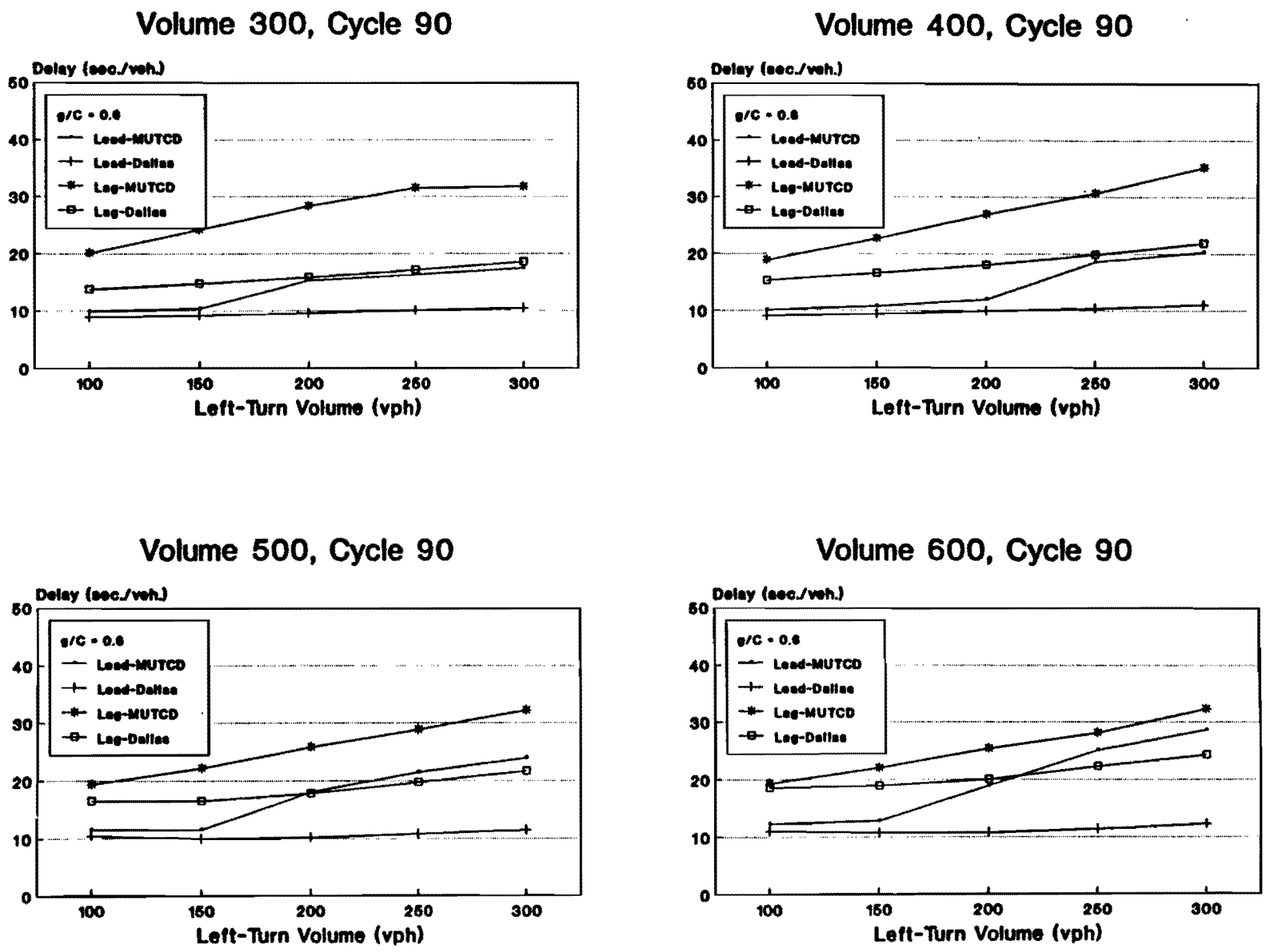

Figure E-9: Predicted Delay vs Left-Turn Volumes (g/C=0.6, Cycle=90 sec.)

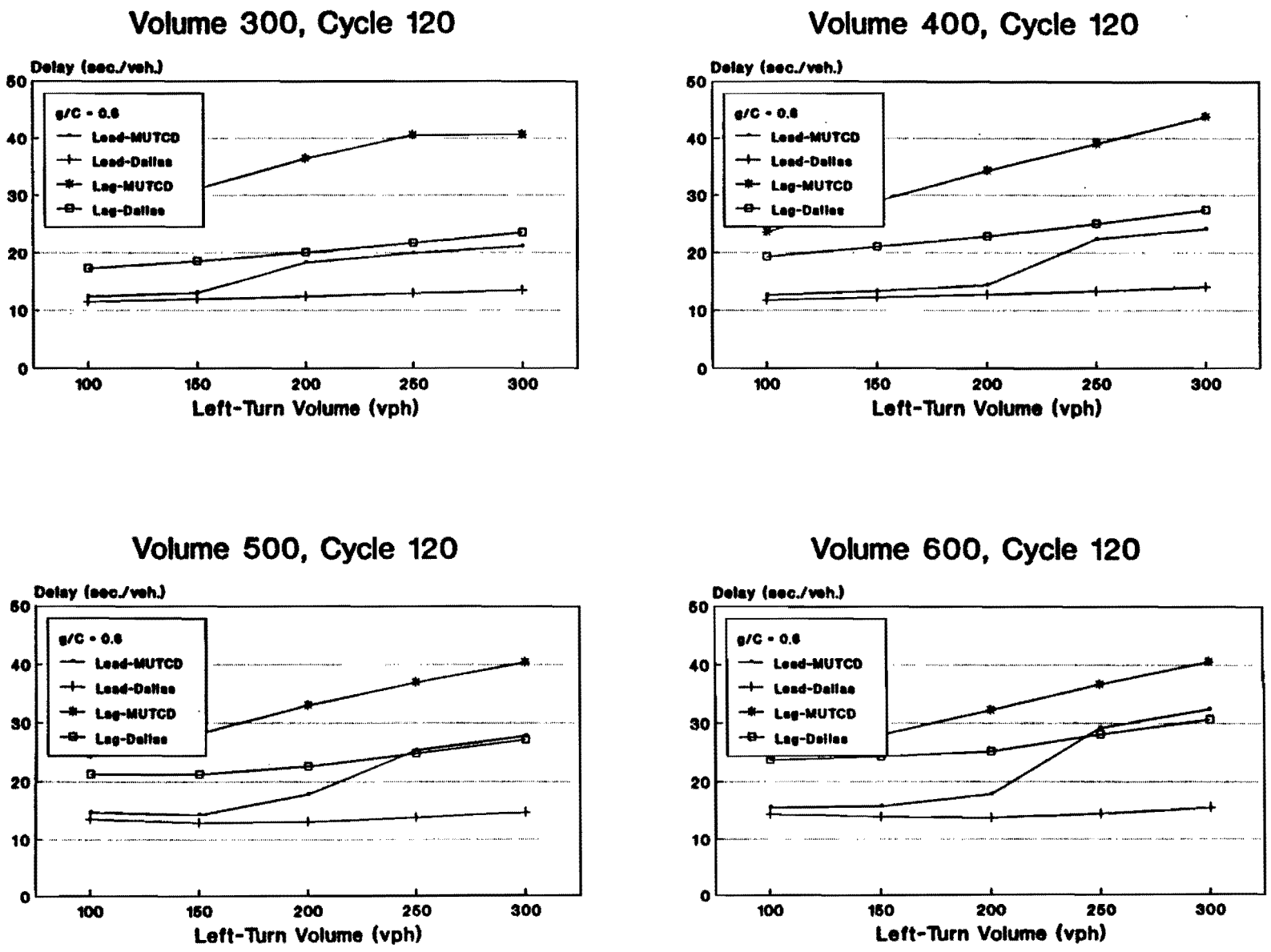

Figure E-10: Predicted Delay vs Left-Turn Volumes (g/C=0.6, Cycle=120 sec.)

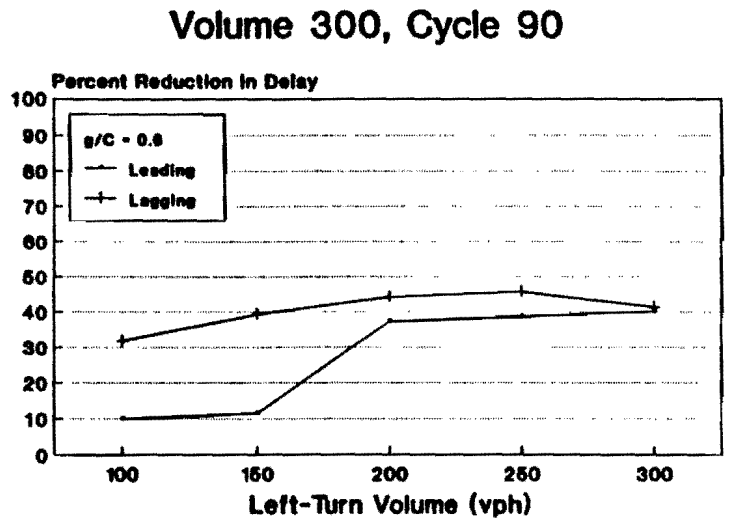

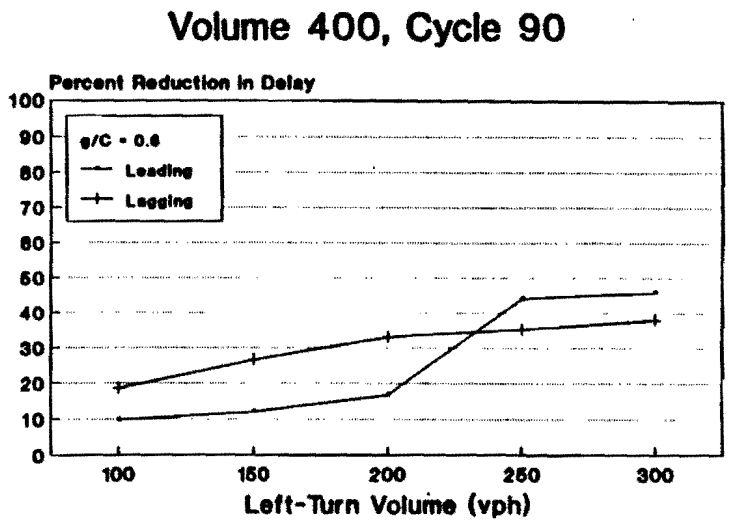

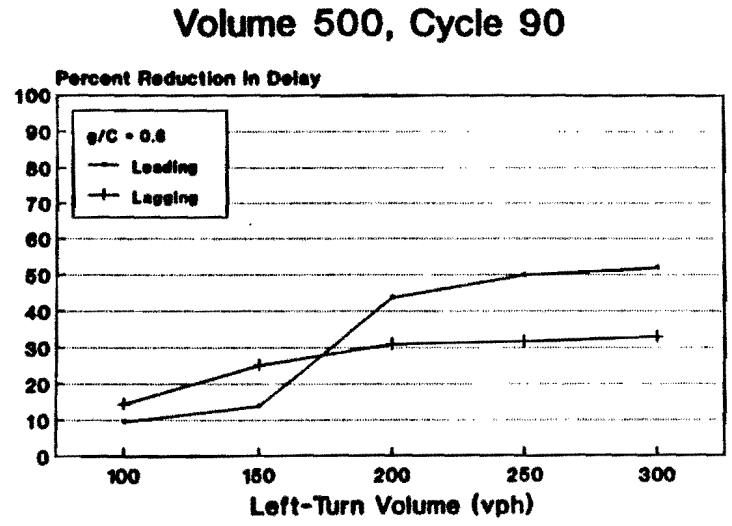

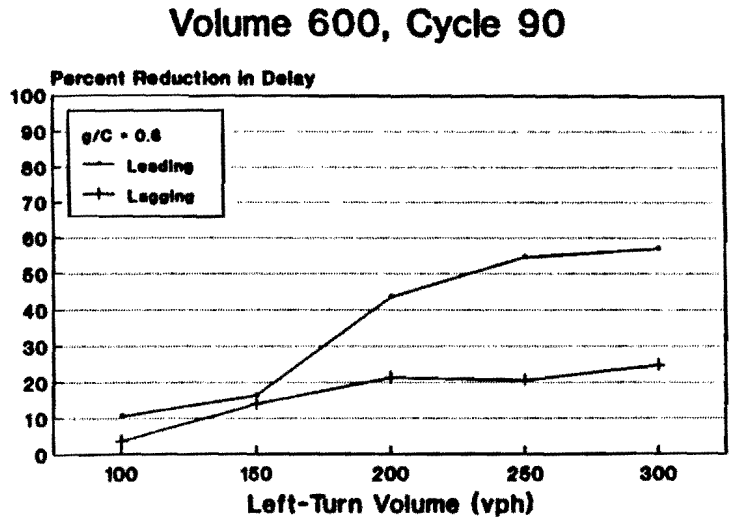

Figure E-11: Reduction In Delay vs Left-Turn Volumes (g/C=0.6, Cycle=90 sec.)